

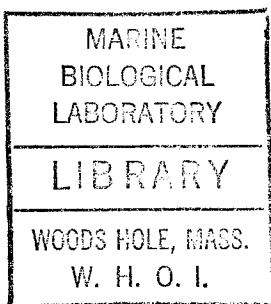
GC  
7.1  
Y75  
1981

THE VERTICAL STRUCTURE OF  
THE WIND-DRIVEN CIRCULATION

by

WILLIAM ROY YOUNG  
B.Sc., M.Sc., Australian National University  
(1977)

SUBMITTED IN PARTIAL FULFILLMENT OF THE  
REQUIREMENTS FOR THE DEGREE OF  
DOCTOR OF PHILOSOPHY



at the

MASSACHUSETTS INSTITUTE OF TECHNOLOGY

and the

WOODS HOLE OCEANOGRAPHIC INSTITUTION

August, 1981

Signature of Author

\_\_\_\_\_  
Joint Program in Oceanography, Massachusetts  
Institute of Technology - Woods Hole  
Oceanographic Institution

Certified by

\_\_\_\_\_  
Thesis Supervisor

Accepted by

\_\_\_\_\_  
Chairman, Joint Oceanography Committee  
in the Earth Sciences, Massachusetts  
Institute of Technology - Woods Hole  
Oceanographic Institution.

THE VERTICAL STRUCTURE OF  
THE WIND-DRIVEN CIRCULATION

by

WILLIAM ROY YOUNG

Submitted to the Joint Program Oceanographic  
Committee in the Earth Sciences, Massachusetts  
Institute of Technology and Woods Hole  
Oceanographic Institution, on August 5, 1981,  
in partial fulfillment of the requirements for  
the degree of Doctor of Philosophy.

ABSTRACT

This thesis consists of three loosely related theoretical studies.

In chapters 1 - 3 the physical mechanisms which determine the three dimensional structure of the currents in the Sverdrup interior of a wind-driven gyre are discussed. A variety of simple analytic models suggest that the subsurface geostrophic contours in a wind gyre are closed and so the flow in these regions is not determined by lateral boundary conditions. Instead a turbulent, quasigeostrophic extension of the Batchelor-Prandtl theorem suggests that the potential vorticity is uniform inside these laterally isolated regions. The requirement that the potential vorticity be uniform leads simply and directly to predictions of the shape and extent of the wind gyre and the vertical structure of the currents within it.

In chapter 4 the propagation of Rossby wave trains through slowly varying forced mean flows is examined by solving the linearized potential

vorticity equation using the WKB method. If the mean flow is forced the action defined by Bretherton and Garrett (1968) is not conserved.

Surprisingly, there is another quadratic wave property which is conserved, the wave enstrophy.

In chapter 5 shear dispersion in an oscillatory velocity field, similar to that of an inertial oscillation, is discussed. The goal of this section is to develop intuition about the role of internal waves in horizontal ocean mixing. The problem is examined using a variety of models and techniques. The most important result is (23.2) which is an expression for the effective horizontal diffusivity produced by the interaction of vertical diffusivity and oscillatory vertical shear. Given an empirical velocity shear spectrum and an estimate of the vertical diffusivity this result could be used to calculate a horizontal eddy diffusivity which parameterizes the horizontal mixing due to the internal wave field.

Thesis Supervisor: Dr. P. B. Rhines

Title: Senior Scientist,

Woods Hole Oceanographic Institution.

## ACKNOWLEDGEMENTS

This is a welcome opportunity to thank my advisor, Peter Rhines. Our partnership has been more exciting and productive than I would have thought possible four brief years ago. His guidance has been inspirational and his approach to science has deeply influenced me.

The remaining members of my thesis committee, Joe Pedlosky and Glenn Flierl, have done much to improve the readability of this thesis. I am also grateful to them for many enlightening conversations and critical questions which forced me to think more clearly.

During my studenthood I have enjoyed the company of a remarkably exciting set of office-mates. Their physical proximity encouraged me to expose them to undigested (and often undigestable) ideas. At W.H.O.I. I benefited from the company of Breck Owens, Dan Wright and John Loder. At M.I.T. the denizens of Think-Tank Central, Ellen Brown, Al Campbell, Teri Chereskin and Bill Dewar, provided a resonant audience. That honorary denizen, Glenn Ierley, has the rare distinction of contributing to both my intellectual progress and my physical comfort; my memories of his pecan pies will long endure.

I'd also like to thank Mary Ann Lucas who cheerfully and efficiently typed this thesis.

Finally, NSF Grant OCE-78-25692 has supported me throughout my stay in the Joint Program.

## TABLE OF CONTENTS

	Page
ABSTRACT	1
ACKNOWLEDGEMENTS	3
CHAPTER 1      A DISCUSSION OF THE VERTICAL STRUCTURE OF THE WIND-DRIVEN CIRCULATION.	9
Abstract of Chapter 1.	9
Section 1      The Sverdrup Balance	11
Introduction - the Sverdrup balance reduces the dimensionality of the circulation problem from three to two.	11
An assumption - separation of the wind-driven and thermohaline circulations.	14
The quasigeostrophic equations.	15
The nondimensional equations; the significance of $U/\beta L^2$ .	15
Scale estimates of $\ell$ and $U$ in terms of external variables.	17
Section 2      Time Dependent, Dissipationless Circulation Problems	20
Introduction - the possibility of determining the vertical structure by solving an initial value problem.	20
A linear initial value problem.	22
Baroclinic flows forced by moving wind-stress patterns -- a linear analysis.	26
Nonlinear effects -- a two-layer quasigeostrophic model.	30
Section 3      Linear, Steady, Dissipative Circulation Problems	37
Introduction - dissipation smooths the singular current distributions suggested by the linear initial value problem.	37
A two layer model with interfacial drag.	37
Continuously stratified models with various dissipative mechanisms.	43

	Page	
Section 4	The Importance of Closed Geostrophic Contours	45
	Introduction - the dynamics of closed and blocked geostrophic contours are compared and contrasted.	45
	A two layer quasigeostrophic model.	46
	A three layer quasigeostrophic model.	50
	Uniform potential vorticity in subsurface layers.	53
Section 5	Some Homogeneous Circulation Problems	56
	Introduction	56
	Topographically closed geostrophic contours.	56
	Sverdrup flow on a broken $\beta$ -plane.	61
CHAPTER 2	POTENTIAL VORTICITY HOMOGENIZATION	64
	Abstract of Chapter 2.	64
Section 6	An Oceanic Analog of the Batchelor-Prandtl Theorem	66
	Introduction - removing degeneracy inside closed streamlines using an integral theorem.	66
	The Batchelor-Prandtl theorem.	67
	Vertical viscosity and a Batchelor-Prandtl theorem for potential vorticity.	68
Section 7	Some Exegetical Remarks on $\overline{v_i'q'} = -\kappa_{ij} q_{,j}$	71
	Introduction - mesoscale eddies and the removal of degeneracy inside closed geostrophic contours.	71
	The eddy flux of potential vorticity.	72
Section 8	Potential Vorticity Homogenization - a Turbulent Extension of the Batchelor-Prandtl Theorem	79
	Introduction - the weak eddy assumption.	79
	The first proof: use $\overline{v_i'q'} = -\kappa_{ij} \overline{q}_{,j}$ explicitly.	79
	The second proof: use the enstrophy equation.	81

	Page	
Section 9	A Generalization of the Zonal Average	84
	Introduction - some geometric preliminaries.	84
	An application of (9.5): high Peclet number, unsteady advection-diffusion.	87
	Definition of a generalized zonal average.	88
	The generalized zonal average of the potential vorticity equation.	92
	Introduction of Lagrangian coordinates.	94
	Effects of weak dissipation in a steady wave field.	96
Appendix A:	Algebra leading to (9.33b)	98
Appendix B:	Algebra leading to (9.39a)	99
CHAPTER 3	SOME GENERAL CIRCULATION MODELS	100
Abstract of	Chapter 3.	100
Section 10	Closed, Interior Geostrophic Contours in a Layered General Circulation Model	102
	Introduction - recapitulation of previous results.	102
	The three layer quasigeostrophic equations.	103
	All the lowest layer geostrophic contours are blocked.	103
	The geostrophic contours of the middle layer can be calculated.	104
	Calculation of weak subsurface flows in blocked regions.	108
Section 11	A Continuously Stratified Theory	110
	Introduction - the continuously stratified model.	110
	The depth of the wind-driven gyre: $z = -D(x,y)$ .	110
	Solution of (11.4).	112
	A model of the Ekman pumping; $w_E = [1 -  y ]$ .	112
	Some remarks on the relationship between the present theory and thermocline theories.	115

	Page	
Section 12	A Nondissipative Model of the Subsurface Western Boundary Layer	119
	Some qualitative arguments concerning western boundary layer dynamics.	119
	The model, assume $\psi_1$ is known.	121
	(12.4) is not as simple as it seems.	121
	A boundary layer with continuous potential vorticity.	129
	Solution of the boundary layer equations.	133
	Conclusion.	135
Section 13	A Frictional Model of the Western Boundary Layer	137
	Introduction - a two layer model with interfacial friction.	137
	Nondimensionalization.	138
	Solution of the barotropic mode equation.	139
	An equation for $\psi_2$ alone.	140
	A preliminary simplification.	140
	The thermal analogy and a general discussion of the role of the western boundary layer.	142
	Limiting case 1: $F = O(\delta)$ .	144
	Limiting case 1: $F = O(\delta^{-1})$ .	145
	The distinguished limit: $F = O(1)$ .	146
	Solution in the interior.	147
	Detailed solution in the boundary layer.	
	Case 1: $0 < y < 1$ .	150
	Detailed solution in the boundary layer.	
	Case 2: $y_* < y < 0$ .	151
	Detailed solution in the boundary layer.	
	Case 3: $-1 < y < y_*$ .	152
	Summary.	153
	Does the potential vorticity homogenize?	153
	The boundary patches at $y = 0$ and $y_*$ .	155
	Some extensions.	155
Appendix A:	Asymptotic expansion of $M(1, b, -\frac{1}{3} aF)$	
	as $aF \gg \infty$ and $b = 1 - \frac{1}{3}(1 - aF)$ .	157



CHAPTER I  
A Discussion of the Vertical Structure of the  
Wind-Driven Circulation

Abstract of Chapter I

The vertically integrated Sverdrup balance provides a qualitative picture of the horizontal characteristics of the wind-driven circulation. This chapter is a preliminary discussion of the mechanisms which determine the vertical structure of the flow.

In section 1 the quasigeostrophic equations are introduced and nondimensionalized. It is argued that in the Sverdrup interior of a wind gyre the vortex stretching is as strong as the  $\beta$ -effect. This assumption leads to estimates of the vertical length scale and horizontal velocity scale in terms of external variables. These estimates do not depend on eddy diffusivities (eqns. (1.13a,b)).

In section 2 a linear dissipationless initial value problem is solved. The goal here is to determine the vertical structure of the steady state by switching on the wind stress and calculating the ensuing circulation. It is found that the Sverdrup circulation becomes as top-trapped as the vertical resolution of the model will permit, and so these linear time dependent problems do not provide a physically sensible answer. The nonlinear initial value problem is also discussed; if there is no dissipation this problem may have no steady state.

In section 3 steady linear dissipative circulation problems are discussed. In these models the vertical scale of the circulation depends on unknown eddy diffusivities.

Section 4 is a preliminary discussion of nonlinear circulation models. The nonlinearity considered is vortex stretching and its most important effect is to close geostrophic contours within the ocean basin. The region within the closed contours is shielded from lateral boundary conditions. It is only in these isolated regions that subsurface flows can exist.

Section 5 is a digression into homogeneous circulation theory. The wind-driven flow within topographically closed geostrophic contours is discussed; when the bottom friction is weak this flow is much faster than the familiar Sverdrup flow in the region where the geostrophic contours are coastally blocked.

## 1. The Sverdrup Balance.

Introduction - the Sverdrup balance reduces the dimensionality of the circulation problem from three to two.

The Sverdrup balance occupies a central place in wind-driven circulation theory. This simple integral constraint on the three dimensional circulation is based on the simplicity of the planetary scale vorticity balance in a stratified fluid:

$$\beta v = f w_z. \quad (1.1)$$

If (1.1) is integrated from the base of the upper Ekman layer,  $z=0$ , down to a "level of no motion",  $z=-D$ , where  $w=0$ , the classical Sverdrup balance:

$$\begin{aligned} \beta \int_{-D}^0 v \, dz &= f w_E \\ &= \nabla \times \left( \frac{\tau}{\rho_0 f} \right) \cdot \hat{z} \end{aligned} \quad (1.2)$$

results. In (1.2)  $w_E$  is the vertical velocity at the base of the Ekman layer produced by the curl of the wind stress  $\tau$ ; (1.2) enables one to calculate the north-south transport from the curl of the wind stress without even considering the underlying stratification,  $\rho(z)$ , of the fluid. Since the vertically integrated transport is approximately horizontally nondivergent the east-west transport is given by

$$\int_{-D}^0 u \, dz = \beta^{-1} \int_x^a \frac{\partial}{\partial y} \left\{ \nabla \times \left( \frac{\tau}{\rho_0 f} \right) \right\} \cdot \hat{z} \, dx' \quad (1.3)$$

where the constant of integration is determined by requiring that the zonal flow vanish at the eastern boundary  $x=a$ .

Equations (1.2) and (1.3) can be used to calculate two dimensional flows driven by the wind. For example the familiar pattern in figure 1

is produced by the convenient choice

$$w_E = -w_0 \cos\left(\frac{\pi}{2} \frac{y}{L}\right) \quad (1.4)$$

which models the Ekman pumping in a subtropical gyre. Historically this has been one of the most important theoretical applications of the Sverdrup balance; it is used to reduce the dimensionality of the full circulation problem. Thus all of homogeneous circulation theory can be interpreted as applying to the vertically integrated transport in a stratified ocean.

There are several obvious deficiencies in the classical theory outlined above. The first is the lack of vertical resolution; how is the transport in (1.2) distributed in the vertical? Secondly, is there any theoretical justification for the existence of a "level of no motion"? The idea that the directly wind-driven flow penetrates only several hundred meters vertically and rests above a circulation driven by thermohaline processes or eddies underpins much theoretical and observational thought. Observational support for a relatively "shallow" (order 700 m) wind-driven circulation is found in the transport calculations of Leetma, Niiler and Stommel (1977). There is a clear need for a theory which explains why the wind-driven flow is as deep as it is and predicts what the vertical profiles of mean currents should look like. Both of the issues outlined above will be discussed in chapters 1-3 of this thesis. The remainder of this section will be devoted to introducing the quasigeostrophic equations and, more importantly, seeing what vertical length scales are suggested by nondimensionalization.

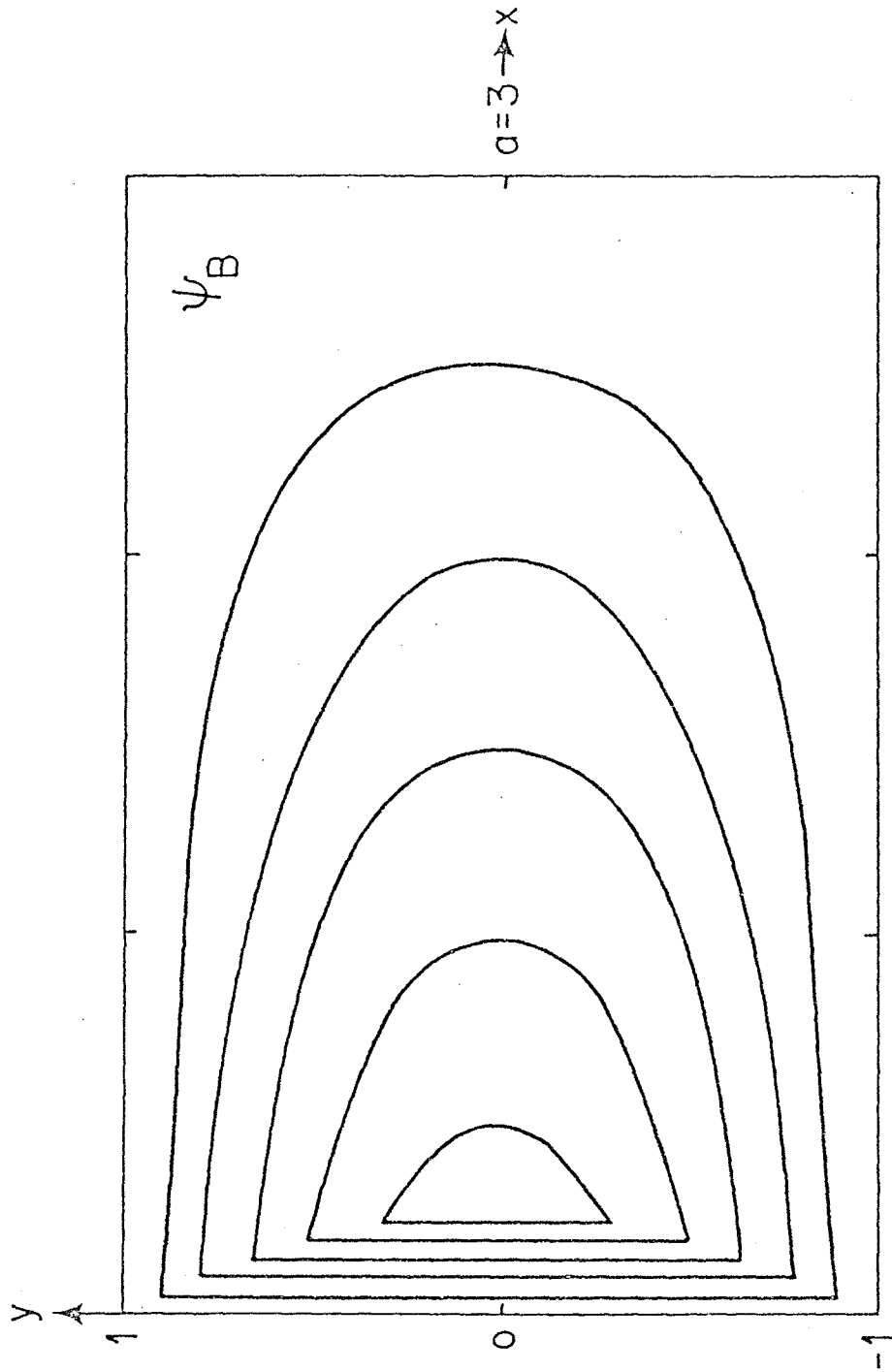


Figure 1. The barotropic streamfunction given by (1.4). The western boundary layer is shown schematically.

An assumption: separation of the wind-driven and thermohaline circulations

Before proceeding I must make explicit a major assumption underlying both this thesis and much of classical wind-driven circulation theory. This is the idea that the thermohaline and wind-driven circulations can be separated to the extent that it is meaningful or informative to consider the density,  $\rho(z)$ , as essentially prescribed by the thermohaline processes. This separation is ensured a priori by using the quasigeostrophic equations in which the density is partitioned as

$$\rho(x,y,z,t) = \rho_0 \left\{ 1 - g^{-1} \int_0^z N^2(z') dz' - g^{-1} b(x,y,z,t) \right\} \quad (1.5)$$

where  $\rho_0$  is (say) the density at the surface,  $N$  the Brunt-Väisälä frequency and  $b$  the buoyancy. All the thermohaline processes are subsumed in the supposedly known function  $N(z)$  and the constant  $\rho_0$ ; the unknown perturbations produced by the wind are contained in  $b(x,y,z,t)$ . The validity of quasigeostrophic approximation requires that

$$N^2 \gg b_z$$

so that the isopycnals are approximately flat. Pedlosky (1979), Section 6.19, discusses the scaling associated with (1.5) more carefully and concludes that the quasigeostrophic approximation remains valid provided the length scale of the flow is much less than the radius of the Earth (this same condition ensures the validity of the  $\beta$ -plane approximation). The gyre scale flows discussed in this thesis only marginally satisfy this condition and indeed the isopycnals in trans-gyre sections show significant deviations from their mean depths and more disastrously (for

the quasigeostrophic approximation at least) may even strike the surface. Nevertheless the simplicity of the quasigeostrophic equations is a compelling reason for using them as the basis of first attempts at circulation modelling.

I shall briefly discuss the role of thermohaline models again at the end of section 11.

### The quasigeostrophic equations

The dimensional quasigeostrophic equations are then (Pedlosky, 1979):

$$q_t + J(\psi, q) = \text{Forcing} + \text{Dissipation} \quad (1.6a)$$

$$q = \psi_{xx} + \psi_{yy} + (F\psi_z)_z + \beta y \quad (1.6b)$$

$$F(z) = f_0^2 N^{-2} \quad (1.6c)$$

$$(u, v) = (-\psi_y, \psi_x) \quad (1.6d)$$

$$b_t + J(\psi, b) = -wN^2 + \text{dissipation} \quad (1.6e)$$

$$b = f_0 \psi_z \quad (1.6f)$$

Equation (1.6e) is conservation of density equation linearized in the quasigeostrophic sense about the mean stratification. This relationship together with the hydrostatic balance (1.6f) is used to calculate  $w$ .

### The nondimensional equations; the significance of $U/\beta L^2$

It is instructive to nondimensionalize (1.6) so that (1.1) and (1.2) are recovered as zero order balances when the nondimensional parameter:

$$\epsilon^2 = U/\beta L^2 \quad (1.7)$$

goes to zero (Pedlosky, 1979). In (1.7)  $U$  is a scale estimate of the horizontal velocity and  $L$  is an external variable viz. the horizontal

length scale of the forcing. We expect that  $L$  will also be characteristic of the horizontal structure of the forced flow. Denoting nondimensional variables by  $*$  then:

$$\Psi = UL \Psi_* \quad (1.8a)$$

$$(x, y) = L(x_*, y_*) \quad (1.8b)$$

$$z = \ell z_* \quad (1.8c)$$

$$N = N_0 N_* \quad (1.8d)$$

where  $\ell$  is the vertical scale of the flow and  $N_0$  is a typical value of  $N$ . It is important to realize that  $\ell$  and  $U$  are unknown a priori; later in this section we will make some assertions about the probable dynamic balance and so obtain expressions for  $\ell$  and  $U$  in terms of the external dimensional variables  $f_0$ ,  $N_0$ ,  $\beta$  etc.

The potential vorticity is:

$$q = \beta L \left[ \epsilon^2 \nabla_*^2 \Psi_* + y_* + s^2 (F_* \Psi_{*z_*})_{z_*} \right] \quad (1.8)$$

where  $\epsilon^2$  is defined in (1.7) and:

$$s^2 = (f_0^2 / N_0^2) (U / \beta L^2) \quad (1.9a)$$

$$F_* = N_*^{-2} \quad (1.9b)$$

Since we are concerned with wind-driven flows it is appropriate to nondimensionalize  $w$  using the amplitude of the imposed Ekman pumping,  $W$ , so that:

$$w = W w_*$$

and then the nondimensional combination of (1.6e and f) is:

$$\psi_{*z}^t + J(\psi_*, s^2 F \psi_{*z}) = -\mu w_* \quad (1.10)$$

where

$$t = (L/U)t_* \quad (1.11a)$$

$$\mu = f_0 W / \beta L U \quad (1.11b)$$

Substituting typical observed values of  $U$  (say  $1 \text{ cm s}^{-1}$ ) and  $L$  (say  $10^8 \text{ cm}$ ) into (1.7) shows that  $\epsilon^2 \sim 10^{-3}$  so that on these large length scales the relative vorticity contributes negligibly to the potential vorticity and the steady version of (1.6a) is:

$$\psi_{*x} + \frac{\partial}{\partial z_*} J(\psi_*, s^2 F \psi_{*z}) = 0(\epsilon^2)$$

or from (1.10)

$$\psi_{*x} = \mu \frac{\partial w_*}{\partial z_*} + 0(\epsilon^2) \quad (1.12)$$

Equation (1.12) is the nondimensional version of (1.1).

Scale estimates of  $\ell$  and  $U$  in terms of external variables.

The internal dimensional variables  $\ell$  and  $U$  are now determined by assuming that

- 1) The Sverdrup balance (1.12) holds so  $\mu=1$ .
- 2) The vortex stretching (i.e. the deformation of the density surfaces) is as strong as the  $\beta$ -effect (Rhines and Holland, 1979) so  $s^2=1$ .

Solving  $s^2=\mu=1$  gives

$$\ell = f_0 (N_0 \beta)^{-2/3} W^{1/3} \quad (1.13a)$$

$$U = \beta^{-1/3} N_0^{2/3} W^{2/3} \quad (1.13b)$$

In Tables 1.1 (a,b) numerical values of  $\mathcal{L}$  and  $U$  are given as functions of  $W$  and  $N_0$  at  $45^\circ$  and (more typically for a subtropical gyre)  $30^\circ$  latitude.

The results (1.13) have been derived here rather formally. In particular I have not attempted to motivate the assumption that the vortex stretching be as strong as the  $\beta$ -effect ( $s^2=1$ ). Rhines and Holland (1979) pointed out that unless this is the case the potential vorticity is dominated by the  $\beta$ -effect and the geostrophic contours (i.e. contours of constant  $q$ ) are blocked by coastal boundaries. We will see in sections 2-4 that possible motions at points threaded by such blocked geostrophic contours are severely constrained. One of the major conclusions of this thesis is that the wind-driven flow avoids these constraints by closing the geostrophic contours in the interior of the basin. This closure is accomplished primarily by balancing the vortex stretching against the  $\beta$ -effect in the Sverdrup interior and so the scaling  $s^2=1$  is expected. Finally note that the estimates of  $\mathcal{L}$  and  $U$  are realistic and do not depend on any unknown eddy diffusivities.

$W \text{ cm s}^{-1} \rightarrow$ $N_0 \text{ s}^{-1} \downarrow$	$5 \times 10^{-5}$	$10 \times 10^{-5}$	$15 \times 10^{-5}$	$20 \times 10^{-5}$	
$5 \times 10^{-4}$	$1.6 \times 10^{-1}$ $2.0 \times 10^5$	$2.5 \times 10^{-1}$ $2.5 \times 10^5$	$3.3 \times 10^{-1}$ $2.9 \times 10^5$	$4.0 \times 10^{-1}$ $3.1 \times 10^5$	$U \text{ cm s}^{-1}$ $\leftarrow$ $l \text{ cm}$
$10^{-3}$	$2.5 \times 10^{-1}$ $1.3 \times 10^5$	$4.0 \times 10^{-1}$ $1.6 \times 10^5$	$5.2 \times 10^{-1}$ $1.8 \times 10^5$	$6.3 \times 10^{-1}$ $2.0 \times 10^5$	$U \text{ cm s}^{-1}$ $\leftarrow$ $l \text{ cm}$
$5 \times 10^{-3}$	$7.3 \times 10^{-1}$ $4.3 \times 10^4$	1.2 $5.4 \times 10^5$	1.5 $6.2 \times 10^5$	1.8 $6.8 \times 10^4$	$U \text{ cm s}^{-1}$ $\leftarrow$ $l \text{ cm}$

(a)  $45^\circ$  latitude;  $f = 1.0 \times 10^{-4} \text{ s}^{-1}$  and  $\beta = 1.6 \times 10^{-13} \text{ cm}^{-1} \text{ s}^{-1}$ .

$W \text{ cm s}^{-1} \rightarrow$ $N_0 \text{ s}^{-1} \downarrow$	$5 \times 10^{-5}$	$10 \times 10^{-5}$	$15 \times 10^{-5}$	$20 \times 10^{-5}$	
$5 \times 10^{-4}$	$1.5 \times 10^{-1}$ $1.2 \times 10^5$	$2.3 \times 10^{-1}$ $1.6 \times 10^5$	$3.0 \times 10^{-1}$ $1.8 \times 10^5$	$3.7 \times 10^{-1}$ $2.0 \times 10^5$	$U \text{ cm s}^{-1}$ $\leftarrow$ $l \text{ cm}$
$10^{-3}$	$2.3 \times 10^{-1}$ $7.9 \times 10^4$	$3.7 \times 10^{-1}$ $9.9 \times 10^4$	$4.8 \times 10^{-1}$ $1.1 \times 10^5$	$5.8 \times 10^{-1}$ $1.2 \times 10^5$	$U \text{ cm s}^{-1}$ $\leftarrow$ $l \text{ cm}$
$5 \times 10^{-3}$	$6.8 \times 10^{-1}$ $2.7 \times 10^4$	1.1 $3.4 \times 10^4$	1.4 $3.9 \times 10^4$	1.7 $4.3 \times 10^4$	$U \text{ cm s}^{-1}$ $\leftarrow$ $l \text{ cm}$

(b)  $30^\circ$  latitude;  $f = 7.3 \times 10^{-5} \text{ s}^{-1}$  and  $\beta = 2.0 \times 10^{-13} \text{ cm}^{-1} \text{ s}^{-1}$

Tables 1.1a & b. Values of  $U$  and  $l$  for various values of the external parameters.

## 2. Time Dependent, Dissipationless Circulation Problems

Introduction - the possibility of determining the vertical structure by solving an initial value problem.

One superficially appealing approach to the problem of vertically resolving the Sverdrup flow is to completely solve an initial value problem. So consider a stratified quiescent ocean and suddenly apply a wind-stress. The eventual steady state must satisfy the Sverdrup balance (1.2) and so by solving the initial value problem we will have determined the vertical structure of the currents.

The two layer linear version of this problem has been discussed by Anderson and Gill (1975), Rhines (1977) and, with north-south topography, by Anderson and Killworth (1977). Since there are two layers the quasigeostrophic equations have two linear Rossby wave solutions with different vertical structures. The first is the barotropic mode which crosses the basin East to West in a few weeks and established a barotropic Sverdrup flow (in which the isopycnals are flat, but rising or falling linearly with time). The second is the much more slowly propagating baroclinic mode which is generated at the eastern boundary and crosses the basin East to West in several years. When the baroclinic mode arrives at a particular longitude the flow in the lower layer is "switched-off" and all the Sverdrup transport is concentrated in the top layer.

As Charney and Flierl (1981) point out, the result is very different if one uses a continuously stratified model. The complete solution of this problem is given later in this section. Strictly speaking, no steady state is ever reached, the Sverdrup flow is increasingly (as  $t \rightarrow \infty$  and

more baroclinic Rossby wave modes arrive at a given longitude) concentrated into a "jet" at the surface. By contrast in a multi-layered model there is a steady state with all the Sverdrup transport in the uppermost layer. Charney and Flierl (1981) did not solve this problem explicitly, but instead argued that since the linearized density equation is (from (1.6e)):

$$b_t + wN^2 = 0 \quad (2.1)$$

any steady state must have  $w=0$  or  $N^2=0$ . It then follows from (1.1) that  $v=u=0$ . This argument can be strengthened to include the nonlinear advective terms in (1.6e); simply integrate over the area enclosed by a closed streamline and these terms vanish leaving:

$$\iint_{\psi} b_t d^2a = -N^2 \iint_{\psi} w d^2a . \quad (2.2)$$

Thus in a steady state  $w$  must change sign within each streamline. This is impossible however if we evaluate (2.2) at  $z=0$  where  $w$  is externally imposed and may have one sign (e.g.  $w < 0$  in a subtropical gyre). Thus, within the context of strictly nondiffusive, quasigeostrophic dynamics, the first term in (2.2) is always nonzero and, as in the linear problem, there is no steady state. It is interesting to note that the layered model avoids all these difficulties since  $N^2=0$  and so gives potentially misleading results.

To summarize, the approach to the vertical resolution problem outlined in the first paragraph of this section is not promising. The fact that the most realistic models (i.e. continuously stratified,

nonlinear) never reach steady states indicates the necessity of including some dissipation. Nevertheless, time dependent problems are worth discussing for their own intrinsic interest and also because they help to motivate the approach to the vertical resolution problem I shall finally adopt. In the remainder of this section I shall concentrate on dissipationless time dependent problems. The next two subsections are devoted to linear problems while in the concluding subsection I briefly discuss the important, qualitative modifications introduced by nonlinearity.

#### A linear initial value problem

The initial value problem whose solution is presented in this section is:

$$[\nabla^2 \psi + \beta y + (F\psi_z)_z]_t + \beta \psi_x = 0 \quad (2.3a)$$

$$w(x, y, 0, t) = w_E(y) \theta(t) \quad (2.3b)$$

$$w(x, y, -H, t) = 0 \quad (2.3c)$$

$$\psi(x, y, z, 0) = 0 \quad (2.4d)$$

$$\psi(a, y, z, t) = 0 \quad (2.5e)$$

$$w(x, y, z, t) = -Ff_0^{-1} \psi_{zt} \quad (2.5f)$$

Equation (2.3a) is the linearized potential vorticity equation. Equations (2.3b,c) are the boundary conditions at  $z=0$  and  $-H$ ;  $\theta(t)$  is the unit step function which "switches on" the Ekman pumping  $w_E(y)$  at  $t=0$ . Equation (2.5e) is the standard no flux Eastern boundary condition. Equation (2.5f) is the linearized expression for  $w$  in terms of  $\psi$ .

This problem is solved by expanding  $\Psi$  in terms of eigenfunctions defined by the Sturm-Liouville problem:

$$(FC_z)_z + \lambda^2 C = 0 \quad (2.6)$$

$$C_z = 0 \quad \text{at } z = 0 \quad \text{and } -H$$

The above problem has an infinite set of solutions:

$$C_n(z) \text{ and } \lambda_n > 0 \quad n = 0, 1, \dots$$

For example when  $F$  is constant:

$$C_n(z) = \cos \lambda z / F \quad \text{and } \lambda_n = n\pi F/H.$$

For reasonably well behaved  $F(z)$ , the  $C_n(z)$  form a complete set and the solution to (2.3) can be represented as:

$$\Psi = \sum \phi_n(x, y, t) C_n(z) \quad (2.7)$$

The evolution equations for the modal amplitudes  $\phi_n$  are obtained using the Galerkin procedure viz. multiply (2.3a) by  $C_n(z)$  and integrate from  $z = -H$  to  $z = 0$ . The term  $(F\Psi_z)_{zt}$  is handled using repeated integration by parts; in this way one avoids the questionable procedure of exchanging differentiation and summation in the representation (2.7). Because the problem is linear and the boundary conditions are simple the equations for  $\phi_n$  are uncoupled; Flierl (1979) has shown how nonlinearity and bottom slope couples the modal evolution equations. With the normalization

$\int_{-H}^0 C_n^2 dz = H$ , the evolution equations for the problem (2.3) are

$$\nabla^2 \phi_{nt} - \lambda_n^2 \phi_{nt} + \beta \phi_{nx} = f_0 C_n(0) H^{-1} w_E(y) e(t) \quad (2.8)$$

Equation (2.8) is essentially the problem discussed by Anderson and Gill (1975). Away from the western boundary the first term is negligible; this amounts to neglecting the relative vorticity see (1.7) and the following discussion. The solution of the simplified equation which satisfies the Eastern boundary condition at  $x = a$  (2.5e) is:

$$\phi_n(x, y, z, t) = \begin{cases} f_0 C_n(0) H^{-1} W_E(y) \theta(t) [\beta^{-1}(x-a)] & \text{if } t > \lambda_n^2 \beta^{-1}(a-x) \\ f_0 C_n(0) H^{-1} W_E(y) \theta(t) [-\lambda_n^{-2} t] & \text{if } t < \lambda_n^2 \beta^{-1}(a-x) \end{cases} \quad (2.9)$$

When  $t$  is small the modal amplitude is proportional to time; when the signal from the Eastern boundary arrives the mode is brought into Sverdrup balance, (see figure 2). Because there are an infinite number of modes, and the higher order ones travel arbitrarily slowly, a steady solution is never reached. However since:

$$H \delta(z) = \sum_{n=0}^{\infty} C_n(0) C_n(z)$$

we can see from (2.7) and (2.9) that

$$t \xrightarrow{\lim} \psi = f_0 W_E(y) \theta(t) [\beta^{-1}(x-a)] \delta(z)$$

The  $\delta$ -function jet in the above is the singular vertical distribution of Sverdrup transport which was alluded to earlier in this section. The unphysical nature of the solution to this simple linear initial value problem motivates us to include additional processes such as dissipation and nonlinearity. Dissipation alone is of course sufficient; one can simply introduce some "eddy viscosity" into (2.3a) or (2.3) which acts selectively on the higher order modes and traps them near the Eastern

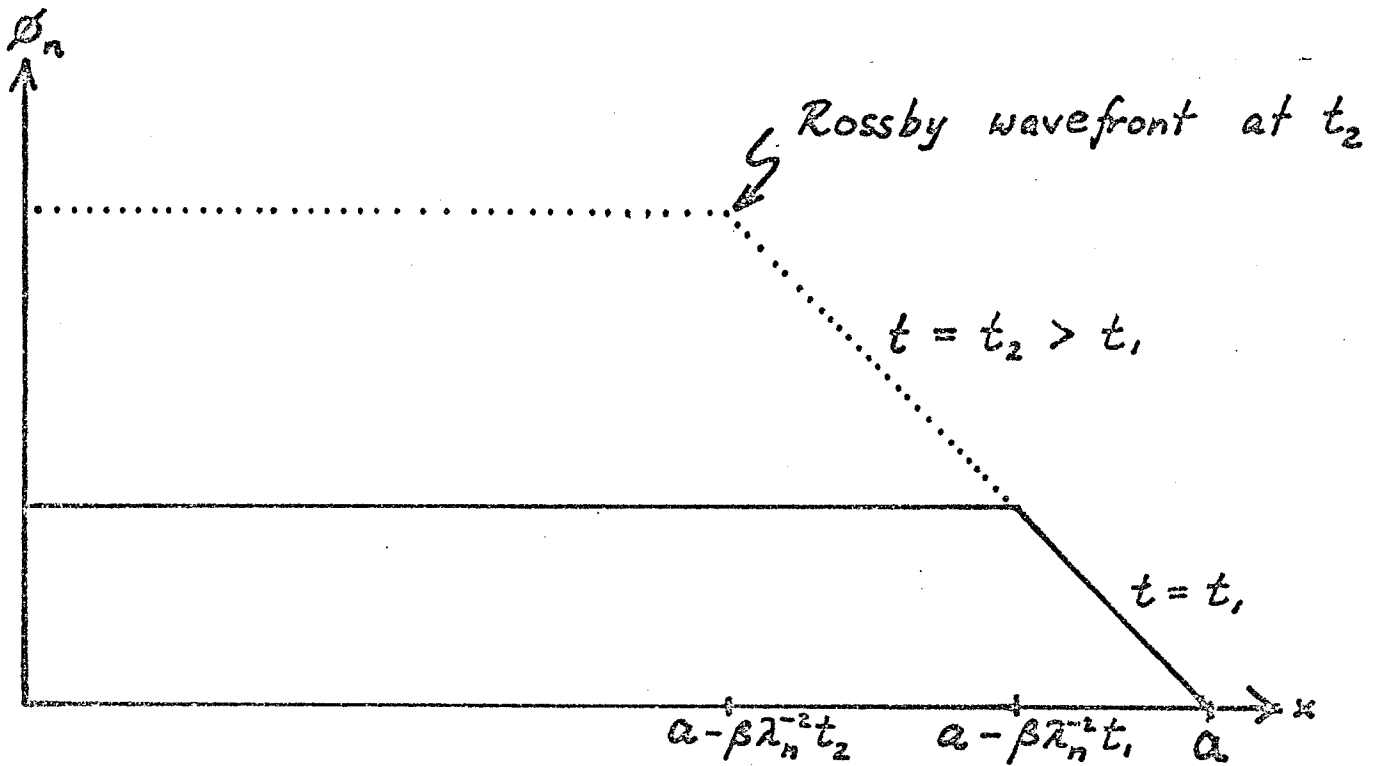


Figure 2. The amplitude of the  $n$ 'th baroclinic Rossby wave mode from (2.9). At the eastern boundary,  $x = a$ , the density surfaces are undisturbed so  $\phi_n = 0$ . Far to the west, where the signal generated at the eastern boundary hasn't arrived,  $\phi_n$  increases linearly with time. The transition between these regions is accomplished by a Rossby wavefront which propagates east to west across the basin.

boundary. This process is unsatisfactory because the vertical scale of the circulation then depends crucially on the value of the eddy viscosity; an example of this is given in section 1.3.

Baroclinic flows forced by moving wind-stress patterns -- a linear analysis

This subsection is a digression which will reinforce the conclusions based on the linear initial value problem. Following Lighthill (1967) I shall consider the steady flow produced by a uniformly translating forcing pattern:

$$w(x,y,o,t) = w_0 \exp(ik\tilde{x} + ily)$$

where

$$\tilde{x} = x - Ut.$$

By considering the limit  $U \gg 0$ , Lighthill was able to recover information about the steady state of the wind-driven flow in a homogeneous ocean. In particular he showed that the Sverdrup balance obtained when  $(k^2 + l^2)U/\beta \ll 1$  (cf (1.7)) and he also obtained the correct boundary condition (no mass flux at an eastern boundary).

It is straightforward to repeat Lighthill's calculation in a constant  $N$  ocean. The linearized potential vorticity equation with boundary conditions is:

$$\frac{\partial}{\partial t} [\nabla^2 \psi + F\psi_{zz}] + \beta \psi_x = 0 \quad (2.10a)$$

$$z = 0: \quad w = -f_0^{-1} F \psi_{zt} = w_0 \exp[ik\tilde{x} + ily] \quad (2.10b)$$

$$z = -H: \quad w = -f_0^{-1} F \psi_{zt} = 0 \quad (2.10c)$$

The solution of (2.10) is:

$$\psi = \frac{if_0 w_0}{kpFU} \frac{\cosh[p(z+H)]}{\sinh[pH]} e^{i(k\tilde{x} + ly)} \quad (2.11a)$$

if:  $F_p^2 = k^2 + \lambda^2 + (\beta/U) > 0$  (2.11b)

and is:

$$\psi = -\frac{if_0 w_0}{kmfU} \frac{\cos[m(z+H)]}{\sin[mH]} e^{i(k\tilde{x} + \lambda y)} \quad (2.12a)$$

if:  $F_m^2 = -k^2 - \lambda^2 - (\beta/U) > 0$ . (2.12b)

We will concentrate on the case of an eastward moving source so that  $U > 0$  and only the solution (2.11) is relevant. The case of a westward moving source is more complicated but can be treated in a similar fashion.

First note that the barotropic limit discussed by Lighthill is obtained from (2.11a) when:

$$pH \ll 1.$$

This means that:

$$k^2 + \lambda^2 + (\beta/U) \gg f_0/NH$$

so that, somewhat surprisingly, large scale forcing ( $k^2 + \lambda^2 > 0$ ) does not necessarily produce a barotropic response. In fact the limit  $k^2 + \lambda^2 > 0$  is just the limit  $\epsilon^2 > 0$  discussed in section 1. In this case the relative vorticity contributes negligibly to the potential vorticity and from (2.11b) the vertical length scale is:

$$p^{-1} = \frac{f_0}{N} \sqrt{\frac{U}{\beta}}. \quad (2.13)$$

As we decrease  $U$ , so that the steady limit is approached, the vertical scale (2.13) decreases and the solution (2.11a) simplifies to the "top-trapped" form:

$$\psi = \frac{iN w_0}{k \sqrt{\beta U}} \exp\left[\frac{N}{f_0} \sqrt{\frac{\beta}{U}} z\right] e^{i(k\tilde{x} + \lambda y)}. \quad (2.14)$$

Note how (2.14) satisfies the Sverdrup balance (1.2). We have solved (2.10) for the simple case of a uniformly translating sinusoidal forcing. Patterns with more interesting spatial structure can be constructed with Fourier analysis; if

$$w(\tilde{x}, y) = \iint dk dl w_0(k, l) e^{i(k\tilde{x} + ly)}$$

then from (2.14):

$$\psi = \frac{iNw_0}{\sqrt{\beta U}} \exp\left[\frac{N}{f_0} \sqrt{\frac{\beta}{U}} z\right] \iint dk dl k^{-1} w_0(k, l) e^{i(k\tilde{x} + ly)}. \quad (2.15)$$

Lighthill (1967) shows that the behaviour of the transform (2.15) in the far field is dominated by the singularity  $k^{-1}$  in the integrand. To invert the transform this singularity is shifted off the real axis by switching on the forcing at  $t = -\infty$  with a slow growth proportional to  $e^{\delta t}$ . This leads to the replacement

$$kU \rightarrow kU + i\delta$$

so that in (2.15) is also proportional to  $e^{\delta t}$ . Thus the singularity in (2.15) is in the lower half  $k$ -plane and so is enclosed by the semi-circular inversion contour only when  $\tilde{x} < 0$ , see figure 3. When  $\tilde{x} > 0$  the contour encloses no singularities, the response is exponentially small and so the usual boundary condition of no motion to the East of the forcing pattern is recovered. The final expression is

$$\psi \sim \begin{cases} 0 & \text{as } x - Ut \rightarrow +\infty \\ -\frac{Nw_0}{\beta U} \exp\left\{\frac{N}{f_0} \sqrt{\frac{\beta}{U}} z\right\} \int_{\tilde{x}}^{\infty} w(x_1, y) dx_1 & \text{as } x - Ut \rightarrow -\infty. \end{cases}$$

The novel aspect of the calculation above is the vertical structure

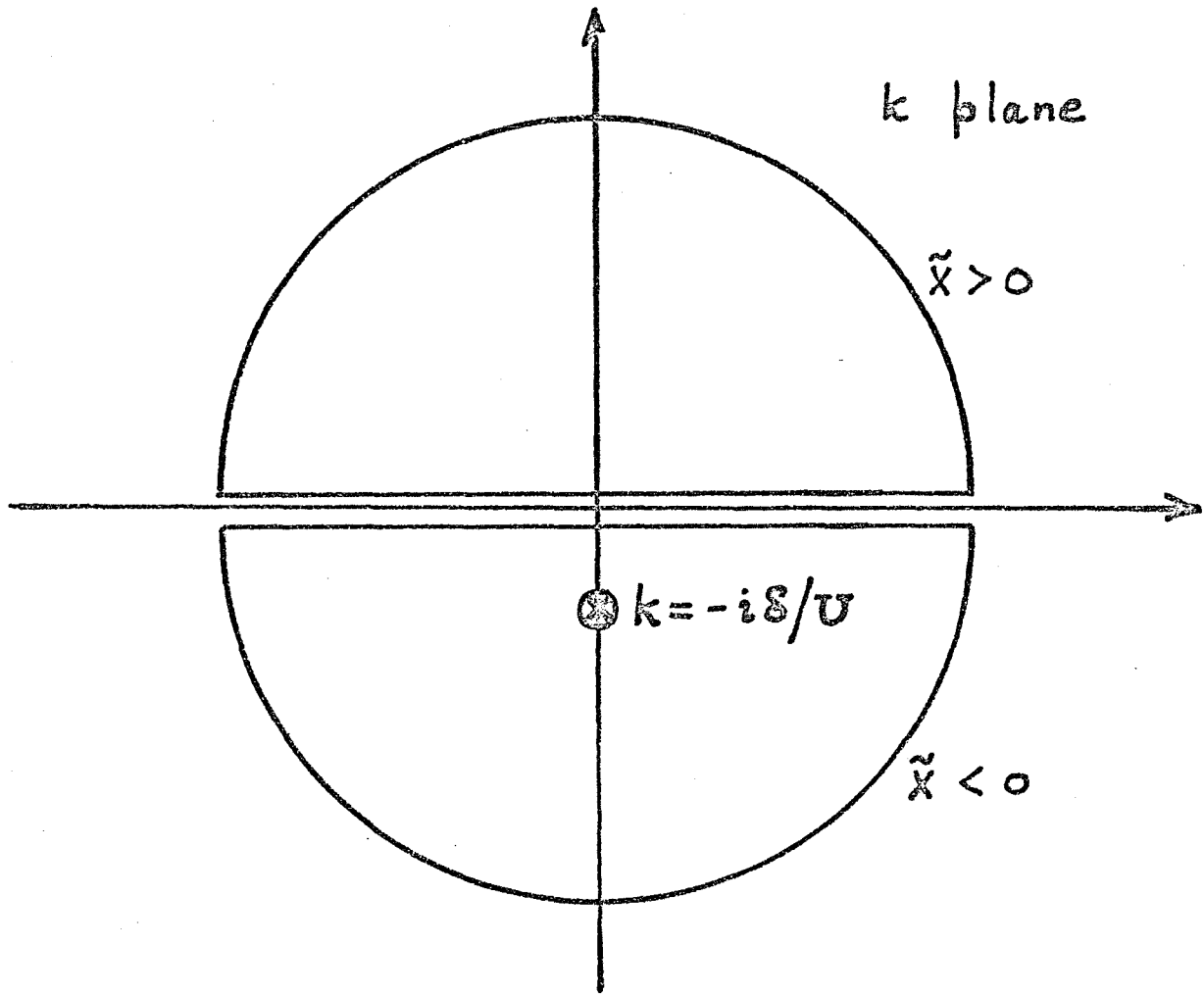


Figure 3. The path of integration in the complex  $k$ -plane used to evaluate the integral (2.15). The singularity is enclosed only when  $\tilde{x} < 0$ .

of the response; note how (2.9) is recovered if  $U > 0$  since:

$$\lim_{n \rightarrow 0} \frac{1}{n} e^{nz} = \delta(z-).$$

Once again a linear theory has given an unphysical answer to the vertical structure problem.

### Nonlinear effects -- a two layer quasigeostrophic model

A simple model which economically displays the important effects of nonlinearity is the well known two layer model. The quasigeostrophic equations in this case are

$$q_{1t} + J(\psi_1, q_1) = f_0 w_E(x, y, t) / H_1 \quad (2.16a)$$

$$q_{2t} + J(\psi_2, q_2) = 0 \quad (2.16b)$$

where

$$q_1 = \nabla^2 \psi_1 + \beta y + F(\psi_2 - \psi_1) \quad (2.17a)$$

$$q_2 = \nabla^2 \psi_2 + \beta y + F(\psi_1 - \psi_2) \quad (2.17b)$$

$$F = f_0^2 / g' H_1 \quad (2.17c)$$

For simplicity the nonessential assumption of equal layer depths has been made.

The system (2.16) has two linear wave modes:

- (i) the barotropic mode which crosses an ocean basin in about a week
- (ii) the baroclinic mode which crosses an ocean basin in about a year.

Thus if large scale forcing is "switched on" impulsively in (2.16) the barotropic flow is established very rapidly. The baroclinic wave then has to propagate through a barotropic flow created by its faster brother.

This nonlinear effect is entirely neglected in the linear models discussed earlier in this section.

To obtain a simple equation describing this interaction suppose that the forcing is large scale, more precisely:

$$L^2 \gg f_0 W / \beta^2 H_1 . \quad (2.18)$$

This condition is equivalent to assuming that  $\epsilon^2$  defined in (1.7) is much less than one;  $U$  is related to the scale estimate of  $w_E$ , denoted by  $W$ , by assuming that the Sverdrup balance holds. The inequality (2.18) ensures that the relative vorticity is negligible in (2.17). Thus the barotropic mode:

$$2\psi_B = \psi_1 + \psi_2 \quad (2.19)$$

satisfies the Sverdrup balance:

$$2\beta\psi_{Bx} = f_0 w_E / H_1 . \quad (2.20)$$

The above result can be used to rewrite (2.16b) in terms of one unknown,  $\psi_2$ :

$$2F\psi_{2t} + J(\hat{q}, \psi_2) = 0 \quad (2.21a)$$

$$\hat{q} = \beta y + 2F\psi_B \quad (2.21b)$$

Equation (2.21a) is just a linear advection equation for  $\psi_2$ , even though the nonlinear term  $J(\psi_1, \psi_2)$  has been retained. If this term is neglected the linear problem:

$$2F\psi_{2t} - \beta\psi_{2x} = 0 \quad (2.22)$$

discussed by Rhines (1977) and Anderson and Gill (1975) is recovered. The initial condition for (2.21a) and (2.22) is that the baroclinic mode is initially zero or equivalently:

$$\psi_2(x, y, 0) = \psi_B(x, y) \quad (2.23)$$

The simplest method of solving (2.21) is to introduce a new coordinate system:

$$\xi = p(x, y) \quad (2.24a)$$

$$\mu = q(x, y) \quad (2.24b)$$

in terms of which:

$$\frac{\partial}{\partial x} = \left(\frac{\partial p}{\partial x}\right) \frac{\partial}{\partial \xi} + \left(\frac{\partial q}{\partial x}\right) \frac{\partial}{\partial \mu}$$

$$\frac{\partial}{\partial y} = \left(\frac{\partial p}{\partial y}\right) \frac{\partial}{\partial \xi} + \left(\frac{\partial q}{\partial y}\right) \frac{\partial}{\partial \mu}$$

so that:

$$J(\hat{q}, \psi_2) = J(\hat{q}, p) \frac{\partial \psi_2}{\partial \xi} \quad (2.25)$$

$\hat{q}$  is known and so it is convenient to define  $p$  by

$$J(p, \hat{q}) = -\beta \quad (2.26)$$

so that (2.21a) is

$$2F\psi_{2t} - \beta\psi_{2\xi} = 0 \quad (2.27)$$

which is formally identical to (2.22).

This formal equivalence does not mean that the solutions of (2.22) and (2.27) are qualitatively similar. The easiest way to appreciate the possible differences is to solve (2.27) with a simple form for  $\hat{q}$ . To this end consider the forcing function:

$$w_E = \begin{cases} \alpha x & \text{if } x^2 + y^2 < R^2 \\ 0 & \text{otherwise} \end{cases} \quad (2.28)$$

which produces the barotropic flow:

$$\psi_B = \begin{cases} (G/F)(R^2 - x^2 - y^2) & \text{if } x^2 + y^2 < R^2 \\ 0 & \text{otherwise} \end{cases} \quad (2.29)$$

where

$$G = -\frac{\alpha f_0 F}{4\beta H_1} \quad (2.30)$$

The field  $\hat{q}$  defined in (2.21b) is then

$$\hat{q} = \begin{cases} \beta y + G(R^2 - x^2 - y^2) & \text{if } x^2 + y^2 < R^2 \\ \beta y & \text{otherwise} \end{cases} \quad (2.27)$$

The  $\hat{q}$  contours given by (2.27) are sketched in figure 5. Inside the circle  $x^2 + y^2 = R^2$  the contours are circles or arcs of circles centered on  $(0, \beta/2G)$ . If this point is inside the circle  $x^2 + y^2 = R^2$  some of  $\hat{q}$  contours are closed; the appearance of closed  $\hat{q}$  contours when the forcing is sufficiently strong is a major qualitative change introduced by nonlinearity.

In solving the initial value problem posed by (2.23) and (2.27) one must consider the regions of open and closed  $\hat{q}$  contours separately.

Consider the open contour case first. This case is qualitatively similar to the linear problem (2.22) and (2.23). The solution of this linear problem is

$$\Psi_2 = \Psi_B(x + (\beta/2F)t, y) \quad (2.28)$$

which shows how the initial disturbance in the lower layer propagates westward out from under the forcing region as  $t \rightarrow \infty$ . If one waits long enough the lower layer comes to rest directly below the forcing region. The solution of the nonlinear problem with open  $\hat{q}$  contours is qualitatively similar; the wavefront no longer advances uniformly as in (2.28), but instead is distorted in a way which reflects the underlying  $q$  geometry. Eventually, however, it escapes westward and leaves the fluid directly under the forcing region quiescent.

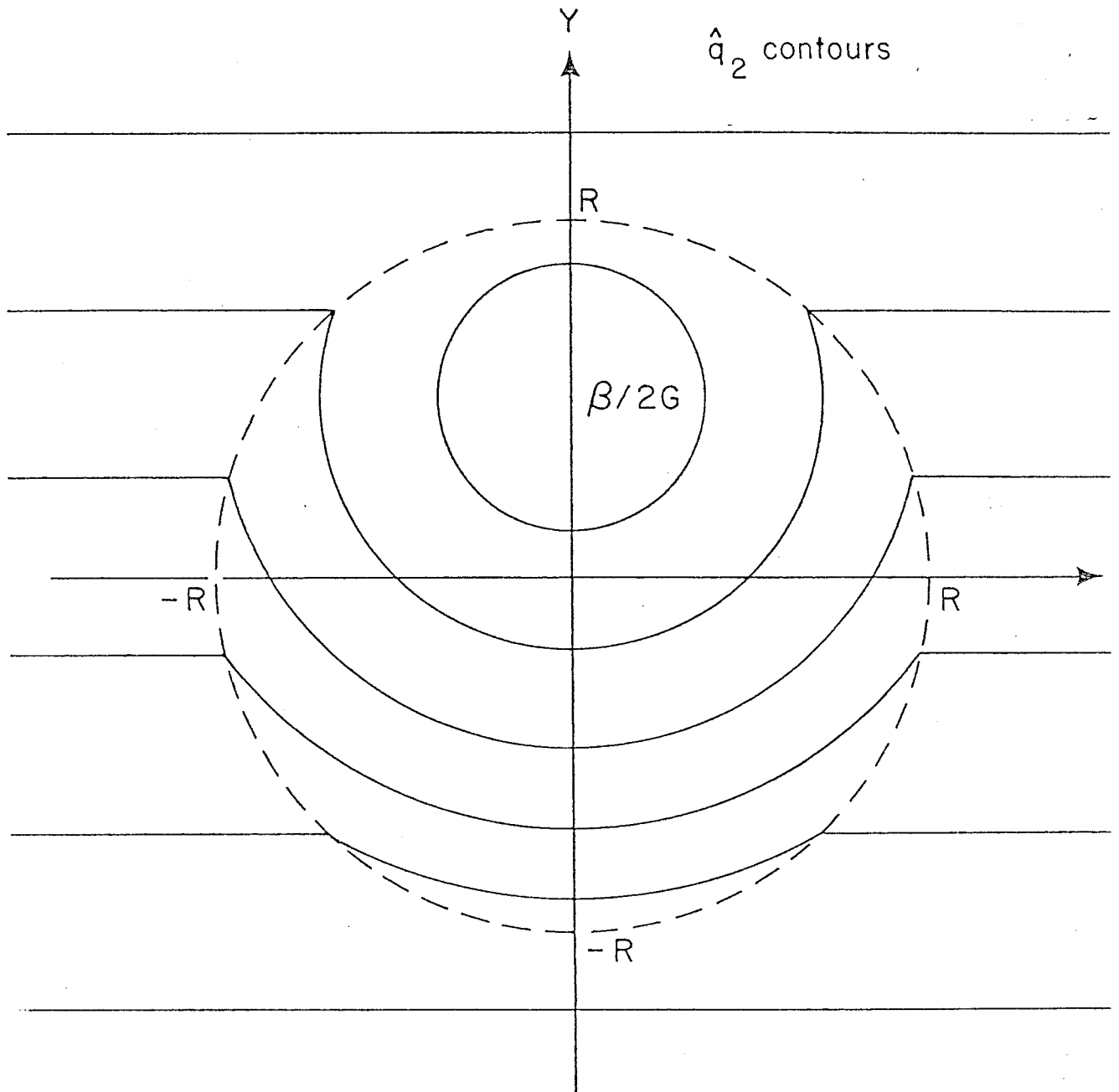


Figure 5. The function  $\hat{q}$  is given by (2.27). Inside the circle  $x^2 + y^2 = R^2$  the contours are circles or arcs of circles centered on  $\beta/2G$ .

Now consider the closed contour case. Since this interesting case has not been discussed in the literature I shall construct an explicit solution based on (2.27). It is obviously convenient to use polar coordinates centered on  $(0, \beta/2G)$ , see figure 5. Thus inside the closed region in figure 5 let:

$$\tilde{x} = x$$

$$\tilde{y} = y - (\beta/2G)$$

then define polar coordinates

$$\tilde{r}^2 = \tilde{x}^2 + \tilde{y}^2$$

$$\tan \tilde{\theta} = \tilde{x}/\tilde{y}$$

so that

$$\hat{q} = G(R^2 - \tilde{r}^2) + (\beta^2/4G)$$

Equations (2.21a) and (2.23) are then

$$F\psi_{2t} - G\psi_{2\tilde{\theta}} = 0$$

$$\psi_2(x, y, 0) = (G/F)[R^2 - \tilde{r}^2 - (\beta/G)\tilde{r} \sin \tilde{\theta} - \beta^2/4G]$$

the solution of which is:

$$\psi_2 = (G/F)[R^2 - \tilde{r}^2 - (\beta/G)\tilde{r} \sin \{\tilde{\theta} + (G/F)t\} - \beta^2/4G] \quad (2.29)$$

Thus  $\psi_2$  oscillates indefinitely inside the closed  $\hat{q}$  contours which is in strong contrast to the behaviour in the open regions where  $\psi_2$  eventually vanishes. This oscillation is clearly a general feature of closed  $\hat{q}$  contours and is not an artifact of the simple choice of forcing function (2.28).

Physically speaking the appearance of closed  $\hat{q}$  contours means that the barotropic flow is strong enough to successfully oppose the westward propagation of the baroclinic Rossby wave; the wave is trapped inside the closed  $\hat{q}$  regions. The unending oscillation in (2.29) clearly suggests the need to include dissipation.

The nonlinear model is interesting because it shows how the tendency of the baroclinic Rossby wave to bring the lower layer to rest can be combated by barotropic advection. Moreover it focuses our attention on closed  $\hat{q}$  contours. Much of this thesis is concerned with the steady flows in these closed regions. The time dependent problem discussed here emphasizes the importance of dissipation and shows that an initial value problem does not suggest a particular steady solution in such regions.

### 3. Linear, Steady, Dissipative Circulation Problems

Introduction - dissipation smooths the singular current distributions suggested by the linear initial value problem.

The vertically singular distributions of wind-driven flow found in the last section by solving linear problems can be made more acceptable mathematically (but not perhaps physically) by including some dissipation which smears out the delta function and smoothly distributes the currents in the vertical. The problem then is that the vertical scale of the circulation depends on the unknown eddy diffusivities. This is in contradistinction to the vertical scale (1.13) derived in section 1 by considering the nonlinear vortex stretching process. The theory I present in chapters 2 and 3 is based on this nonlinear process and naturally gives (1.13) as the relevant vertical scale. The inadequacies of the linear, dissipative models discussed in this section are instructive because they will eventually be used to highlight the important differences between flow in regions threaded by blocked geostrophic contours and flow in regions where the contours close.

#### A two layer model with interfacial drag

The model described here is similar to that of Welander (1968). It differs from his model in that I use the quasigeostrophic approximation and obtain exact solutions, whereas Welander allowed the interface to undergo large vertical excursions and used boundary layer analysis. Philosophically this section is also different from Welander: he thought of his two layers as comprising the full vertical extent of the ocean. He assumed that the lower layer was much thicker than the upper layer and

this allowed him to rigorously neglect the vortex stretching nonlinearity since the lower layer is then at rest. I consider the two layer model in this section to comprise the upper thermocline waters which lie above a much deeper, quiescent lowest layer. Thus, roughly speaking, the two layers in this model correspond to Welander's upper layer. The neglect of the nonlinearity in this situation is entirely ad hoc and unjustified; the principal goal of this section is to make this point very clearly by evaluating the neglected nonlinear terms with the linear solution and showing they are as large as the terms retained. Thus the linear problem solved by Welander is, in a sense, unstable: when the vertical resolution is increased by adding more layers, terms which were previously negligible become important and the nature of the solution changes qualitatively.

For future reference the 3 layer quasigeostrophic equations are

$$\begin{aligned} J(\psi_1, q_1) &= f_0 H_1^{-1} w_E + \text{dissipation} \\ J(\psi_2, q_2) &= \text{dissipation} \\ J(\psi_3, q_3) &= \text{dissipation} \end{aligned}$$

the potential vorticities are

$$\begin{aligned} q_1 &= f + \nabla^2 \psi_1 + (f_0^2/g'H_1)(\psi_2 - \psi_1) \\ q_2 &= f + \nabla^2 \psi_2 + (f_0^2/g'H_2)(\psi_1 - \psi_2) + (f_0^2/g''H_2)(\psi_3 - \psi_2) \\ q_3 &= f + \nabla^2 \psi_3 + (f_0^2/g''H_3)(\psi_2 - \psi_3) \end{aligned}$$

where

$$f = f_0 + \beta y$$

is the Coriolis frequency.  $H_i$  is the mean thickness of the  $i$ 'th layer

and the reduced gravities  $g'$  and  $g''$  are:

$$g' = g \left( \frac{\rho_2 - \rho_1}{\rho_0} \right) \quad \text{and} \quad g'' = g \left( \frac{\rho_3 - \rho_2}{\rho_0} \right)$$

If  $H_3 \gg H_1, H_2$ , so that  $\psi_3 = 0$ , and  $g' = g''$ , then the 3 layer equations simplify and become an equivalent 2 layer system:

$$J(\psi_1, q_1) = f_0 H_1^{-1} w_E + v_1 \nabla^2 (\psi_2 - \psi_1) \quad (3.1a)$$

$$J(\psi_2, q_2) = v_2 \nabla^2 (\psi_1 - \psi_2) - \delta \nabla^2 \psi_2 \quad (3.1b)$$

where

$$q_1 = \nabla^2 \psi_1 + \beta y + (f_0^2 / g' H_1) (\psi_2 - \psi_1)$$

$$q_2 = \nabla^2 \psi_2 + \beta y + (f_0^2 / g' H_2) (\psi_1 - 2\psi_2)$$

$\delta$  = bottom drag or drag on a motionless lowest layer

$v_1$  and  $v_2$  are interfacial drag coefficients

The barotropic mode equation (the two layer analog of a vertical integral of the potential vorticity equation) is obtained by forming the sum  $H_1$  (3.1a) +  $H_2$  (3.1b). Because the interfacial stresses only transfer momentum between the layers and do not act as sources or sinks for vertically integrated momentum:

$$H_1 v_1 = H_2 v_2 \quad (3.2)$$

and the interfacial stress terms cancel leaving:

$$\beta H \frac{\partial \psi_B}{\partial x} = f_0 w_E - \delta H_2 \nabla^2 \psi_2 \quad (3.3)$$

where

$$H = H_1 + H_2$$

$$H \psi_B = H_1 \psi_1 + H_2 \psi_2$$

To obtain (3.3) the relative vorticity was neglected using the  $U/\beta L^2 \ll 1$  approximation. Note how the nonlinear vortex stretching terms in (3.1a,b) cancel when the barotropic mode equation is formed. Thus although these terms may be large in the ocean interior they do not appear in the vertically integrated potential vorticity equation. If the bottom stress term in (3.3) is neglected the Sverdrup balance (1.2) is recovered. I shall return to the simple result (3.3) when I discuss the nonlinear problem. For the moment I shall solve the linear version of (3.1a,b):

$$\beta \psi_{1x} = f_0^w E / H_1 - v_1 \nabla^2 \psi_1 + v_1 \nabla^2 \psi_2 \quad (3.4a)$$

$$\beta \psi_{2x} = \quad + v_2 \nabla^2 \psi_1 - (v_2 + \delta) \nabla^2 \psi_2 \quad (3.4b)$$

The above system can be reduced to a very familiar problem by forming a linear combination: (3.4a) +  $\gamma$  (3.4b). The multiplier  $\gamma$  is chosen to ensure that only one linear combination of  $\psi_1$  and  $\psi_2$  appears. The sum is:

$$\beta (\psi_1 + \gamma \psi_2)_x = (f_0^w E / H_1) - \nabla^2 \left\{ (v_1 - \gamma v_2) \psi_1 + (-v_1 + v_2 \gamma + \delta \gamma) \psi_2 \right\} \quad (3.5)$$

and the condition that the linear combinations on the left and right hand sides be identical is

$$v_2 \gamma^2 + (v_2 + \delta - v_1) \gamma - v_1 = 0 \quad (3.6)$$

The quadratic (3.6) has two roots:

$$\gamma_+ = \frac{1}{2v_2} \left\{ (v_1 - \delta - v_2) + \sqrt{\Delta} \right\}$$

$$\gamma_- = \frac{1}{2v_2} \left\{ (v_1 - \delta - v_2) - \sqrt{\Delta} \right\}$$

$$\begin{aligned}\Delta &= (v_2 + \delta - v_1)^2 + 4v_1v_2 \\ &= \delta^2 + 2\delta(v_2 - v_1) + (v_1 + v_2)^2\end{aligned}$$

This procedure has transformed (3.4) into two uncoupled Stommel (1948) circulation problems for the functions:

$$\theta_+ = \psi_1 + \gamma_+ \psi_2 \quad (3.7a)$$

$$\theta_- = \psi_1 + \gamma_- \psi_2 \quad (3.7b)$$

In terms of  $\theta$ , (3.5) is:

$$\beta \theta_{\pm x} = (f_0^w w_E / H_1) - (v_1 - \gamma_{\pm} v_2) \nabla^2 \theta_{\pm} \quad (3.8)$$

so that these two problems have identical Sverdrup interiors but different frictional boundary layers. The solution is shown schematically in figure 4.

The fact that the Sverdrup interiors are identical is significant since

$$\begin{aligned}\psi_2 &= (\gamma_+ - \gamma_-)^{-1} (\theta_+ - \theta_-) \\ &\approx 0 \quad \text{in the Sverdrup interior}\end{aligned} \quad (3.9)$$

Equation (3.9) is a result which is by now familiar from section 2: the subsurface layers of the Sverdrup interior are at rest. More precisely, it can easily be shown that  $\psi_2$  is order  $\nu$  relative to the total Sverdrup transport. Thus when the vertical resolution of Welander's model is increased by the addition of an extra layer in the thermocline, most of the Sverdrup flow migrates to the uppermost layer.

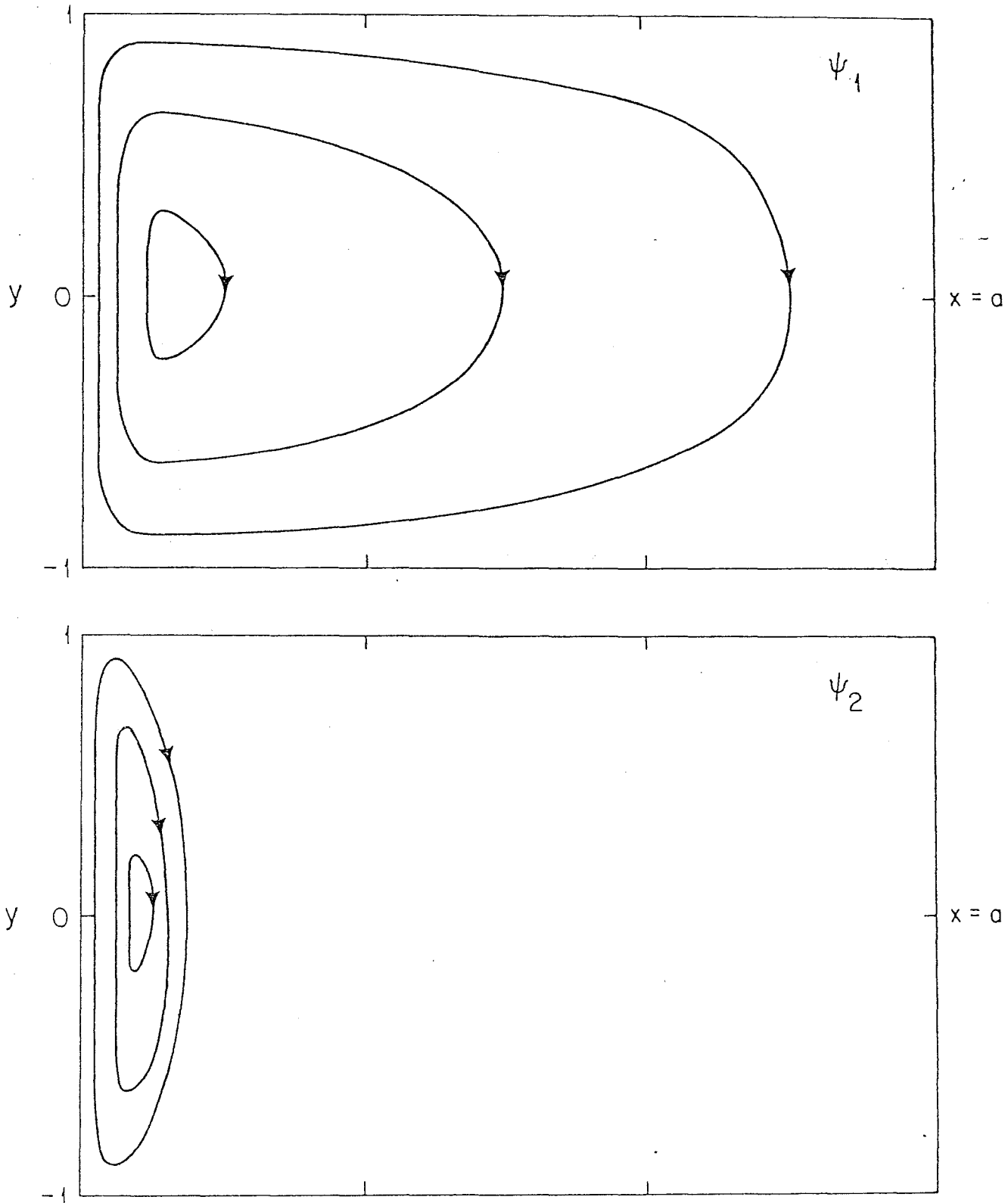


Figure 4. The streamfunctions  $\psi_1$  and  $\psi_2$ .  $\psi_2$  is zero in the interior, all the Sverdrup transport is in the upper layer.

The fact that  $\theta_+$  and  $\theta_-$  are different in the frictional boundary layers is also significant since the neglected nonlinear term is:

$$\begin{aligned} J(\psi_1, \psi_2) &= (\gamma_- - \gamma_+)^{-1} J(\theta_+, \theta_-) \\ &= \text{order one in the boundary layer.} \end{aligned}$$

An important exception to the above is the case considered by Welander:

$$\frac{v_1}{v_2} = \frac{H_2}{H_1} \gg 1$$

which implies that  $(\gamma_- - \gamma_+)^{-1} = O(v_2/v_1) = O(H_1/H_2)$  so that the nonlinearity is negligible even in the boundary layer.

Continuously stratified models with various dissipative mechanisms.

Finally to complete this section I shall discuss some continuously stratified models in which the wind driven flow is vertically distributed by various dissipative mechanisms. The rather obvious point of this subsection is that the vertical scale depends on the unknown eddy diffusivities.

For simplicity I consider a constant  $N$  ocean in which the steady, linear planetary momentum and density equations with dissipation are

$$\begin{aligned} +fu &= -f_0 \psi_y + \mu(v_{xx} + v_{yy}) + \nu v_{zz} \\ -fv &= -f_0 \psi_x + \mu(u_{xx} + u_{yy}) + \nu u_{zz} \\ wN^2 &= -\delta b + \lambda(b_{xx} + b_{yy}) + \kappa b_{zz} \end{aligned}$$

The equations above were written down primarily to define the various eddy diffusivities  $\mu$ ,  $\nu$ ,  $\delta$ ,  $\lambda$  and  $\kappa$ . The potential vorticity equation is then

$$\frac{\beta \psi_x}{(1)^x} = \frac{-\delta F \psi}{(2)^{zz}} + \frac{(\nu + \lambda F) \nabla^2 \psi}{(3)} + \frac{\kappa F \psi}{(4)^{zzzz}} + \frac{\mu \nabla^4 \psi}{(5)} \quad (3.10)$$

where  $\nabla^2$  above is the horizontal Laplacian and  $F$  is defined in (1.6c).

If there was any reason to believe one of the dissipative mechanisms above was particularly realistic, (3.10) could easily be solved exactly. One can however simply relate the vertical and horizontal length scales by straightforward scale analysis of (3.10). Suppose, for example, that the dominant diffusive process is thought to be vertical density diffusion. This would suggest a balance between terms (1) and (4) in (3.10) and would lead to:

$$\text{vertical length scale} = \left\{ \kappa F (\text{horizontal length scale}) / \beta \right\}^{1/4}$$

The above is the familiar Linenkin scale;  $\kappa$  can be adjusted to make it reasonable.

#### 4. The Importance of Closed Geostrophic Contours

Introduction - the dynamics of closed and blocked geostrophic contours are compared and contrasted.

From the previous sections one is led to conclude that there is a strong tendency for the wind driven circulation to be concentrated at the surface. This result follows from a fundamental constraint imposed by conservation of potential vorticity and density. Because both these quantities are conserved in an unforced dissipationless interior, a fluid element is confined to a geostrophic contour (i.e. a curve defined by the intersection of a potential vorticity surface with a density surface). Rhines and Holland (1979) and Rooth, Stommel and Veronis (1978) realized that this implied that if a geostrophic contour struck a coastal boundary, where a no mass flux condition is imposed, then the fluid must be motionless at all interior points threaded by that contour. The latter authors couched their arguments in terms of layered models but it is clear that this restriction is unnecessary.

This argument explains why the linear models of sections 2 and 3 produced top-trapped wind driven flows: in these models the potential vorticity is just  $\beta y$  and all the geostrophic contours are blocked. Thus the steady motion is confined to the uppermost layer which is directly forced by the wind.

Clearly one way of avoiding the severe constraints imposed by blocked geostrophic contours is for the flow to oppose the  $\beta$ -effect with vortex stretching and close the contours in the basin. In this section I shall discuss some simple nonlinear models in which this is the case. The

nonlinear initial value problem of section 2 has already been used to illustrate some of the consequences of closed geostrophic contours. One point that was not emphasized in that section is that  $\hat{q}$  defined in (2.21b) is essentially the field of geostrophic contours in the lower layer. The solution (2.29) shows how closed geostrophic contours "trap" Rossby waves and prevent an inviscid system reaching a steady state. The simple models discussed in this section (especially the three layer model) were suggested by Rhines (personal communication).

#### A two layer quasigeostrophic model

As in section 3 the two layers in this model are thought of as being thermocline layers above a much deeper, motionless abyssal layer. The quasigeostrophic equations are

$$J(\psi_1, q_1) = (f_0 w_E / H_1) \quad (4.1a)$$

$$J(\psi_2, q_2) = 0 \quad (4.1b)$$

where the potential vorticities are (assuming  $\epsilon^2 \ll 1$ ):

$$q_1 = \beta y + \frac{f_0^2}{g'H_1} (\psi_2 - \psi_1) \quad (4.2a)$$

$$q_2 = \beta y + \frac{f_0^2}{g''H_2} (\psi_1 - \psi_2) - \frac{f_0^2}{g''H_2} \psi_2 \quad (4.2b)$$

In section 3 I assumed that  $g' = g''$ ; this assumption is not made here.

For simplicity I shall use the simple forcing function introduced in section 2:

$$w_E = \begin{cases} \alpha x & \text{if } x^2 + y^2 < R^2 \\ 0 & \text{otherwise} \end{cases} \quad (4.3)$$

This simple choice for the forcing produces a simple barotropic response obtained by solving (3.3) with  $\delta = 0$ :

$$\psi_B = \begin{cases} -\frac{f_0 \alpha}{2\beta H} \{R^2 - x^2 - y^2\} & \text{if } x^2 + y^2 < R^2 \\ 0 & \text{otherwise} \end{cases} \quad (4.4)$$

where  $H\psi_B = H_1\psi_1 + H_2\psi_2$  and  $H = H_1 + H_2$ .

Note that since:

$$\int_{-\infty}^{\infty} w_E dx = 0$$

the barotropic streamlines close naturally and it is not necessary to append Western boundary layers.

Once  $\psi_B$  is known we can rewrite (4.2b) as:

$$q_2 = \beta y + \frac{f_0^2 H}{g^1 H_1 H_2} \psi_B - f_0^2 \left( \frac{1}{g^1 H_1} + \frac{1}{g^1 H_2} \right) \psi_2 \quad (4.5)$$

Now from (4.1b):

$$q_2 = Q(\psi_2) \quad (4.6)$$

which is just a statement that flow is along geostrophic contours. From (4.5) and (4.6) it follows that  $q_2$  and  $\psi_2$  are functions of the known quantity:

$$\hat{q}_2 = \beta y + \frac{f_0^2 H}{g^1 H_1 H_2} \psi_B \quad (4.7)$$

which is familiar from the nonlinear initial value problem of section 2.

The significance of  $\hat{q}_2$  can be understood by considering two limits. First suppose that the forcing is weak in which case:

$$\hat{q}_2 = \beta y$$

This means that the geostrophic contours are all blocked by coastal boundaries and  $\psi_2 = 0$  everywhere in agreement with section 2. On the other hand if the forcing is strong then:

$$\hat{q}_2 \propto \psi_B$$

and if the  $\psi_B$  contours close, as in (4.4), then the geostrophic contours also close.

The transition between the two limiting cases can be appreciated by explicitly calculating  $\hat{q}_2$  using (4.4); if  $x^2 + y^2 < R^2$  then:

$$\hat{q}_2 = \beta y + G(R^2 - x^2 - y^2) \quad (4.8)$$

where

$$G = -\left(\frac{f_0 \alpha}{2\beta H}\right) \left(\frac{f_0^2 H}{g' H_1 H_2}\right)$$

It follows that if  $x^2 + y^2 < R^2$  the  $\hat{q}_2$  contours are circles or arcs of circles while if  $x^2 + y^2 > R^2$  the  $\hat{q}_2$  contours are just  $\beta y$  contours i.e.:

$$\left(y - \frac{\beta}{2G}\right)^2 + x^2 = \frac{\beta^2}{4G^2} + R^2 - \frac{\hat{q}_2}{G} \quad \text{if } x^2 + y^2 < R^2$$

$$\beta y = \hat{q}_2 \quad \text{otherwise}$$

The contours are sketched in figure 5 with  $\alpha < 0$  or  $G > 0$ . The closed contours exist only if the forcing is sufficiently strong, specifically only if

$$\left|\frac{2G}{\beta}\right| \geq R^{-1} \quad (4.9)$$

Using the equivalences:

$$N^2 \sim g'/H$$

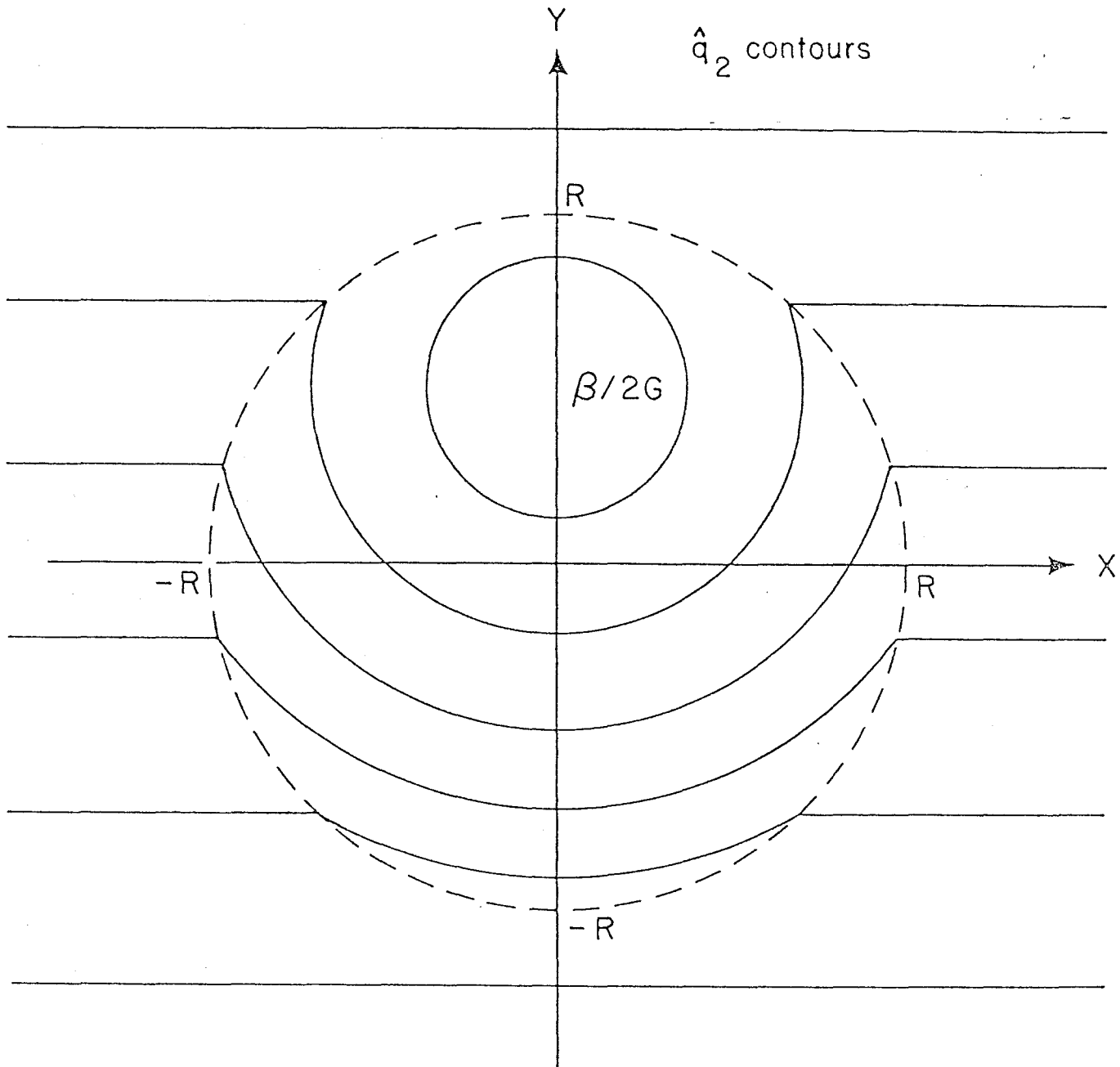


Figure 5. The contours of the function  $\hat{q}_2$  defined in (4.7). If  $\psi_B$  is given by (4.4) the contours are circles or arcs of circles centered on  $\beta/2G$ .

$$W \sim \alpha R$$

$$l^3 \sim H_1 H_2 H$$

it follows that (4.9) is equivalent to (1.13a) so that this solution is a specific example of the flows discussed abstractly in section 1.

The most important point to realize is that in the region where  $\hat{q}$  contours close,  $\psi_2$  need not be zero. In fact it is arbitrary to the extent that any choice of  $Q$  in (4.6) is permissible; within the context of an eddyless inviscid theory, where the right hand side of (4.1b) is identically zero, there is no preferred relation between  $\psi_2$  and  $q_2$ . A major theme of chapters 2 and 3 is that to determine  $Q$  we must consider the small nonconservative processes which should appear on the right hand side of (4.1b). As a first approximation these are negligible and we get (4.6). If the geostrophic contours are closed (i.e. if the forcing is sufficiently strong) we are not compelled by no flux boundary conditions to conclude that  $\psi_2$  is zero. The problem of determining  $Q$  in this case is discussed in chapter 2. Ironically, even though there are an infinite number of steady solutions in the closed regions, the nonlinear initial value problem of section 2 fails to "find" any of them; see (2.29).

#### A three layer quasigeostrophic model

In order to see how the results above depend upon the vertical resolution I shall discuss the closure of geostrophic contours using a three layer quasigeostrophic model. For simplicity I shall assume the layers have equal mean thicknesses,  $H_1 = H_2 = H_3$ , and the density jumps are also equal,  $g' = g''$ . The quasigeostrophic equations are then

$$J(\psi_1, q_1) = f_0 w_E / H_1 \quad (4.10a)$$

$$J(\psi_2, q_2) = 0 \quad (4.10b)$$

$$J(\psi_3, q_3) = 0 \quad (4.10c)$$

where the potential vorticities are

$$q_1 = \beta y + F(\psi_2 - \psi_1) \quad (4.11a)$$

$$q_2 = \beta y + F(\psi_1 - 2\psi_2 + \psi_3) \quad (4.11b)$$

$$q_3 = \beta y + F(\psi_2 - \psi_3) \quad (4.11c)$$

where

$$F = \frac{f_0^2}{g'H_1}.$$

If (4.10a,b,c) are added the equation for the barotropic streamfunction:

$$3\psi_B = \psi_1 + \psi_2 + \psi_3$$

results. If  $w_E$  is given by (4.3), then when  $R^2 < x^2 + y^2$ :

$$\psi_B = -\frac{f_0 \alpha}{6\beta H_1} (R^2 - x^2 - y^2) \quad (4.12)$$

and  $\psi_B$  is zero otherwise.

Rhines (personal communication) first observed that using  $3\psi_B = \psi_1 + \psi_2 + \psi_3$ , (4.11b) can be written as:

$$q_2 = \beta y + 3F\psi_B - 3F\psi_2 \quad (4.13)$$

But from (4.10b)

$$q_2 = Q_2(\psi_2) \quad (4.14)$$

so that (4.13) implies that  $q_2$  and  $\psi_2$  are functions of

$$q_2 = \beta y + 3F\psi_B \quad (4.15)$$

This solution is obviously very similar to that discussed using the two layer model earlier in this section. Using (4.12),  $\hat{q}_2$  can be plotted as in figure 5. The complete flow is not determined yet however -- we only know  $\psi_1 + \psi_2 + \psi_3$  and by plotting  $\hat{q}_2$  we locate a region where  $\psi_2$  may be nonzero. To make further progress we need to know  $\psi_2$ , or equivalently  $Q_2$  in (4.14), in this region where the contours close. I shall discuss the consequences of the completely arbitrary choice:

$$q_2 = a\psi_2 + b \quad \text{in the closed contours.} \quad (4.16)$$

The results of chapters 2 and 3 will give the case  $a = 0$  an almost mesmeric appeal. For the moment however regard (4.16) as a convenient ad hoc specification of  $Q_2$ .

Eliminating  $q_2$  between (4.16) and (4.13) gives  $\psi_2$  in terms of known fields:

$$\psi_2 = \frac{1}{3F + a} \left\{ \beta y + 3F\psi_B - b \right\} \quad (4.17)$$

We can now attack the bottom layer. Using (4.17), (4.11c) gives:

$$q_3 = \left( \frac{4F + a}{3F + a} \right) \beta y + \left( \frac{3F^2}{3F + a} \right) \psi_B - \left( \frac{bF}{3F + a} \right) - F\psi_3 \quad (4.18)$$

Reasoning as before we see from (4.10c) that  $\psi_3$  and  $q_3$  are functions of:

$$\hat{q}_3 = \left( \frac{4F + a}{3F + a} \right) \beta y + \left( \frac{3F^2}{3F + a} \right) \psi_B$$

Once again  $\hat{q}_3$  can be plotted; it is apparent that the  $\beta$ -effect contributes more strongly to  $\hat{q}_3$  than to  $\hat{q}_2$ , so that the region of closed  $\hat{q}_3$  contours is smaller and lies below the region of closed  $\hat{q}_2$  contours. It may be that none of the  $\hat{q}_3$  contours close, in which case there is no flow in the lowest layer. If there are some closed

$\hat{q}_3$  contours we once again have the problem of specifying a functional relationship between  $\psi_3$  and  $q_3$  (analogous to 4.16). Once this is done, either by an ad hoc choice or by considering the small dissipative processes neglected in (4.10c), (4.18) can be solved for  $\psi_3$  in terms of known fields. With  $\psi_2$ ,  $\psi_3$  and  $\psi_B$  now known,  $\psi_1$  is found from  $3\psi_B = \psi_1 + \psi_2 + \psi_3$ .

### Uniform potential vorticity in subsurface layers

As was mentioned previously, the results of chapters 2 and 3 will indicate that uniform potential vorticity in the subsurface layers is an important special case. I shall discuss the solution of this special case in detail. If  $q_2$  and  $q_3$  are constant in the regions where the geostrophic contours close, it follows that:

$$\begin{aligned} \psi_2 &= \frac{1}{F} \left( \frac{1}{3} \beta y + F \psi_B - q_2 \right) \quad \text{inside closed } \hat{q}_2 = \beta y + 3F\psi_B \text{ contours} \\ &= 0 \quad \text{otherwise} \end{aligned}$$

$$\begin{aligned} \psi_3 &= \frac{1}{F} \left( \frac{4}{3} \beta y + F \psi_B - \frac{1}{3} q_2 - q_3 \right) \quad \text{inside closed } \hat{q}_3 = \frac{4}{3} \beta y + F \psi_B \text{ contours} \\ \psi_3 &= 0 \quad \text{otherwise} \end{aligned}$$

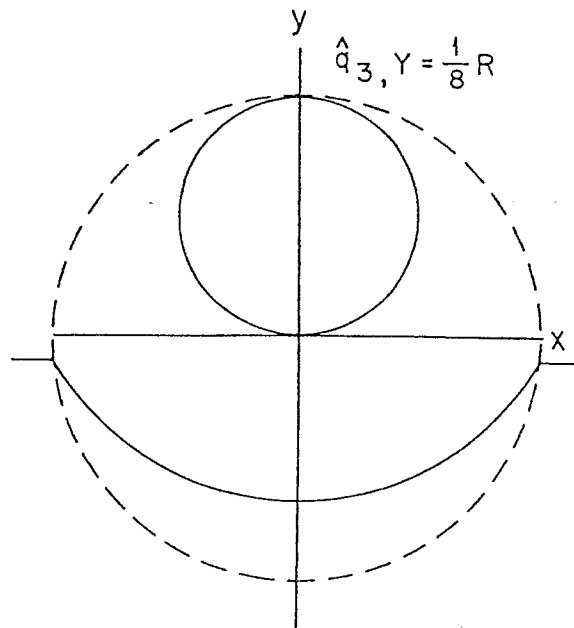
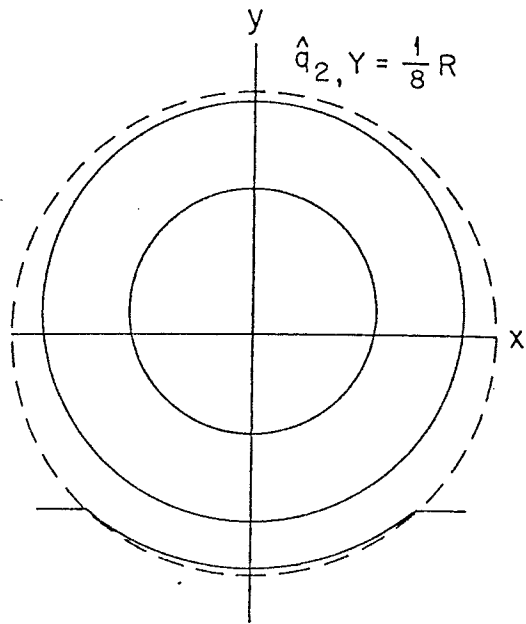
$$\psi_1 = 3\psi_B - \psi_2 - \psi_3.$$

If  $\psi_B$  is given by (4.12) it follows, as in the two layer model, that when  $x^2 + y^2 < R^2$  the  $\hat{q}_2$  contours are circles or arcs of circles

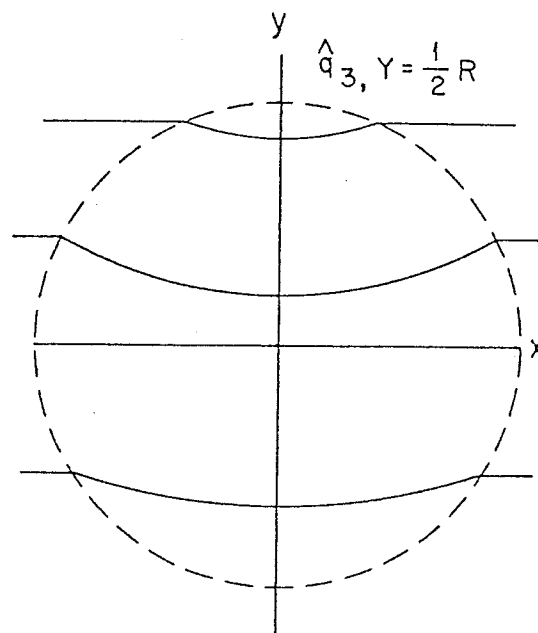
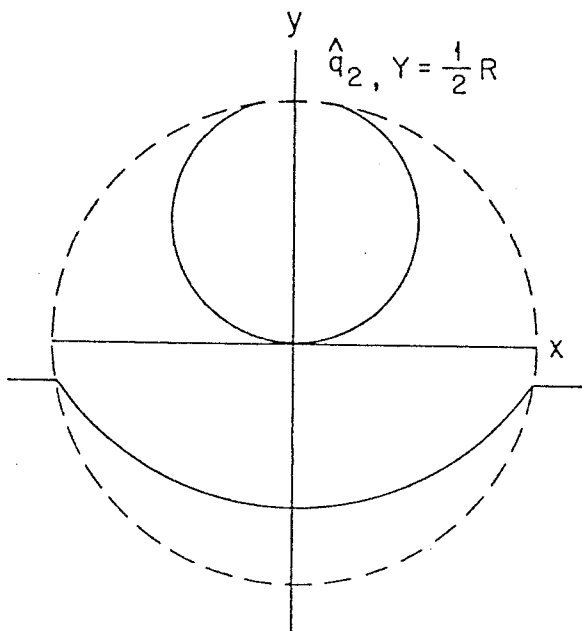
centered on  $(0, Y = -\frac{\beta^2 H_1}{f_0 \alpha F})$ . Similarly the  $\hat{q}_3$  contours are centered on

$(0, 4Y)$ . These contours have been sketched in figure 6 for the special

cases  $Y = \frac{1}{2}R$  and  $Y = \frac{1}{8}R$  with  $\alpha < 0$ . In the former case the forcing is not



(a)



(b)

Figure 6. The functions  $\hat{q}_2$  and  $\hat{q}_3$  (a) In this case the forcing is strong enough to produce closed  $\hat{q}_3$  contours. (b) This case is less strongly forced so all the  $\hat{q}_3$  contours are open.

sufficiently strong to close the contours in the lowest layer and  $\psi_3 = 0$  everywhere. In the latter, more strongly forced, case there are closed  $\hat{q}_3$  contours and  $q_3$  is constant within this region.

The nonlinear models discussed in this section have many appealing features: the size and shape of the region containing the subsurface flows does not depend on any unknown eddy viscosities, and the depth of penetration of the flow increases with the forcing (figure 6) in a sensible fashion. As is observed the gyre center shifts northward as one goes deeper.

## 5. Some Homogeneous Circulation Problems

### Introduction

This final section of chapter 1 is a digression into some uninvestigated aspects of homogeneous circulation theory. I shall consider two problems. Firstly the wind driven flow which develops in regions where  $f/h$  contours (i.e. geostrophic contours) are closed by topography. Secondly, flow on a "broken  $\beta$ -plane" where  $\beta$  changes discontinuously, perhaps because of topography.

These problems are not directly relevant to the vertical structure problem discussed in the previous sections. The first problem is however instructive and performing the scaling associated with it is a good intuition building exercise.

### Topographically closed geostrophic contours.

The steady linearized potential vorticity equation is:

$$J(\psi, q) = (f_0 w/H) - \delta \nabla^2 \psi \quad (5.1)$$

$$q = f/h \quad (5.2)$$

The first term is advection of potential vorticity; it has been assumed that the length scale of the flow is sufficiently large to allow the relative vorticity to be neglected. The second term is the Ekman pumping which drives the motion. Note that  $H$  in (5.1) is the constant mean depth of the fluid whereas  $h$  in (5.2) is the actual varying depth of the fluid. The last term is the dissipation provided by a bottom Ekman layer.

For orientation note, that if  $h$  is constant (5.1) reduces to the familiar Stommel circulation problem. Welander (1968) introduced a helpful "thermal analogy" according to which  $\psi$  is a passive scalar

advected by the streamfunction  $q$ . The second term is a source while the third is diffusion.

The most familiar state of affairs is when the first two terms in (5.1) balance, once again the Sverdrup balance. This problem is solved subject to the eastern boundary condition:

$$\psi(a, y) = 0$$

by introducing a new coordinate system (Pedlosky, 1979):

$$\xi = p(x, y) \quad (5.2a)$$

$$\mu = q(x, y). \quad (5.2b)$$

In terms of these new coordinates:

$$\frac{\partial}{\partial x} = \left(\frac{\partial p}{\partial x}\right) \frac{\partial}{\partial \xi} + \left(\frac{\partial q}{\partial x}\right) \frac{\partial}{\partial \mu}$$

$$\frac{\partial}{\partial y} = \left(\frac{\partial p}{\partial y}\right) \frac{\partial}{\partial \xi} + \left(\frac{\partial q}{\partial y}\right) \frac{\partial}{\partial \mu}$$

so that:

$$J(\psi, q) = J(p, q) \frac{\partial \psi}{\partial \xi}.$$

$q$  is of course known and so we choose  $p$  so that:

$$J(p, q) = 1 \quad (5.3)$$

With this choice (5.1) becomes:

$$\frac{\partial \psi}{\partial \xi} = (f_0 w / H) + O(\delta) \quad (5.4)$$

and this equation, apart from some potential complications at the boundary, is identical to that in a flat bottomed ocean.

When the  $q$ -contours close however we have a very different problem. To see this integrate (5.1) over the area enclosed by a  $q$ -contour. It is easy to see that the first term in the equation vanishes and we're left with

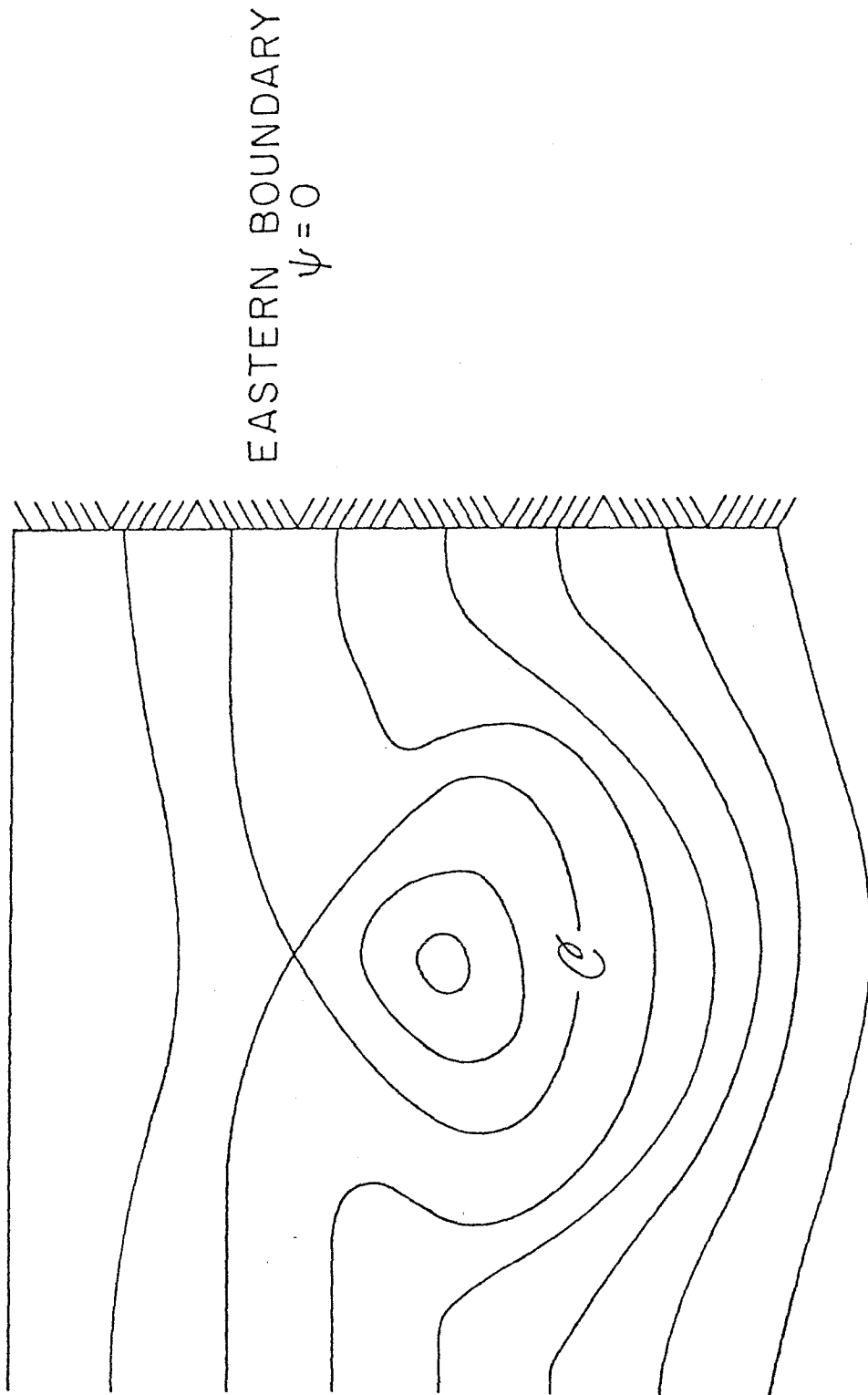


Figure 7. A schematic illustration of closed  $\bar{q}$  contours. An isolated topographic feature produces a patch of closed  $\bar{q}$  contours on a  $\beta$ -plane.

$$\iint_q (f_0 w/H) d^2 a = \delta \oint_q \nabla \psi \cdot \hat{n} dl \quad (5.4)$$

where  $\hat{n}$  is the outward normal. Now the left hand side of (5.4) is order one, unless  $w$  is contrived, so that the frictional term cannot be negligible no matter how small  $\delta$  is. This is in contrast to the Sverdrup balance in which the frictional term is neglected at first order.

The integral theorem suggests the rescaling

$$\hat{\psi} = \delta \psi \text{ or } \psi = \delta^{-1} \hat{\psi} \quad (5.5)$$

so that (5.1) and (5.4) are

$$J(\hat{\psi}, q) = \delta \left\{ (f_0 w/H) - \nabla^2 \hat{\psi} \right\} \quad (5.6a)$$

$$\iint_q (f_0 w/H) d^2 a = \oint_q \nabla \hat{\psi} \cdot \hat{n} dl \quad (5.6b)$$

In the rescaled variables the right hand side of (5.6a) is small and so

$$\hat{\psi} = F(q) + O(\delta) \quad (5.7)$$

where  $F$  is some undetermined function. This solution is reminiscent of the situation in section 4 where we arbitrarily specified a functional relationship between  $\psi$  and  $q$ , e.g. (4.16). In this problem however we determine  $F$  by explicitly considering the small right hand side of (5.6a). This is essentially done by forming the integral relation (5.6b), the large left hand side of (5.6a) vanishes leaving only the small right hand side. Physically (5.6b) states that the fluid pumped into the area enclosed by the  $q$  contour at the top leaves via the bottom Ekman layer. It can also be interpreted as an integral balance between the torque of the wind stress at the top, and the frictional drag at the bottom, on the

column of fluid enclosed by the  $q$  contour. In any case if (5.7) is substituted into (5.6b) there results:

$$\frac{dF}{dq} = \iint_q (f_0 w/H) d^2 a / \oint_q \nabla q \cdot \hat{n} dl \quad (5.8)$$

Equation (5.8) is a differential equation for  $F$  which in principle can be solved once  $w$  and  $q$  are specified.

The most important aspect of the solution (5.8) is the scaling (5.5). This shows that in a basin with both open and closed geostrophic contours, such as that shown schematically in figure 7, the flow in the blocked regions is order  $\delta$  smaller than the flow in the closed regions.

This can be understood intuitively by considering the thermal analogy. In the blocked regions a positive source term in (5.1) is ultimately balanced by advection of "cool fluid" from the eastern boundary. In the closed regions this is not possible and a final balance is achieved between conduction and the source term -- this is essentially the content of (5.6b). If the conductivity is small the temperature,  $\psi$ , must become very large (i.e. order  $\delta^{-1}$ ) relative to the temperature in the blocked region, before these terms balance.

This observation is relevant to the baroclinic problems discussed in section 4. In these problems sufficiently strong forcing produces closed geostrophic contours in subsurface layers by deforming the density surfaces. The results of sections 2 and 3 might suggest that all the Sverdrup transport should be confined to the uppermost layer. Suppose, however, there is weak vertical friction between the layers, say a drag proportional to the velocity difference between them. When the upper layer flow is above blocked lower layer geostrophic contours this friction

produces weak lower layer flow (i.e. the bulk of the Sverdrup transport is in the upper layer). When, however, the upper layer flow is above closed lower layer geostrophic contours the friction acts effectively to spin-up a strong subsurface flow. The amplitude of this flow is ultimately limited by friction on either the bottom or an even deeper layer. The result is that when equilibrium is finally established a substantial fraction of the Sverdrup transport has migrated to the lower layer.

There is apparently a very complicated matching problem at the  $q$ -contour which separates blocked and closed regions in figure 7. I have not been able to satisfactorily discuss this problem analytically. In attempting to analyze the probable structure of the boundary layer in this region I was led to consider the "broken  $\beta$ -plane" model in the next subsection.

#### Sverdrup flow on a broken $\beta$ -plane

In this subsection I discuss the solution of (5.1) when

$$q = \begin{cases} \beta_+ & \text{if } y > 0 \\ \beta_- & \text{if } y < 0 \end{cases} \quad (5.9)$$

and

$$w = \begin{cases} w_0 & \text{if } x < 0 \\ 0 & \text{if } x > 0 \end{cases} \quad (5.10)$$

The solution of (5.1) away from the break at  $y = 0$  is:

$$\psi = \begin{cases} x/\beta_+ & y > 0 \\ x/\beta_- & y < 0 \end{cases} \quad (5.11)$$

This solution has a discontinuity in derivative at  $y = 0$  which corresponds to a discontinuity in north-south transport at the break. This is removed

by an order  $\delta^{1/2}$  thick boundary layer in which the friction is important.

To discuss the boundary layer it is convenient to use the equation for  $v = \psi_x$ . From (5.1):

$$\beta v_x = (f_0 w_0 \delta(x)/H) - \delta \nabla^2 v \quad (5.12)$$

where  $\beta$  is given by (5.9) and  $w_0 \delta(x)$  in the second term is the derivative of (5.10) and should not be confused with the amplitude of the friction in the third term.

In the boundary layer region, introduce a scaled length scale:

$$\mu = \delta^{1/2} y$$

so that (5.12) is

$$\beta v_x = -v_{\mu\mu} + O(\delta) \quad (5.13)$$

The solution of (5.13) which matches smoothly onto the outer solution

$$v = \begin{cases} 1/\beta_- & \text{as } \mu \rightarrow -\infty \\ 1/\beta_+ & \text{as } \mu \rightarrow +\infty \end{cases}$$

is

$$v = \begin{cases} \frac{1}{\sqrt{\beta_+\beta_-}} + \frac{(\beta_- - \beta_+)}{\beta_+(\beta_- + \sqrt{\beta_+\beta_-})} \operatorname{erf}\left[\frac{1}{2}\sqrt{\frac{\beta_+}{|\mu|}} \mu\right] & \text{if } y > 0 \\ \frac{1}{\sqrt{\beta_+\beta_-}} + \frac{(\beta_- - \beta_+)}{\beta_-(\beta_+ + \sqrt{\beta_+\beta_-})} \operatorname{erf}\left[\frac{1}{2}\sqrt{\frac{\beta_-}{|\mu|}} \mu\right] & \text{if } y < 0 \end{cases} \quad (5.14)$$

In (5.14) both  $v$  and  $v_x$  are continuous at  $\mu = 0$ . The streamfunction is recovered from (5.14) using:

$$\psi = - \int_x^0 v(x', \mu) dx'$$

The most important point to note about the above solution is the way the friction acts to smooth the discontinuity in north-south mass

transport at the break. This model was originally introduced as a first step toward understanding the matching problem at the dividing  $q$ -contour in figure 7. The connection is rather tenuous and the broken  $\beta$ -plane has been discussed here only for the sake of completeness.

## CHAPTER 2

## Potential Vorticity Homogenization

## Abstract of Chapter 2

In section 6 the problem of determining  $Q$  inside closed geostrophic contours is discussed and an analogy with the classical Batchelor-Prandtl theorem is drawn. The analogy is strongest, and the formulation mathematically simplest, when the principal dissipative process is horizontal diffusion of potential vorticity.

In section 7 the parameterization

$$\overline{v_i'q'} = -K_{ij}\overline{q}_{,j}$$

in the context of geostrophic turbulence is critically discussed. It is argued that the analogy with the turbulent diffusion of a passive scalar is misleading and additional processes must be invoked to justify the above relation.

Section 8 is the most important section in this chapter; two different, but related, proofs of a quasigeostrophic, turbulent extension of the Batchelor-Prandtl theorem are given. The principal result is that inside closed geostrophic contours the potential vorticity is uniform.

Section 9 is a digression in which a new averaging procedure, essentially a generalization of the familiar meteorological zonal average, is discussed. As in the zonal case, the introduction of Lagrangian coordinates emphasizes the importance of transience and dissipation in

enabling the fluctuations to alter the mean flow. A third homogenization proof, this one valid for a steady, weakly dissipative, wave field is given at the end of this section.

## 6. An Oceanic Analog of the Batchelor-Prandtl Theorem.

### Introduction - removing degeneracy inside closed streamlines using an integral theorem.

In section 4 it was shown how sufficiently strong forcing produces closed geostrophic contours in subsurface density layers. Because both the forcing and dissipation is weak in these regions the approximate solution of the potential vorticity equation is

$$q = Q(\psi, z) + (\text{small corrections due to weak dissipation, etc.}) \quad (6.1)$$

(here, unlike in section 4, I'm using a continuously stratified model in which  $z$  is the vertical coordinate). Because the contours are closed, the solution  $\psi = 0$  is not required by the imposition of no flux boundary conditions. In fact the function  $Q$  cannot be determined except by considering the weak dissipative processes neglected in deriving (6.1).

This degeneracy associated with closed streamlines is a familiar problem in fluid mechanics. Usually the degeneracy is removed (i.e.  $Q$  is uniquely determined) by invoking a small amount of dissipation or viscosity and proving an integral constraint which must be satisfied by the flow no matter how small (or large) the dissipation is.

An example of this procedure has already been given in section 5 where the flow within topographically closed geostrophic contours was determined using the integral theorem (5.4). A more familiar example is Batchelor's (1956) proof that the relative vorticity becomes uniform within two-dimensional, steady, closed streamlines at high Reynolds number. For completeness Batchelor's proof is given later in this section. Other similar examples are found in dynamo theory; Weiss (1966)

and Proctor (1975) (see Moffatt (1978) for a review) proved that magnetic flux lines are expelled from two-dimensional eddies using essentially the same idea.

### The Batchelor-Prandtl Theorem

The steady two-dimensional Navier-Stokes equation can be reduced to:

$$J(\psi, \nabla^2 \psi) = \nu \nabla^4 \psi \quad (6.2)$$

where  $\psi$  is the streamfunction and  $\nu$  the kinematic viscosity. If the viscosity is small, more precisely if

$$\text{Reynolds Number} = \frac{UL}{\nu} \gg 1,$$

the solution of (6.2) is plausibly:

$$\nabla^2 \psi = F(\psi) + O(\text{Reynolds Number})^{-1}. \quad (6.3)$$

Now if the streamlines are open (i.e. do not close) then  $F$  is determined by boundary conditions externally imposed at the source. On the other hand if the streamlines close  $F$  is undetermined.

Now observe that if (6.2) is integrated over the area enclosed by a closed streamline then the large left hand side vanishes identically leaving

$$\nu \oint \nabla (\nabla^2 \psi) \cdot \hat{n} \, dl = 0 \quad (6.4)$$

where  $\hat{n}$  is the unit normal,  $\nabla \psi / |\nabla \psi|$ , to the closed streamline. Equation (6.4) is the integral theorem alluded to earlier in this section; it is clearly valid no matter how small or large the Reynolds number is. When the Reynolds number is large however, we use both (6.3) and (6.4) to obtain

$$\nu \oint \nabla (F(\psi)) \cdot \hat{n} \, dl = 0$$

or since  $F'(\psi)$  is constant on the path of integration and  $\oint \nabla \psi \cdot \hat{n} \, dl = \oint \underline{v} \cdot \underline{dl}$

$$\nu F'(\psi) \oint \underline{v} \cdot \underline{dl} = 0. \quad (6.5)$$

Since the circulation round the streamline must be nonzero (6.5) implies:

$$F' = 0$$

or equivalently:

$$\nabla^2 \psi = \text{constant within the closed streamlines} \quad (6.6)$$

The statement that the vorticity is uniform within closed streamlines is known as the Batchelor-Prandtl theorem.

There is an important assumption in the above derivation which should be made explicit. This is the notion that the viscous term in (6.2) is small everywhere on the closed contour. Thus flow in which every streamline passes through a viscous boundary layer are excluded. Some of the simplest and most useful theoretical models in oceanography, such as the Stommel (1948) circulation pattern, fall into this category.

#### Vertical Viscosity and a Batchelor-Prandtl Theorem for Potential Vorticity.

Returning now to the geophysical context, consider the form of the dissipative term produced in the potential vorticity equation by vertical diffusion of momentum in the horizontal momentum equation:

$$\frac{Dv}{Dt} + zxfv = -\nabla p + (v_{v_z})_z \quad (6.7)$$

There are undoubtedly other important dissipative processes such as vertical density diffusion; for reasons which will become clear when mesoscale eddies are discussed I shall focus on vertical friction. One of the most important mean flow effects of eddies is the vertical transmission of stress. The frictional term in (6.7) can be thought of as a simplistic model of these processes. For the moment however simply regard  $(v_{v_z})_z$  as laminar friction. The heuristic argument given

in section 5 suggests that vertical friction acts effectively to produce flow in regions where geostrophic contours close. The integral theorem (6.10) below is a first step towards quantifying the argument given in that section; it is simply a statement that in the final equilibrium state the frictional forces on the annulus of fluid within a closed contour balance.

The planetary scale potential vorticity equation is then (e.g. section 1):

$$J(\psi, q) = (\nu \nabla^2 \psi_z)_z \quad (6.8a)$$

$$q = \beta y + (F \psi_z)_z \quad (6.8b)$$

$$F(z) = f_0^2 N^{-2}. \quad (6.8c)$$

As in section 4 one can think of the flow being forced by Ekman pumping at the surface. When the forcing is sufficiently strong there will be closed geostrophic contours in which:

$$q = Q(\psi, z) + O(\nu) \quad (6.9)$$

(it is assumed that the vertical friction is weak).

Now, as in the earlier proof of the Batchelor-Prandtl theorem, observe that if (6.8a) is integrated over the area enclosed by a closed streamline the large left hand side vanishes and leaves:

$$\oint \nabla (\nu \psi_z)_z \cdot \hat{n} \, dl = 0$$

(c.f. (6.4)). Using (6.8b) and (6.9) the above can be put in the form

$$\oint Q_\psi \oint \underline{v} \cdot \underline{dl} + \nu_z F \oint \underline{v}_z \cdot \underline{dl} = 0 \quad (6.10a)$$

$$\underline{v} = \underline{v}(z)/F(z) \quad (6.10b)$$

Now there is one particular case in which the integral theorem (6.10a) gives a straightforward answer. That is when  $v_z = 0$  or equivalently:

$$v \propto F \propto N^{-2} \quad (6.11)$$

In this case (6.10a) implies

$$Q = 0$$

i.e. the potential vorticity is a function of z only.

Note with the particular model of vertical friction in (6.11) the potential vorticity equation is:

$$J(\psi, q) = \nabla^2 q \quad (6.12)$$

so only one particular type of vertical friction is equivalent to horizontal diffusion of potential vorticity. In this case there is a very close analogy between the proof that potential vorticity is uniform and the Batchelor-Prandtl theorem. In section 7 I shall argue that horizontal potential vorticity diffusion is really a more fundamental process than laminar vertical friction as in (6.7) and so (6.12) is really a more important model equation than (6.8a). This means that the mathematically simplest version of (6.10a) is also the most physically relevant.

The observation that not all forms of vertical friction horizontally homogenize potential vorticity is potentially important since it allows one to discriminate between processes. For instance, if it is observed that the potential vorticity is indeed uniform in some part of the ocean one could argue that this homogenization was accomplished by horizontal diffusion of potential vorticity and not by some arbitrary vertical friction due to say, internal waves. (Unless of course there was some reason for believing that vertical stress transmission by internal waves should be modelled as in (6.11)!) )

7. Some Exegetical Remarks on:  $\overline{v'_i q'_i} = -\kappa_{ij} \overline{q}_{,j}$

Introduction - mesoscale eddies and removal of degeneracy inside closed geostrophic contours.

In section 6 the importance of dissipation in removing degeneracy (i.e. determining  $Q$  in (6.1)) was emphasized. The examples discussed in that section were all based on laminar viscosity. In discussing the wind-driven general circulation we are faced with a difficult problem because it is not obvious a priori which small scale process to invoke. In my opinion the most important is plausibly the eddy flux of potential vorticity associated with the mesoscale motions. Thus if an overbar denotes some as yet unspecified averaging process then the mean potential vorticity equation is

$$\overline{q}_t + \underline{\overline{v}} \cdot \nabla \overline{q} = -\nabla \cdot \underline{\overline{v'q'}} + \overline{\Delta} \quad (7.1a)$$

$$\overline{\Delta} = \text{other smaller scale processes} \quad (7.1b)$$

e.g., internal waves

In (7.1a)  $\underline{\overline{v}}$  is now the mean flow, supposedly driven by the wind, upon which is superimposed the more energetic mesoscale eddies. If the right hand side of (7.1a) is small and the motion is steady then we have the familiar situation:

$$\underline{\overline{v}} = \hat{z} \times \nabla \overline{\psi} \quad (7.2a)$$

$$\overline{q} = Q(\overline{\psi}, z) + (\text{small corrections due to RHS}) \quad (7.2b)$$

The assertion that the right hand side of (7.1a) is small, even though  $|\underline{\overline{v'}}| \gg |\underline{\overline{v}}|$ , depends on the correlation in  $\underline{\overline{v'q'}}$  being small.

In section 8 I shall determine  $Q$  in (7.2a) by proving a turbulent extension of the Batchelor-Prandtl theorem. In this section I shall discuss some general results concerning the eddy flux of potential vorticity which will be used in the course of the proof. These results rely heavily on the notion of averaging. For reasons which will emerge later it is clearest to think of ensemble averaging rather than time averaging. Because of the complications of oceanic geometry it is difficult to generalize the zonal averaging procedure which is so convenient in meteorology. Nevertheless a tentative generalization is discussed in section 9; because this generalization is unfamiliar, section 9 has been set aside as a digression.

#### The eddy flux of potential vorticity

Rhines (1977) and Rhines and Holland (1979) have argued that the potential vorticity flux is related to the mean gradients by:

$$\overline{v_i' q'} = - K_{ij} \bar{q}_{,j} \quad (7.3a)$$

where  $K_{ij}$  is the Lagrangian diffusivity of the fluid particles:

$$K_{ij} = \overline{v_i' \xi_j'} \quad (7.3b)$$

$$\xi_j' = \text{particle displacement from mean trajectory} \quad (7.3c)$$

The arguments leading to (7.3) in this section will be couched in terms of turbulence, rather than nonlinear waves. The principal physical difference between these two regimes is that when the fluctuations are stationary (i.e., statistical properties such as velocity autocorrelations are independent of time)  $K_{11}$  and  $K_{22}$  are zero for waves but not

for turbulence. The case of a nonstationary wave field is probably best treated using the formulation in section 9.

The principal assumption made by Rhines (1977) and Rhines and Holland (1979) to obtain (7.3a) is

$$\gamma_1 = U'T'/\bar{L} \ll 1 \quad (7.4a)$$

$$\gamma_2 = T'/T_\Delta \ll 1 \quad (7.4b)$$

where

$\bar{L}$  = length scale of mean fields such as  $\bar{q}, \overline{q'^2}$ .

$U'$  = root mean square velocity of the turbulence

$T'$  = time scale over which the fluctuating velocity becomes decorrelated. See Figure 8.

$T_\Delta$  = time scale over which a particle's potential vorticity changes due to forcing, dissipation, etc.

One argument given is based on the similarity between the potential vorticity equation:

$$\frac{Dq}{Dt} = \Delta \quad (7.5)$$

and the advection equation of a passive scalar in a turbulent velocity field. The latter problem was solved by Taylor (1921). I shall present a slightly more modern version of Taylor's proof and emphasize the assumptions additional to (7.4) required to obtain (7.3a) when  $q$  is the potential vorticity.

The principal reason for requiring (7.4) is that it enables one to divide the time axis into intervals of length  $\tau$  which satisfy the double inequality

$$T' \ll \tau \ll \bar{T} \text{ and } T_\Delta \quad (7.6)$$

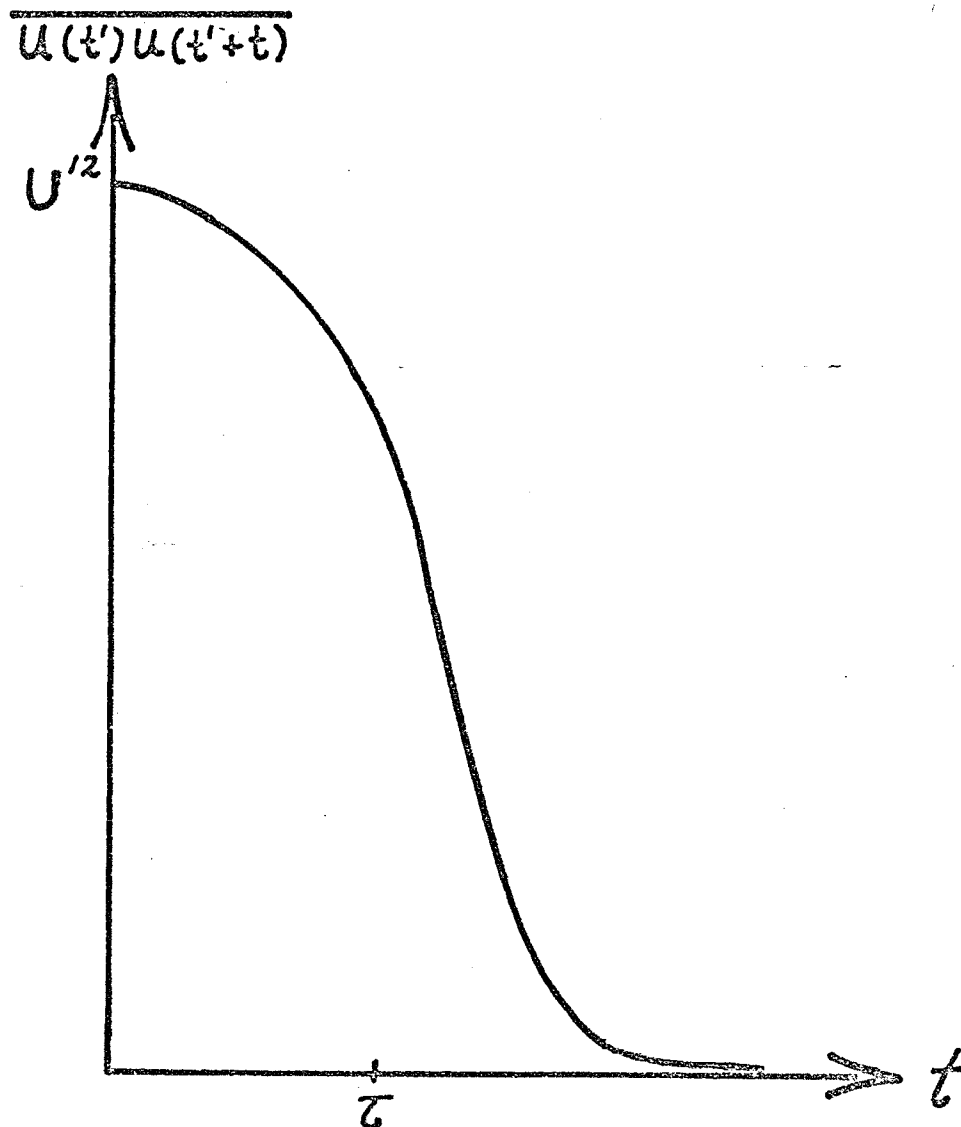


Figure 8. A schematic illustration of the Lagrangian velocity correlation function. By assumption the fields discussed in this section are turbulent so this function decreases to zero at infinity and has nonzero area under it.

where  $\bar{T}$  = time scale over which  $\bar{q}$  changes. (7.7)

Note that (7.6) is not an additional assumption but is a consequence of (7.4).

Now if:

$$q(\underline{x}, 0) = q_0(\underline{x}) \quad (7.8a)$$

then the solution of (7.5) at  $t = \tau$  is approximately

$$q(\underline{x}, \tau) = q_0(\underline{x} - \underline{\xi}(\underline{x}, \tau)) \quad (7.8b)$$

where:  $\underline{x} - \underline{\xi}(\underline{x}, \tau)$  = position at  $t=0$  of the particle at  $\underline{x}$  at time  $\tau$ .

Note that (7.4b) and (7.6) were used to obtain (7.8b). Now using (7.4a), (7.8b) is

$$q(\underline{x}, \tau) = q_0 - \underline{\xi} \cdot \nabla q_0 + O(\tau_1^2) \quad (7.9a)$$

or ensemble averaging

$$\bar{q}(\underline{x}, \tau) = \bar{q}_0 - \bar{\underline{\xi}} \cdot \nabla \bar{q}_0 - \overline{\underline{\xi}' \cdot \nabla q_0'} \quad (7.9b)$$

Subtracting (7.9b) from (7.9a) gives

$$q'(\underline{x}, \tau) = q_0' - \underline{\xi}' \cdot \nabla \bar{q}_0 - \bar{\underline{\xi}} \cdot \nabla q_0' - \underline{\xi}' \cdot \nabla q_0' + \overline{\underline{\xi}' \cdot \nabla q_0'} \quad (7.10)$$

and multiplying the above by  $v'_i(\underline{x}, \tau)$  and ensemble averaging gives:

$$\overline{v'_i q'} = -K_{ij} \bar{q}_{0,j} - \overline{v'_i \{ q_0' - \underline{\xi}' \cdot \nabla q_0' - \underline{\xi}' \cdot \nabla q_0' \}} \quad (7.11a)$$

(1)                      (2)                      (3)

$$K_{ij} = \overline{v'_i \xi'_j} \quad (7.11b)$$

When  $q$  is a passive scalar a major simplification of (7.11a) is possible: term 3 is zero because there is no reason to expect the velocity field at time  $\tau$  to be correlated with the  $q'$  field at time 0. It might be objected that this is not the case when  $q$  is potential vorticity. This objection cannot have much weight since the putatively important term is a

correlation between two fluctuating quantities separated by an interval  $\tau$ . Since the field is turbulent, time separation is sufficient to allow the velocity field forget its past; and so unless the correlation between  $\underline{v}'$  and  $q'$  has a much longer memory (indeed a decorrelation time comparable to  $T_\Delta$  or  $\bar{T}$ ), term 3 will also be negligible when  $q$  is the potential vorticity. In this case one has:

$$\overline{v'_i q'} = -\kappa_{ij} \bar{q}_{0,j} \quad (7.12)$$

and combining this with (7.1a) gives:

$$\bar{q}_t + \bar{v} \cdot \nabla \bar{q} = (\kappa_{ij} \bar{q}_{0,j})_{,i} + \bar{\Delta} \quad \text{at } t = \tau \ll \bar{T}. \quad (7.13)$$

The diffusive term in (7.13) contains  $q_0$  not  $q(\underline{x}, \tau)$ .

To obtain a mean field equation valid for  $t = O(\bar{T}) \gg \tau$  replace  $q_0$  by  $q$  in the diffusive term to obtain:

$$\bar{q}_t + \bar{v} \cdot \nabla \bar{q} = (\kappa_{ij} \bar{q}_{,j})_{,i} + \bar{\Delta}. \quad (7.14)$$

When  $q$  is a passive scalar this is justified by asserting that at  $t = \tau$  one can restart the ensemble without changing the  $q$  distribution in any realization, but with different velocity fields, entirely uncorrelated with those in the previous ensemble. Because the  $q$  distribution in each realization is unchanged,  $\bar{q}(\underline{x}, \tau)$  is only infinitesimally different from  $\bar{q}_0$  and can be computed from (7.13). On the other hand because the velocity fields have been "scrambled" the correlation between  $\underline{v}'$  and  $q'$  created during the first  $\tau$  interval (see (7.12)) is again zero. Thus in the second interval one can proceed exactly as in the first to compute  $\bar{q}$  at  $t = 2\tau$ . The transition to the continuous evolution equation (7.14) is justified because  $\bar{q}$  changes only slightly in each  $\tau$  interval.

Put differently, on the coarse time scale  $\tau$  the evolution of  $\bar{q}$  is a Markov process and so in each  $\tau$  interval one may use unbiased velocity statistics (i.e.  $K_{ij}$ ) rather than averages conditioned by knowledge of what happened in the previous interval. This process of dividing the time axis into intervals such that random fields are uncorrelated from interval to interval while mean fields change slightly is standard in statistical physics e.g. Chandrasekhar (1943), Van Kampen (1976).

When  $q$  is the potential vorticity the argument given after equation (7.14) cannot go through without modification; it is impossible to change the velocity field in each realization without also changing the potential vorticity field. This means that if  $\overline{v'q'}$  initially had some nonzero value (unlike the passive scalar case we cannot assume that this correlation is zero initially) it may not be possible to "scramble" the fluctuations  $\underline{v}'$  and  $q'$  at  $t = \tau$  in such a way that  $\bar{q}(\underline{x}, \tau)$  computed from (7.13) is unchanged while  $\overline{v'q'}(\underline{x}, \tau)$  is also reinitialized. Thus it is not clear that the evolution of the ensemble in the second  $\tau$  interval is independent of, and statistically identical to, the evolution in the first interval.

The difficulties associated with the derivation of (7.3) via the passive scalar analogy have not passed unnoticed in the literature; the discussion above is intended to make explicit what I believe are the strongest objections to this argument. To circumvent these difficulties Rhines (1977) proposed a simple model in which the potential vorticity perturbation,  $q'$ , is subject to Rayleigh damping and the restriction

(7.4b) is removed. de Verdiere (1980) explicitly calculated  $\kappa_{ij}$  in this case for a weakly nonlinear wave field.

In general, however, even for turbulence, provided (7.4a) is satisfied, Rhines finds that:

$$\kappa_{ij} = \int_0^{\infty} R_{ij}(\tau) e^{-\tau/T_{\Delta}} d\tau$$

$R_{ij}$  = the Lagrangian velocity correlation  
(figure 8)

$T_{\Delta}$  = time scale of the Rayleigh damping

This particular damping mechanism ensures that in each interval of  $T_{\Delta}$  the evolution of the ensemble is independent of that in the previous interval. It is not clear whether different dissipative processes are qualitatively similar. What is clear, however, is that one is relying on dissipation to destroy correlations between  $\underline{v}'$  and  $q'$  and this is philosophically quite different from the "scrambling" procedure described after (7.14).

## 8. Potential Vorticity Homogenization - a Turbulent Extension of the Batchelor-Prandtl Theorem

### Introduction - the weak eddy assumption.

In this section I combine the ideas of sections 6 and 7 and give two proofs of the generalized Batchelor-Prandtl theorem. The first explicitly uses (7.3a) while the second does not. Both rely on the assumption that the right hand side of (7.1a) is small so that as a first approximation, when the ensemble average is steady:

$$\bar{q} \cong Q(\bar{\psi}, z) \quad (8.1)$$

Note that it is necessary to neglect  $\nabla \cdot \underline{v}'q'$  even in the western boundary layers i.e. it is assumed that (8.1) is a good approximation everywhere on a streamline. This is the weak eddy assumption which I cannot convincingly defend a priori. I shall return to this point in section 12 when I discuss western boundary layer dynamics.

The first proof: use  $\overline{v'_i q'_j} = -\kappa_{ij} \bar{q}_{,j}$  explicitly

This proof is virtually identical to those given in section 6 for laminar friction. Integrate the steady version of (7.1a) over a closed streamline to obtain:

$$\oint \underline{v}'q' \cdot \hat{n} dl = \iint \bar{\Delta} d^2a \quad (8.2)$$

where  $\hat{n} = \nabla\bar{\psi}/|\nabla\bar{\psi}|$  is the normal to the streamline. Now (7.3a) and (8.1) imply

$$\frac{\partial Q}{\partial \bar{\psi}} \oint \kappa_{ij} \bar{\psi}_{,j} n_i dl = \iint \bar{\Delta} d^2a \quad (8.3)$$

If  $\bar{\Delta}$  is very small i.e. mesoscale eddies are much stronger than all the

small processes subsumed in  $\Delta$ , then (8.3) implies that  $\frac{\partial Q}{\partial \Psi} \cong 0$  or the potential vorticity is uniform.

One possible objection to this conclusion is that the line integral on the left hand side of (8.3) may be very small, even though mesoscale eddies are dominant, because the integrand may have both signs and significant cancellation may occur. However, since the integrand of the line integral is

$$\kappa_{ij} \bar{\Psi}_{,j} n_i = \kappa_{ij} \bar{\Psi}_{,j} \bar{\Psi}_{,i} / |\nabla \bar{\Psi}| \quad (8.4a)$$

$$= S_{ij} \bar{\Psi}_{,i} \bar{\Psi}_{,j} / |\nabla \bar{\Psi}| \quad (8.4b)$$

where

$$S_{ij} = \frac{1}{2} \{ \Psi_{ij} + \Psi_{ji} \} \quad (8.5)$$

= symmetric part of  $\kappa_{ij}$ ,

and the symmetric part of  $\kappa_{ij}$  is related to the spread of a cloud of particles about its center of mass (Rhines, 1977), reversals in the sign of the integrand must, in some sense, correspond to a contraction of the cloud about its center of mass. This is unlikely in a turbulent fluid. I shall return to this point in the next subsection.

The argument in the preceding paragraph may not be entirely convincing, but in any case (8.3) certainly suggests strongly that variations in  $q$  can only be due to the small scale processes subsumed in  $\Delta$ . The assumption that these are small and  $\bar{q}$  is uniform leads to a theory of the wind driven circulation which is so simple that it deserves extensive investigation before one turns to the much more complicated theories suggested by the alternatives.

Finally, note that the major conclusion, uniform potential vorticity, is based principally on the assumption that  $K_{ij}$  exists; it is not necessary to actually be able to calculate  $K_{ij}$  or make strong simplifying assumptions such as taking  $K_{ij}$  to be an isotropic constant tensor.

The second proof: use the enstrophy equation

Because of the uncertainties associated with the parametrization (7.3a) it is worthwhile attempting to construct a proof of potential vorticity homogenization which does not use  $K_{ij}$  explicitly. The proof here is based on the enstrophy equation which is obtained by multiplying the fluctuation potential vorticity equation:

$$q'_t + \bar{v} \cdot \nabla q' + \underline{v}' \cdot \nabla \bar{q} + \underline{v}' \cdot \nabla q' - \overline{\underline{v}' \cdot \nabla q'} = \Delta' q' \quad (8.6)$$

by  $q'$  and ensemble averaging. If the statistics are stationary there results:

$$\bar{v} \cdot \nabla \overline{\frac{1}{2} q'^2} + \overline{\underline{v}' q'} \cdot \nabla \bar{q} + \overline{\underline{v}' \cdot \nabla \frac{1}{2} q'^2} = \overline{\Delta' q'} \quad (8.7)$$

Integrating the above over the area enclosed by a closed mean streamline gives:

$$\iint \overline{\underline{v}' q'} \cdot \nabla \bar{q} \, d^2a + \iint \nabla \cdot \overline{\underline{v}' \frac{1}{2} q'^2} \, d^2a = \iint \overline{\Delta' q'} \, d^2a \quad (8.8)$$

Equation (8.8) is the integral balance equation for perturbation enstrophy. A similar expression for the mean enstrophy is obtained by multiplying the steady version of (7.1a) by  $\bar{q}$  and integrating over the same area as in (8.8):

$$\iint \bar{q} \nabla \cdot \overline{\underline{v}' q'} \, d^2a = \iint \bar{q} \bar{\Delta} \, d^2a \quad (8.9)$$

Integrating the first term by parts and using (8.1) and (8.2) to rewrite the boundary contribution gives:

$$\iint \overline{v'q'} \cdot \nabla \bar{q} \, d^2a = Q(\psi_*, z) \iint \bar{\Delta} \, d^2a - \iint \bar{q} \bar{\Delta} \, d^2a \quad (8.10)$$

$\psi_*$  = the value of the streamfunction on the closed streamline which encloses the area of integration.

Whereas (8.8) and (8.9) are exact, (8.10) is approximate because (8.1) was used as an intermediate step.

Eliminating  $\iint \overline{v'q'} \cdot \nabla \bar{q}$  between (8.8) and (8.10) gives:

$$\iint \overline{\Delta'q'} \, d^2a = \oint \overline{\frac{1}{2}q'^2} \cdot \hat{n} \, dl + \left\{ \iint \bar{q} \bar{\Delta} \, d^2a - Q(\psi_*, z) \iint \bar{\Delta} \, d^2a \right\} \quad (8.11)$$

Now if the right hand side of (8.11) is small (the physical justification of this will be discussed later) then:

$$\iint \overline{\Delta'q'} \, d^2a \approx 0 \quad (8.12)$$

For particular forms of the fluctuation dissipation such as:

$$\Delta' = -\delta q' \text{ or } v \nabla^2 q' \quad (8.13)$$

(8.12) allows us to conclude that:

$$q' \approx 0. \quad (8.14)$$

This, together with observation that  $q'$  is created by displacing fluid particles from mean potential vorticity contours e.g. (7.10), implies that

$$\nabla \bar{q} = 0. \quad (8.16)$$

The third term in (8.11) is negligible because it is unlikely that processes other than  $\nabla \cdot \overline{v'q'}$  are important on the large length scales characteristic of the general circulation. This is essentially the same assumption made in the first proof after (8.3). The second term is

negligible because of the two scale approximation  $\gamma_1 \ll 1$ . This amounts to asserting that the dominant balance in (8.7) is:

$$\overline{v'q'} \cdot \nabla \bar{q} \approx \overline{\Delta'q'} \quad (8.17)$$

Rhines (1979) has argued that this is the case for either weak wavelike disturbances, or more appropriately, turbulence in which  $\gamma_1 \ll 1$ .

Using (7.3a), (8.17) can be rewritten as

$$\kappa_{ij} \bar{q}_{,i} \bar{q}_{,j} = \overline{\Delta'q'} \quad (8.18)$$

or with (8.1)

$$\left(\frac{\partial Q}{\partial \bar{\psi}}\right)^2 \kappa_{ij} \bar{\psi}_{,i} \bar{\psi}_{,j} = \overline{\Delta'q'} \quad (8.19)$$

The result emphasizes another similarity between the two proofs of potential vorticity homogenization; the assertion that the integrand of the line integral in (8.3) is positive definite is equivalent to  $\overline{\Delta'q'} > 0$  and this is guaranteed for the particular forms of  $\Delta'$  in (8.13). Rhines and Holland (1979) have discussed the circumstances in which  $\overline{\Delta'q'}$  may be negative and conclude that these exceptions are rare.

## 9. A Generalization of the Zonal Average

### Introduction, some geometric preliminaries.

In sections 7 and 8 the discussion of wave-mean flow interaction was in terms of turbulent eddy fields and much of the discussion was based on ensemble averaging. As was explained in section 7 there are some conceptual difficulties in this formulation which obscure the circumstances in which (7.3) applies.

In this section I shall discuss weak wave fields, not in the familiar atmospheric context where a zonal average is sensible, but in the oceanic context where it is first necessary to generalize this averaging procedure. I shall first present some simple geometric results used in course of the definition.

Consider some closed curves in the  $x$ - $y$  plan (see Figure 9) which are the level contours of some scalar function  $\eta(x,y)$ . Given some other scalar function,  $F(x,y)$ , we can construct a function of  $\eta$  alone by:

$$I(\eta) = \iint_{R_\eta} F(x,y) d^2a \quad (9.1)$$

where the integral is over the region enclosed by the  $\eta$  contour; this region will be denoted by  $R_\eta$  and its area is:

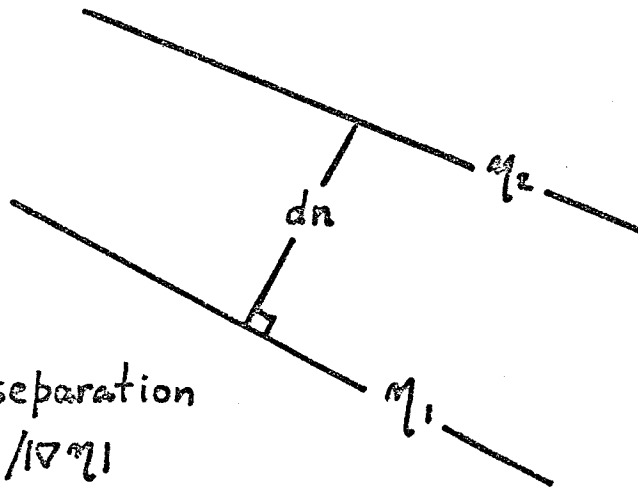
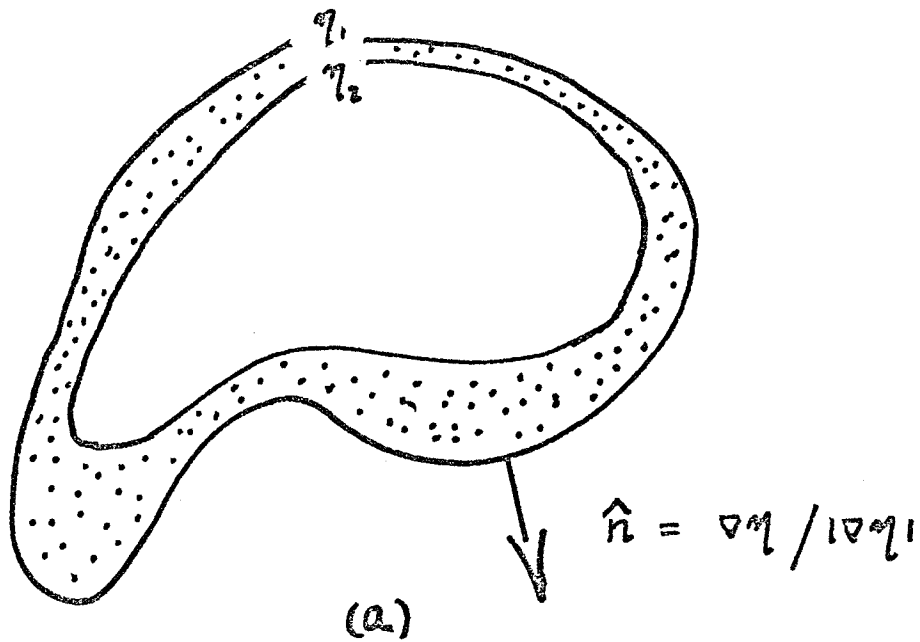
$$A(\eta) = \iint_{R_\eta} d^2a . \quad (9.2)$$

Now that  $I(\eta)$  has been defined by (9.1), how does one calculate its derivative? We have

$$I(\eta_1) - I(\eta_2) = \iint_{\delta R_\eta} F d^2a \quad (9.3)$$

where

$\delta R_\eta$  = the "tubular" region between two adjacent  $\eta$  contours. See Figure 9.



$dn = \text{normal separation}$   
 $\equiv (\eta_1 - \eta_2) / |\nabla\eta|$

Figure 9. This figure defines some of the geometric quantities discussed in the text. (a) Two  $\eta$ -contours and the "tubular" area between them (b) The relationship between the normal separation of the contours and  $|\nabla\eta|$ .

As  $\eta_1 \rightarrow \eta_2$  the area integral in (9.3) can be reduced to a line integral around the contour. Since the normal separation of the contours is

$$dn = (\eta_1 - \eta_2) / |\nabla \eta|$$

it follows that the elemental area in (9.3) is:

$$\begin{aligned} d^2a &= dn \, dl \\ &= (\eta_1 - \eta_2) \, dl / |\nabla \eta|. \end{aligned} \quad (9.4)$$

Substituting (9.4) into (9.3) gives:

$$\begin{aligned} \frac{dI}{d\eta} &= \lim_{\eta_1 \rightarrow \eta_2} \frac{I(\eta_1) - I(\eta_2)}{\eta_1 - \eta_2} \\ &= \oint_{\eta} F \frac{dl}{|\nabla \eta|} \end{aligned} \quad (9.5)$$

Equation (9.5) is the principal result of this subsection. In (9.5) and the following  $\oint_{\eta}$  denotes a line integral round a closed  $\eta$  contour.

As a particular application of (9.5), consider steady homogeneous quasigeostrophic flow with closed streamlines. In this application  $\eta = \psi$ . The total amount of kinetic energy inside a particular streamline is given by an integral like (9.1) viz

$$K(\psi) = \iint_{R_{\psi}} \frac{1}{2} \nabla \psi \cdot \nabla \psi \, d^2a \quad (9.6)$$

Differentiating the above using (9.5) gives

$$\begin{aligned} \frac{dK}{d\psi} &= \frac{1}{2} \oint_{\psi} \nabla \psi \cdot \nabla \psi \frac{dl}{|\nabla \psi|} \\ &= \frac{1}{2} \oint \nabla \psi \cdot \hat{n} \, dl \\ &= \frac{1}{2} \left\{ \text{circulation of the streamline} \right\} \end{aligned} \quad (9.7)$$

Equation (9.7) is a surprising connection between the kinetic energy density and the circulation.

An application of (9.5): high Peclet number, unsteady advection-diffusion

As another application of (9.5) I shall develop an approximate solution of the advection-diffusion problem

$$\theta_t + J(\psi, \theta) = \kappa \nabla^2 \theta \quad (9.8a)$$

$$\theta(x, y, 0) = \mathbb{H}(\psi, 0) \quad (9.8b)$$

when the Peclet number

$$P_e = \frac{UL}{\kappa}$$

is large. This condition, together with the choice of initial condition (9.8b), ensures that the second term in (9.8a) dominates the other two so that

$$\theta(x, y, t) = \mathbb{H}(\psi, t) + O(P_e^{-1}) \quad (9.9)$$

Our goal is an evolution equation for  $\mathbb{H}$ .

Begin by integrating (9.8a,b) over the area enclosed by a closed streamline; the large advective term vanishes identically leaving:

$$\iint_{R_\psi} \theta_t \, d^2a = \kappa \oint_\psi \nabla \theta \cdot \hat{n} \, dl. \quad (9.10)$$

Substitute (9.9) into (9.10):

$$\iint_{R_\psi} \mathbb{H}_t \, d^2a = \kappa \mathbb{H}_\psi \oint_\psi \nabla \psi \cdot \hat{n} \, dl; \quad (9.11)$$

as  $t \rightarrow \infty$  the temperature distribution becomes steady and (9.11) shows that it also becomes uniform i.e.  $\mathbb{H}_\psi = 0$ . This is by now a familiar result. To obtain an evolution equation which describes how (9.8b) evolves towards the uniform distribution, differentiate (9.11) with respect to  $\psi$  using (9.5):

$$\left(\frac{H}{t}\right) \oint \frac{dl}{|\nabla\psi|} = \kappa \left\{ \oint \nabla\psi \cdot \hat{n} dl \left(\frac{H}{\psi}\right) \right\} \quad (9.12)$$

Equation (9.12) is the desired evolution equation for  $\left(\frac{H}{t}\right)$ .

Definition of a generalized zonal average

Suppose there is a set of closed contours in the  $(x,y)$  plane given by:

$$\eta(x,y) = \text{constant}$$

and one has some reason for believing that strong mean flow exists about these contours.

For example:

- (i) in the periodic  $\beta$ -plane representation of a spherical Earth attention is naturally focused on the curves  $y = \text{constant}$  which close at infinity.
- (ii) in a homogeneous ocean, where the  $(f/h)$  contours are closed topographically,  $\eta = (f/h)$  is a natural choice.
- (iii) in an inertially balanced flow,  $q_0 = Q(\psi_0, z)$ , which is perturbed slightly, an obvious choice is the initial streamlines,  $\eta = \psi_0$ .
- (iv) in section 4, where the subsurface geostrophic contours are closed by the deformation of the isopycnal surfaces,  $\eta = \hat{q}$ .

I shall argue that a sensible generalization of the zonal average of a scalar is:

$$\bar{F}(\eta) = \oint_{\eta} F \frac{dl}{|\nabla\eta|} / \oint_{\eta} \frac{dl}{|\nabla\eta|} \quad (9.13)$$

The fluctuation is defined as:

$$F' = F - \bar{F} \quad (9.14)$$

Clearly, in example (i) above  $F$  is just a zonal average.

What is not obvious initially is why the factors  $|\nabla\eta|^{-1}$  appear in (9.13) -- it might seem that

$$\oint_{\eta} F \, dl / \oint_{\eta} dl \quad (9.15)$$

is more natural. There are several reasons for preferring (9.13), three important ones are:

(i) with definition (9.13):

$$\overline{z \times \nabla\eta \cdot \nabla F} = \oint_{\eta} \nabla F \cdot \frac{dl}{|\nabla\eta|} / \oint_{\eta} \frac{dl}{|\nabla\eta|} = 0$$

and this is analogous to  $\overline{\partial F / \partial x} = 0$  in the case of a zonal average.

The identity (9.16) is not valid if the average is defined by (9.15)

(ii) using (9.5), (9.13) can be interpreted geometrically as an area average. Let

$$\begin{aligned} A(\eta) &= \iint_{\eta} d^2a \\ &= \text{area enclosed by an } \eta \text{ contour} \end{aligned}$$

and then

$$\frac{\partial A}{\partial \eta} \overline{F} = \oint_{\eta} F \frac{dl}{|\nabla\eta|} = \frac{\partial}{\partial \eta} \iint_{\eta} F \, d^2a$$

so

$$\overline{F} = \frac{\partial}{\partial A} \iint_{\eta} F \, d^2a \quad (9.16)$$

Equation (9.16) can be used as an alternative definition.

(iii) if  $\eta$  is a streamfunction and  $\theta$  is a passive scalar satisfying:

$$\theta_t + J(\eta, \theta) = 0 \quad (9.17)$$

then the average of  $\theta$  defined by:

$$\bar{\theta} = \oint_{\eta} \theta \frac{dl}{|\nabla \eta|} \bigg/ \oint_{\eta} \frac{dl}{|\nabla \eta|}$$

is equal to the Eulerian time average.

To understand points (ii) and (iii) geometrically, divide the "tube" between two adjacent  $\eta$  contours into  $N$  small sections of length  $\delta l_n$  (see Figure 10). As in (9.4) the area of each compartment is:

$$\delta A_n = (\delta l_n)(\delta \eta) / |\nabla \eta| \quad (9.18)$$

At  $t = 0$  the  $\theta$  distribution can be represented arbitrarily accurately (as  $N \rightarrow \infty$ ) by taking  $\theta$  to be piecewise constant in each compartment. This construction enables one to interpret the average (9.13) geometrically

$$\bar{\theta} = \frac{\sum_{n=1}^N \theta_n (\delta A_n)}{\sum_{n=1}^N (\delta A_n)} \quad (9.19)$$

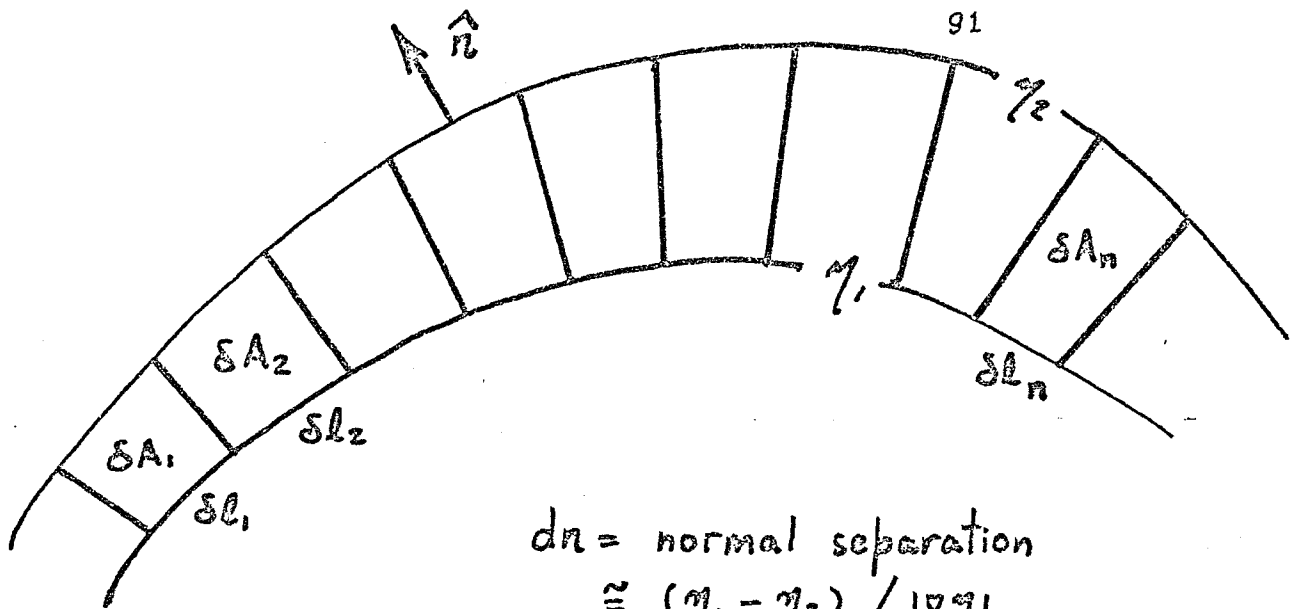
i.e. (9.13) is really an area weighted average. It easily follows from point (i) and (9.17) that  $\theta_t = 0$ .

Now suppose that one is making Eulerian measurements i.e. sitting at a fixed point on the tube and measuring  $\theta$ . Since the fluid moves around the tube one obtains a periodic time series and

$$\langle \theta \rangle = \lim_{T \rightarrow \infty} \frac{1}{T} \int_0^T \theta dt$$

exists. The average above can be related to (9.19) by realizing that as the  $N$  compartments constructed at  $t = 0$  are swept around the tube by the flow their area is unchanged. Moreover, the transit time of the  $n$ 'th compartment past the fixed measuring station is:

$$\begin{aligned} (\delta t_n) &= (\text{length of the compartment at the station}) / (\text{speed of the flow}) \\ &= (\delta l_n) / |\nabla \eta| \end{aligned}$$



$$dn = \text{normal separation} \\ \cong (\eta_1 - \eta_2) / |\nabla \eta_1|$$

$$\Rightarrow \delta A_n = (\delta l_n) dn \\ \cong (\delta l_n) (\eta_1 - \eta_2) / |\nabla \eta_1|$$

Figure 10. The area between two adjacent  $\eta$  contours is divided into small sections at  $t = 0$ . As the compartment is swept around the tube by the flow its area is unchanged.

$$= (\delta A_n) / (\delta n) \quad (\text{from (9.18)})$$

and consequently:

$$\begin{aligned} \langle \theta \rangle &= \sum \theta_n (\delta t_n) / \sum (\delta t_n) \\ &= \sum \theta_n (\delta A_n) / \sum (\delta A_n) \\ &= \bar{\theta} \text{ from (9.19)}. \end{aligned}$$

The above equality, together with the geometric interpretation (9.19), helps one to intuitively understand results based on the average (9.13).

The generalized zonal average of the potential vorticity equation

Using the definitions (9.13) the streamfunction and potential vorticity can be decomposed into mean and fluctuation:

$$\Psi = \bar{\Psi}(n, t) + \psi' \quad (9.20a)$$

$$q = \bar{q}(n, t) + q' \quad (9.20b)$$

It is convenient to define:

$$\bar{\underline{v}} = \hat{z} \times \nabla \bar{\Psi} \quad (9.21a)$$

$$= \frac{\partial \bar{\Psi}}{\partial n} |\nabla \eta| \hat{S} \quad (9.21b)$$

$$\hat{S} = z \times \hat{n} = \text{tangent vector to an } \eta \text{ contour} \quad (9.21c)$$

Since  $\bar{\underline{v}} \cdot \nabla \bar{q} = 0$ , the mean potential vorticity equation is:

$$\bar{q}_t + \overline{\nabla \cdot \underline{v}' q'} = \bar{\Delta} \quad (9.22)$$

The eddy flux term can be rewritten using (9.5):

$$\overline{\nabla \cdot \underline{v}' q'} = \oint_n \nabla \cdot \underline{v}' q' \frac{dl}{|\nabla \eta|} / \oint_n \frac{dl}{|\nabla \eta|}$$

$$\begin{aligned}
&= \left\{ \frac{\partial}{\partial \eta} \iint_{R_\eta} \nabla \cdot \underline{v}' q' d^2 a \right\} / \oint_\eta \frac{dl}{|\nabla \eta|} \\
&= \left\{ \frac{\partial}{\partial \eta} \oint_\eta \underline{v}' q' \cdot \hat{n} dl \right\} / \oint_\eta \frac{dl}{|\nabla \eta|} \quad (9.23)
\end{aligned}$$

so that (9.22) is

$$\bar{q}_t + \frac{\frac{\partial}{\partial \eta} \oint_\eta \underline{v}' q' \cdot \hat{n} dl}{\oint_\eta \frac{dl}{|\nabla \eta|}} = \bar{\Delta} \quad (9.24)$$

The fluctuation potential vorticity equation is obtained by subtracting (9.22) from:

$$\frac{Dq}{Dt} = \Delta$$

There results

$$q'_t + \underline{\bar{v}} \cdot \nabla q' + \underline{v}' \cdot \nabla \bar{q} + F' = \Delta' \quad (9.25a)$$

$$F' = \nabla \cdot \underline{v}' q' - \overline{\nabla \cdot \underline{v}' q'} \quad (9.25b)$$

The fluctuation enstrophy equation is obtained by multiplying (9.25a) by  $q'$  and averaging:

$$\left( \frac{1}{2} \overline{q'^2} \right)_t + \overline{\underline{v}' q' \cdot \nabla \bar{q}} + \overline{\nabla \cdot \frac{1}{2} \underline{v}' q'^2} = \overline{\Delta' q'} \quad (9.26)$$

It is revealing to rewrite the second term in (9.26):

$$\begin{aligned}
\overline{\underline{v}' q' \cdot \nabla \bar{q}} &= \oint_\eta \underline{v}' q' \cdot \nabla \bar{q} \frac{dl}{|\nabla \eta|} / \oint_\eta \frac{dl}{|\nabla \eta|} \\
&= \left\{ \frac{\partial \bar{q}}{\partial \eta} \right\} \oint_\eta \underline{v}' q' \cdot \hat{n} dl / \oint_\eta \frac{dl}{|\nabla \eta|} \quad (9.27)
\end{aligned}$$

so that (9.26) is:

$$\left(\frac{1}{2} \overline{q'^2}\right)_t + \left\{ \frac{\oint_{\eta} \underline{v}' \cdot \hat{n} \, dl}{\oint_{\eta} \frac{dl}{|\nabla \eta|}} \right\} \left\{ \frac{\partial \bar{q}}{\partial \eta} \right\} + \overline{\nabla \cdot \frac{1}{2} \underline{v}' \cdot \underline{v}'^2} = \overline{\Delta' q'} \quad (9.28)$$

Equation (9.24) and (9.28) are the principal results of this subsection; note how it's possible to eliminate  $\oint_{\eta} \underline{v}' \cdot \hat{n} \, dl$  between these two relations. In zonal geometry this elimination leads to relationships which emphasize the role of wave transience and dissipation in mean flow generation, see Rhines (1977), Rhines and Holland (1979) and McEwan, Thompson and Plumb (1980). A similar application in a non-zonal geometry is given in the next subsection.

#### Introduction of Lagrangian coordinates.

Following Rhines (1977) it is informative to rewrite (9.24) and (9.28) using Lagrangian coordinates. I shall use the small amplitude version of Andrews and McIntyres (1978) generalized Lagrangian mean formulation. The disturbance associated particle displacement  $\underline{\xi}'$  is defined by

$$\left(\frac{\partial}{\partial t} + \bar{\underline{v}} \cdot \nabla\right) \underline{\xi}' = \underline{v}^{\ell} \quad (9.29a)$$

$$= \underline{v}' + (\underline{\xi}' \cdot \nabla) \bar{\underline{v}} \quad (9.29b)$$

where  $\bar{\underline{v}}$  is defined in (9.21) and  $\underline{v}^{\ell}$  is the Lagrangian disturbance velocity. If we also define  $\delta'$  by

$$\Delta' = \left(\frac{\partial}{\partial t} + \bar{\underline{v}} \cdot \nabla\right) \delta' \quad (9.30)$$

then the linearized fluctuation potential vorticity equation

$$\left(\frac{\partial}{\partial t} + \bar{\underline{v}} \cdot \nabla\right) q' + \underline{v}' \cdot \nabla \bar{q} = \Delta' \quad (9.31)$$

reduces to

$$q' = \delta' - \underline{\xi}' \cdot \nabla \bar{q} \quad (9.32)$$

if  $\bar{\Delta} = 0$ .

It is easy to verify (9.32) by direct calculation. Let

$$\bar{D} = \frac{\partial}{\partial t} + \underline{v} \cdot \nabla$$

and then

$$\begin{aligned} \bar{D}(q' + \underline{\xi}' \cdot \nabla \bar{q}) &= (\Delta' - \underline{v}' \cdot \nabla \bar{q}) + (\underline{v}' + (\underline{\xi}' \cdot \nabla) \underline{v}) \cdot \nabla \bar{q} \\ &\quad + \underline{\xi}' \cdot \bar{D} \nabla \bar{q} \\ &= \bar{D} \delta' + (\underline{\xi}' \cdot \nabla) (\bar{D} \bar{q}) \\ &= \bar{D} \delta' \end{aligned}$$

if  $\bar{\Delta} = 0$ . Integrating the above relation from the initial time gives (9.32).

From (9.24) it is apparent that changes in  $q$  are induced by

$\oint_{\eta} \underline{v}' q' \cdot \hat{n} dl$ . Using (9.32) one can obtain an alternative expression for this integral:

$$\oint_{\eta} \underline{v}' q' \cdot \hat{n} dl = \oint_{\eta} \delta' \underline{v}' \cdot \hat{n} dl - \oint_{\eta} (\underline{\xi}' \cdot \nabla \bar{q}) \underline{v}' \cdot \hat{n} dl \quad (9.33a)$$

$$\oint_{\eta} \underline{v}' q' \cdot \hat{n} dl = \oint_{\eta} \delta' \underline{v}' \cdot \hat{n} dl - \frac{\partial \bar{q}}{\partial t} \oint_{\eta} \left\{ \frac{1}{2} \nabla \cdot (\eta \underline{\xi}')^2 \right\} t \frac{dl}{|\nabla \eta|} \quad (9.33b)$$

The transition from (9.33a) to (9.33b) is complicated algebraically and the intermediate steps are relegated to Appendix A at the end of this chapter. Equation (9.33b) emphasizes the importance of dissipation and transience in producing changes in the mean state. When (9.33b) and (9.24) are combined there results:

$$\oint_{\eta} \frac{dl}{|\nabla\eta|} \bar{q}_t - \frac{\partial}{\partial\eta} \left\{ \oint_{\eta} \frac{1}{2} (\nabla \cdot \eta \xi')^2 \right\}_t \frac{dl}{|\nabla\eta|} \frac{\partial \bar{q}}{\partial \eta} - \oint_{\eta} \delta' \underline{v}' \cdot \hat{n} dl \Big\} = \oint_{\eta} \frac{dl}{|\nabla\eta|} \bar{\Delta} \quad (9.34)$$

The above form emphasizes the diffusive effects of wave transience; the effective diffusivity is:

$$\oint_{\eta} \frac{1}{2} (\nabla \cdot \eta \xi')^2 \frac{dl}{|\nabla\eta|} = \frac{\partial}{\partial \eta} \iint_{\eta} (\nabla \eta \cdot \underline{\xi}') (\nabla \eta \cdot \underline{\xi}'_t) d^2a$$

and so is positive if the particle displacements along  $\nabla\eta$  are growing.

In the next subsection I shall show that in a steady wave field small Rayleigh damping also produces diffusion of  $\bar{q}$ .

#### Effects of weak dissipation in a steady wave field

It is difficult to make general statements about the term  $\oint_{\eta} \delta' \underline{v}' \cdot \hat{n} dl$  in (9.34). In this subsection I shall consider weak "Rayleigh damping"

$$\Delta' = -\lambda q' = \bar{D} \delta' \quad (9.35)$$

and suppose that the wave field is steady (i.e.  $\overline{a' b'_t} = 0$ ).

In this case the enstrophy equation (9.28) shows that

$$\oint_{\eta} \underline{v}' q' \cdot \hat{n} dl \frac{\partial \bar{q}}{\partial \eta} = -\lambda \oint_{\eta} q'^2 \frac{dl}{|\nabla\eta|} < 0 \quad (9.36)$$

or from (9.33b)

$$\oint_{\eta} \delta' \underline{v}' \cdot \hat{n} dl \frac{\partial \bar{q}}{\partial \eta} = -\lambda \oint_{\eta} q'^2 \frac{dl}{|\nabla\eta|} \quad (9.37)$$

so that the flux of potential vorticity is down gradient in accord with the notion that the eddies have a diffusive effect. For the simple

damping in (9.35) this idea can be made more precise.

Begin by defining

$$\underline{\xi} = \delta' \underline{\xi}'$$

and then (9.29b) shows that

$$\bar{D} \zeta_i + \lambda q' \xi_i = \delta' v_i' + (\underline{\xi} \cdot \nabla) \bar{v}_i \quad (9.38)$$

Multiplying the above by  $n_i$  and integrating round an  $n$  contour gives:

$$\oint_n \delta \underline{v}' \cdot \hat{n} \, dl = \lambda \oint_n q' \underline{\xi}' \cdot \hat{n} \, dl \quad (9.39a)$$

$$= \oint_n \underline{v}' q' \cdot \hat{n} \, dl \quad (9.39b)$$

(see Appendix B). If the dissipation  $\lambda$  is sufficiently small then to a first approximation (9.32) is

$$q' = - \underline{\xi}' \cdot \nabla \bar{q} = - \frac{\partial \bar{q}}{\partial n} \underline{\xi}' \cdot \nabla n$$

and (9.39a) becomes

$$\oint_n \delta \underline{v}' \cdot \hat{n} \, dl = - \lambda \frac{\partial \bar{q}}{\partial n} \oint_n (\underline{\xi}' \cdot \nabla n)^2 \frac{dl}{|\nabla n|}$$

Equation (9.34) is then

$$\left\{ \oint_n \frac{dl}{|\nabla n|} \right\}_{q_t} - \frac{\partial}{\partial n} \left\{ \frac{\partial \bar{q}}{\partial n} \lambda \oint_n (\nabla \cdot n \underline{\xi}')^2 \frac{dl}{|\nabla n|} \right\} = \oint_n \frac{dl}{|\nabla n|} \bar{\Delta} \quad (9.40)$$

A third proof of potential vorticity homogenization follows from (9.40); if  $q_t = \Delta = 0$ , then:

$$\frac{\partial \bar{q}}{\partial n} \left\{ \lambda \oint_n (\nabla \cdot n \underline{\xi}')^2 \frac{dl}{|\nabla n|} \right\} = \text{constant}$$

If the region is simply connected the constant must be zero since we can evaluate the above relation on the limiting  $\eta$  contour with zero area. Presumably the left hand side must vanish there. In this case it follows that  $q = \text{constant}$ .

## Appendix A

### Algebra leading to (9.33b)

The last term in (9.33a) is:

$$\oint_{\eta} (\underline{\xi}' \cdot \nabla \bar{q}) \underline{v}' \cdot \hat{n} \, dl = \frac{\partial \bar{q}}{\partial \eta} \frac{\partial}{\partial \eta} \iint (\underline{\xi}' \cdot \nabla \eta) (\underline{v}' \cdot \nabla \eta) \, d^2 a \quad (\text{A1})$$

where (9.5) was used. Replace  $\underline{v}'$  in the above using (9.29b) and use  $\nabla \cdot \underline{\xi}' = \nabla \cdot \underline{v}' = 0$ . The desired result follows if:

$$\iint \left\{ \nabla \cdot (\underline{\xi}' \eta) \right\} \nabla \times (\underline{\bar{v}} \times \underline{\xi}') \cdot \nabla \eta \, d^2 a = 0 \quad (\text{A2})$$

$$\begin{aligned} \text{Since } \nabla \times (\underline{\bar{v}} \times \underline{\xi}') \cdot \nabla \eta &= \nabla \cdot \left\{ (\underline{\bar{v}} \times \underline{\xi}') \times \nabla \eta \right\} \quad (\nabla \times \nabla \eta = 0) \\ &= -\nabla \cdot \left\{ \underline{\bar{v}} \underline{\xi}' \cdot \nabla \eta \right\} \quad (\underline{\bar{v}} \cdot \nabla \eta = 0) \\ &= -(\underline{\bar{v}} \cdot \nabla) \nabla \cdot (\underline{\xi}' \eta) \quad (\nabla \cdot \underline{\bar{v}} = 0) \end{aligned}$$

the left hand side of (A2) is

$$-\iint \nabla \cdot (\underline{\xi}' \eta) (\underline{\bar{v}} \cdot \nabla) \nabla \cdot (\underline{\xi}' \eta) \, d^2 a$$

which in turn is equal to

$$-\iint (\underline{\bar{v}} \cdot \nabla) \left\{ \frac{1}{2} \nabla \cdot (\underline{\xi}' \eta)^2 \right\} \, d^2 a = -\iint \underline{\bar{v}} \cdot \left\{ \underline{\bar{v}} \frac{1}{2} \nabla \cdot (\underline{\xi}' \eta)^2 \right\} \, d^2 a .$$

Using the divergence theorem this is zero since  $\underline{\bar{v}} \cdot \hat{n} = 0$ .

## Appendix B

Algebra leading to (9.39a)

Equation (9.38) is:

$$\overline{D}\underline{\xi} - (\underline{\xi} \cdot \nabla)\underline{\overline{v}} = \delta' \underline{v}' - \lambda q' \underline{\xi}' \quad (B1)$$

$$= \delta' \underline{\xi}' \quad (B2)$$

To get (9.39a) multiply (B1) by  $n$  and integrate around a closed  $n$  contour. Because the wave field is assumed to be steady

$$\begin{aligned} \oint_n \underline{\xi}_t \cdot \hat{n} \, dl &= \oint_n (\delta' \underline{\xi}')_t \cdot \hat{n} \, dl \\ &= \oint_n \frac{dl}{|\nabla n|} (\overline{\delta' \underline{\xi}' \cdot \nabla n})_t \\ &= 0 \end{aligned}$$

The remaining terms on the left hand side are:

$$\begin{aligned} \oint_n \nabla \times (\underline{\xi} \times \underline{\overline{v}}) \cdot n \, dl &= \frac{\partial}{\partial n} \iint \nabla \times (\underline{\xi} \times \underline{\overline{v}}) \cdot \nabla n \, d^2a \\ &= \frac{\partial}{\partial n} \iint \nabla \cdot \{ (\underline{\xi} \times \underline{\overline{v}}) \times \nabla n \} \\ &= \frac{\partial}{\partial n} \iint \nabla \cdot \{ (\underline{\xi} \cdot \nabla n) \underline{\overline{v}} \} \\ &= \frac{\partial}{\partial n} \oint_n (\underline{\xi} \cdot \nabla n) \underline{\overline{v}} \cdot \hat{n} \, dl \\ &= 0 \quad (\underline{\overline{v}} \cdot \hat{n} = 0) \end{aligned}$$

CHAPTER 3  
General Circulation Models  
and Western Boundary Layer Closures

Abstract of Chapter 3

This chapter uses the results of the previous sections to construct baroclinic models of the wind-driven circulation.

In section 10 it is shown in the context of a two layer model how closed geostrophic contours in the lower layer naturally form in the northwest corner of an ocean basin. Order one flows in the lower layer are confined to this region and calculated by requiring the potential vorticity to be uniform within it.

In section 11 a similar calculation is performed with a continuously stratified model. The goal here is to determine the shape of the region of uniform potential vorticity which bounds the subsurface wind-driven gyre. It is found that the gyre is deepest in the northwest and shoals as one moves south and east.

In section 12 western boundary layer dynamics are considered for the first time. This section is an attempt to construct a completely inviscid, lower layer boundary closure. The model consists of specifying a simple form for  $\Psi_1$ , (12.3a), and then calculating the lower layer boundary flow by requiring the potential vorticity to be uniform at all points connected to the interior region of homogeneous potential vorticity by streamlines. All the frictional processes in this model are subsumed into the form assumed for  $\Psi_1$ .

By contrast section 13 is an investigation of a frictionally dominated western boundary layer. This model emphasizes how dependent the homogenization results of previous sections are on the assumption that dissipation is negligible everywhere on a streamline. In this model the potential vorticity is not uniform within the closed geostrophic contours but rather is determined by the conditions within the frictional boundary layers.

## 10. Closed, Interior Geostrophic Contours in a Layered General Circulation Model

### Introduction - recapitulation of previous results.

The principal components of a baroclinic theory of the wind driven circulation have now been discussed. It remains to assemble them into a coherent whole. In section 4 it was shown how sufficiently strong forcing produces closed geostrophic contours in subsurface density layers. In section 5 it was shown, in the context of a homogeneous model, that rapid circulation is induced around such closed geostrophic contours by weak forcing. This suggests that in a baroclinic model, where the geostrophic contours are closed by the deformation of density surfaces, weak vertical stress transmission will act effectively in the closed regions to produce strong flows. The obvious smaller scale process capable of transmitting vertical stress is the mesoscale eddy field. In sections 6 and 7 it was shown that the usual parametrization of the mesoscale eddy field as a horizontal diffusivity of potential vorticity is equivalent to vertical friction with a coefficient proportional to  $N^{-2}$ . The quasigeostrophic, turbulent extension of the Batchelor-Prandtl theorem in section 8 shows that horizontal diffusivity of potential vorticity or equivalently, vertical diffusion of momentum, produces uniform potential vorticity within the region of closed contours. Thus the picture which emerges is of subsurface flow, driven by weak vertical stress, confined to a region of uniform potential vorticity. In this chapter it is shown how the extent of this region, and the vertical structure of the wind-driven flow, follows directly from the requirement that the potential vorticity be uniform within it.

Three layer quasigeostrophic equations.

In the remainder of this section I shall use the three layer quasigeostrophic equations introduced in section 3. It was shown in that section how the barotropic flow:

$$H\Psi_B = H_1\Psi_1 + H_2\Psi_2 + H_3\Psi_3$$

$$H = H_1 + H_2 + H_3$$

satisfies the simple equation

$$\beta H \frac{\partial \Psi_B}{\partial x} = f_0 w_E + (\text{bottom drag term}) \quad (10.1)$$

If the bottom drag is neglected the Sverdrup balance is recovered and (10.1) can be solved for  $w_E$ ; with the simple choice:

$$w_E = -w_0 \cos\left(\frac{\pi}{2} \frac{y}{L}\right) \quad (10.2)$$

and has

$$\Psi_B = \left(\frac{f_0 w_0}{\beta H}\right) (a - x) \cos\left(\frac{\pi}{2} \frac{y}{L}\right) \quad (10.3)$$

where  $x = a$  is the eastern boundary. The streamlines calculated from (10.3) are shown in figure 1. This is as far as classical theory goes.

The vertical structure of the currents is undetermined.

All the lower layer geostrophic contours are blocked

To make further progress I assume that:

$$H_3 \gg H_1, H_2. \quad (10.4)$$

This ensures that the displacement of the lowest interface cannot produce fractional depth changes comparable to the  $\beta$ -effect in the lowest layer.

Thus away from inertial boundary layers:

$$q_3 \approx \beta y$$

and all the deep geostrophic contours in the lowest layer are blocked by coastal boundaries. This implies that the flow in the lowest layer is weak, since weak vertical stresses produce only weak flow across blocked contours (see section 5). According to this reasoning then, a negligible fraction of the Sverdrup transport is in the lowest layer and

$$H\psi_B \approx H_1\psi_1 + H_2\psi_2 \quad (10.5)$$

The assumption that the lower layer is motionless reduces the three layer model to an equivalent two layer model. The boundary layer analysis in this chapter is based on this two layer model. It is important to realize that the two layers model the upper thermocline waters rather than the complete column.

The geostrophic contours of the middle layer can be calculated

The next step in determining the vertical structure is to focus on the middle layer. In the interior, away from inertial boundary layers:

$$q_2 = \beta y + F(\psi_1 - 2\psi_2) \quad (10.6a)$$

$$F = (f_0^2 / g'H_1) \quad (10.6b)$$

where I have made the nonessential assumption that:

$$g' = g'' \quad \text{and} \quad H_1 = H_2.$$

Using (10.5), (10.6a) is:

$$q_2 = \beta y + F\left(\frac{H}{H_1}\right)\psi_B - 3F\psi_2 \quad (10.7a)$$

$$= \hat{q}_2 - 3F\psi_2 \quad (10.7b)$$

Since the motion in the second layer is almost dissipationless and unforced, (10.7b) shows that:

$$q_2 = Q_2(\hat{q}_2) \quad \text{and} \quad \psi_2 = \Psi_2(q_2). \quad (10.8)$$

The function  $\hat{q}_2$  is contoured for various values of the forcing in figure 11. Note how the  $\hat{q}_2$  contours are closed in the northwest corner of the basin; the extent of this region increases as the parameter

$$F = \left( \frac{f_0 w_0}{\beta^2 H_1} \right) F \quad (10.9a)$$

$$= \left( \frac{f_0^3 w_0}{g' \beta^2 H_1^2} \right) \quad (10.9b)$$

increases.

In the region where the  $\hat{q}_2$  contours close,  $q_2$  is constant and so:

$$\psi_2 = \frac{1}{3F} \left\{ \hat{q}_2 - q_2 \right\} \quad (10.10a)$$

$$\psi_1 = \left( \frac{H}{H_1} \right) \psi_B - \psi_2 \quad (10.10b)$$

The constant  $q_2$  in (10.10a) is chosen to make  $\psi_2$  continuous on the outermost closed  $\hat{q}_2$  contour. Since  $\psi_2$  is zero on the boundary and this outermost contour strikes the northern boundary where  $y = L$  and  $\hat{q}_2 = \beta L$ ,  $q_2 = \beta L$ .

In the region where the  $q_2$  contours are blocked the solution is

$$\psi_1 = \left( \frac{H}{H_1} \right) \psi_B \quad (10.11a)$$

$$\psi_2 = 0 \quad (10.11b)$$

The streamline pattern calculated from (10.10) and (10.11) is sketched in figure 12 for the case  $F = 1$ .

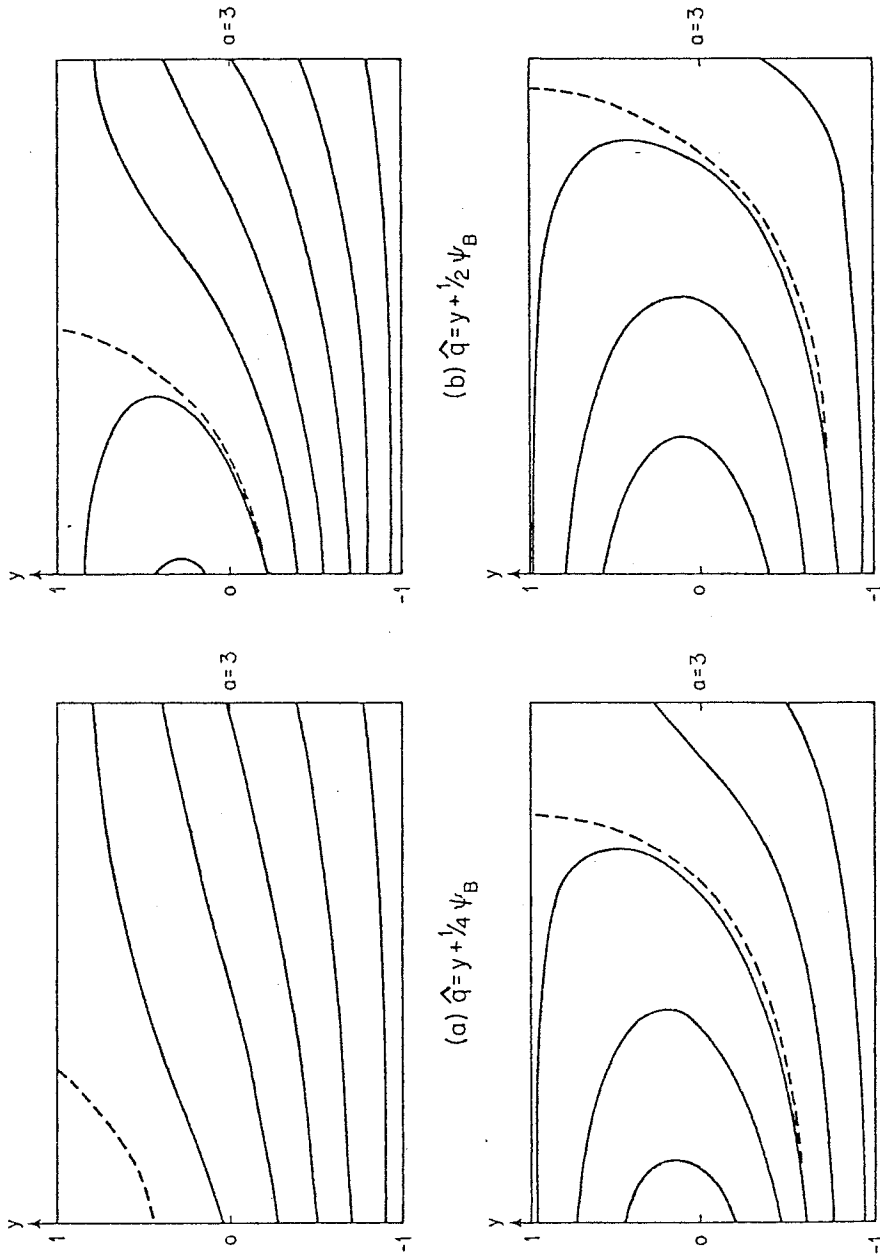
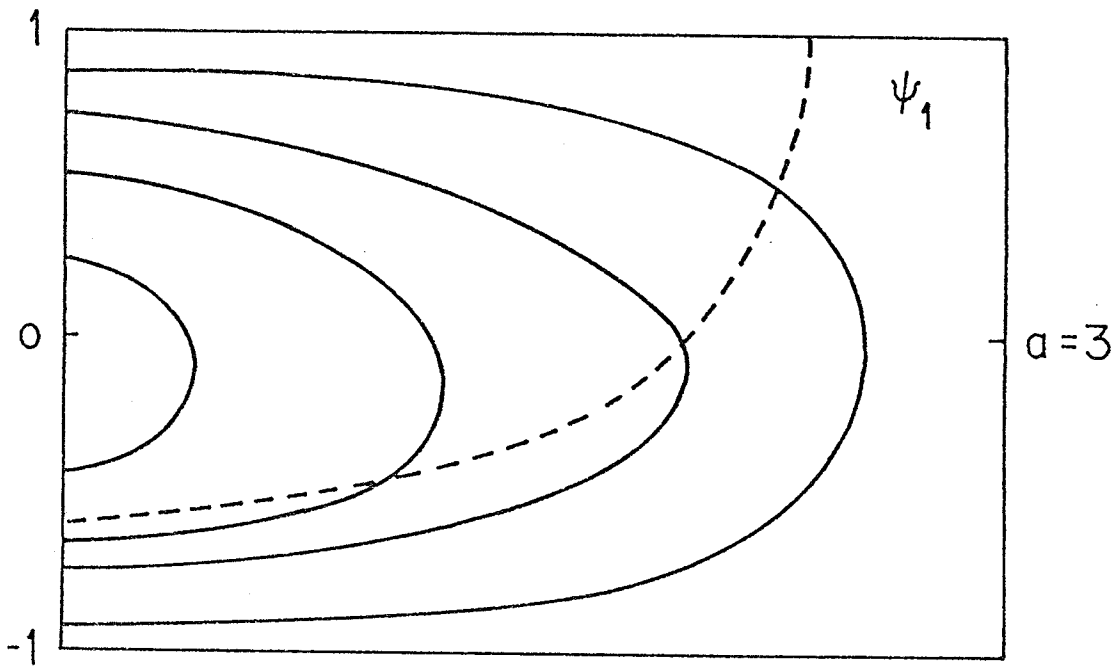
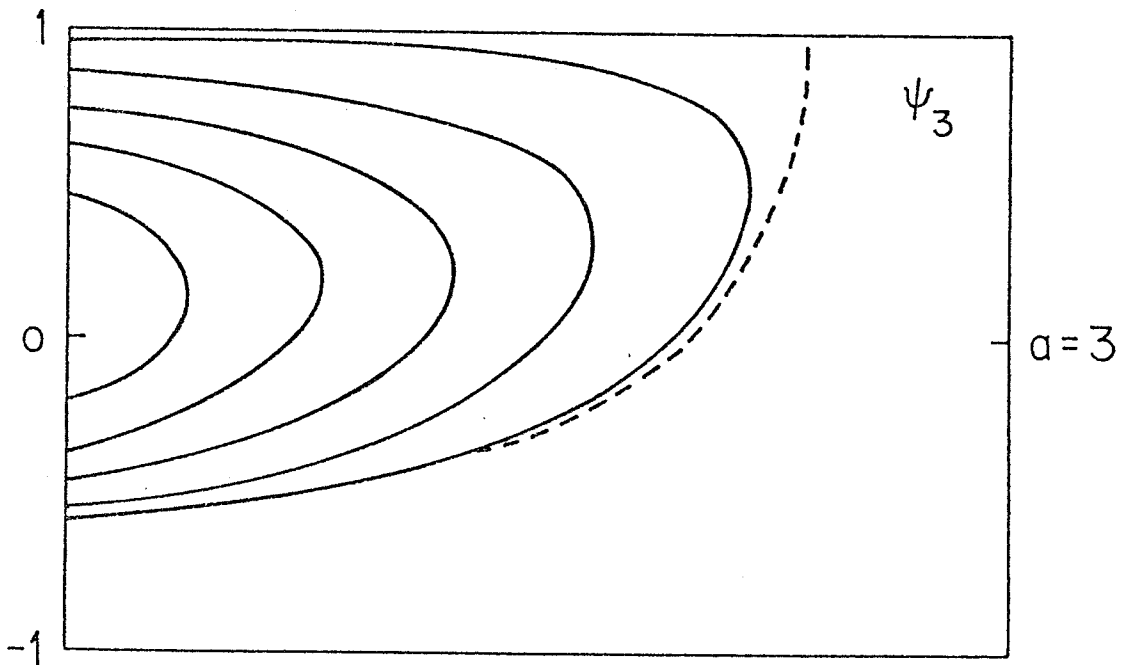


Figure 11. The function  $\hat{q} = y + \bar{F}(a - x) \cos(\frac{\pi}{2} y)$  for various values of  $\bar{F}$ . The outermost closed contour is dashed. As the strength of the forcing increases the closed contour region expands southwards and eastwards.



(a)



(b)

Figure 12. The streamline pattern corresponding to (10.10). The dashed curve is the outermost closed  $\hat{q}_2$  contour inside of which the potential vorticity is uniform in the lower layer.

Calculation of weak subsurface flows in blocked regions.

Now that first approximations of  $\psi_i$  have been obtained using the homogenization theory it is instructive to indicate how the weak flows in the blocked regions could be calculated. This is important because it further elucidates the distinction between closed regions, where weak stresses drive order one flows, and blocked regions, where weak stresses drive weak flows.

Consider, for simplicity, the blocked regions in the middle layer. The first order solution in this region is given by (10.11) with:

$$q_2 = \beta y + F\left(\frac{H}{H_1}\right)\psi_B$$

The form of the next correction depends in detail on how the eddy flux on the right hand side of

$$J(\overline{\psi}_2, \overline{q}_2) = - \overline{J(\psi'_2, q'_2)} \quad (10.12)$$

is parameterized. (In (10.12) the overbar denotes an average, previously in this section it has been taken for granted that  $\psi_1$  and  $\psi_2$  denoted the average streamfunctions.) For illustrative purposes I shall use the simplest parametrization:

$$J(\psi_2, q_2) = \kappa \nabla^2 q_2 \quad (10.13)$$

Implicit in the preceding development is the assumption that  $\kappa$  is small so if  $\psi_2$  is to be order one it must be inertially balanced, see (10.8). In the blocked regions considered here an inertial flow is impossible since it violates the eastern boundary condition. Thus in (10.13)  $\psi_2$  is order  $\kappa$ :

$$\psi_2 = \kappa \phi_2 \quad (10.14)$$

Putting (10.14) into (10.13) and neglecting all the obviously small terms gives a familiar balance:

$$J(\phi_2, \beta y + F(\frac{H}{H_1})\psi_B) = F(\frac{H}{H_1}) \nabla^2 \psi_B \quad (10.15)$$

Equation (10.15) is the turbulent Sverdrup balance described by Rhines and Holland (1979). The  $q_2$  field is the  $\beta$ -effect modified by variations in layer thickness. The "wind stress" on the right hand side is the curl of the Sverdrup flow in the upper layer. At the eastern boundary

$\frac{\partial}{\partial y} \left\{ \beta y + F(\frac{H}{H_1})\psi_B \right\} > 0$  so that (10.15) can be solved in principle by

integrating westward in the usual way. The main point is that if  $\kappa$  is small,  $\psi_2$  is small and the vertically integrated Sverdrup transport is confined to the upper, directly forced layer.

## 11. A Continuously Stratified Theory

### Introduction - the continuously stratified model

In this section I extend the results of section 10 to a continuously stratified model. The goal here is to develop more intuition about the shape of the bowl which contains the wind driven circulation; to this end the vertical resolution will be increased by using the continuously stratified model introduced in section 1.

With the scalings in (1.13a,b) and  $\epsilon^2 \ll 1$  the nondimensional potential vorticity equation is

$$J(\psi, q) = \kappa \nabla^2 q \quad (11.1)$$

$$q = y + (F \psi_z)_z \quad (11.2)$$

where  $F$  is defined in (1.8d) and (1.9b). If  $N^2$  is constant then without loss of generality  $F = 1$ . The vertical boundary conditions are then

$$w = -J(\psi, \psi_z) \quad (11.3a)$$

$$= w_E(y) \quad \text{at } z = 0 \quad (11.3b)$$

$$\psi, \psi_z \rightarrow 0 \quad \text{as } z \rightarrow -\infty \quad (11.3c)$$

The first boundary condition is the standard condition applied at the base of the upper Ekman layer. The second is based on the expectation that the wind driven circulation is shallow, relative to the depth of the ocean; this is in accord with (1.13a) and the numbers in table 1.

### The depth of the wind driven gyre: $z = -D(x,y)$

Now suppose that the wind driven circulation lies between  $z = 0$  and  $z = -D(x,y)$ ; the surface  $z = -D(x,y)$  is a "bowl" which vertically bounds

the wind driven flow. The goal of this section is to calculate  $D$  in terms of the forcing  $w_E(x,y)$  and the basin geometry. This formulation was suggested by Rhines (personal communication).

In accord with the weak eddy assumption  $\kappa \ll 1$ :

$$q = Q(\psi, z) \quad \text{if } 0 > z > -D$$

and then using the homogenization arguments of chapter 2:

$$\frac{\partial Q}{\partial \psi} = 0 \quad \text{if } 0 > z > -D(x,y)$$

so that:

$$q = y + \psi_{zz} = y_0(z) \quad \text{if } 0 > z > -D(x,y) \quad (11.4)$$

Outside the bowl  $0 > z > -D(x,y)$  the wind driven flow vanishes so that in the absence of deep thermohaline forcing or flow imposed by distant sources of fluid (e.g. deep water formation):

$$\psi = 0 \quad \text{if } z < -D(x,y)$$

Now as in section 10 (see the discussion after (10.10)) the function  $y_0(z)$  in (11.4) is determined from the matching condition at the outermost closed geostrophic contour. Anticipating that these contours will resemble those of the layered model shown in figure 11, we see that they are contiguous with the northern boundary of the gyre where  $q = y = 1$  so that:

$$y_0(z) = 1. \quad (11.5)$$

Since the comparison with the layered model in section 10 may not be entirely convincing I shall assume that  $y_0$  is a constant (rather than a function of  $z$ ) and examine the consequences of the alternatives to (11.5). I hope this will further motivate the choice  $y_0 = 1$ .

Solution of (11.4)

The solution of (11.4) which satisfies:

$$\Psi = \Psi_z = 0 \quad \text{on } z = -D(x,y)$$

is:

$$= \frac{1}{2} (z + D)^2 (y_0 - y) \quad \text{if } -D < z < 0 \quad (11.6a)$$

$$= 0 \quad \text{if } z < -D. \quad (11.6b)$$

$D(x,y)$  is determined by requiring that (11.6a) satisfy the upper boundary condition (11.3a,b). The vertical velocity is

$$w = \frac{1}{2} (z + D)^2 (y_0 - y) \left( \frac{\partial D}{\partial x} \right) \quad (11.7)$$

so that (11.3b) implies

$$\frac{\partial}{\partial x} (D^3) = 6(y_0 - y)^{-1} w_E$$

or

$$D^3 = 6(y_0 - y)^{-1} \Psi_B \quad (11.8)$$

where

$$\Psi_B = (x - a) w_E \quad (11.9a)$$

$$a = \text{position of eastern boundary} \quad (11.9b)$$

A model of the Ekman pumping:  $w_E = -\{1 - |y|\}$ .

The streamline pattern corresponding to (11.6) and (11.8) is surprisingly difficult to visualize. It is helpful to consider the simple forcing function

$$w_E = -\{1 - |y|\} \quad (11.10)$$

since in this case the streamlines are simple algebraic curves. This is only for convenience, all plausible models of the Ekman pumping in a subtropical gyre produce qualitatively similar patterns.

With  $w_E$  given by (11.10),  $D[6(a-x)]^{-1/3}$  is plotted against  $y$  in figure 13. Clearly the choice  $y_0 < 1$  leads to unphysical results and can be excluded. The choice  $y_0 > 1$  leads to superficially reasonable results. There are analogous patterns in the three layer model of section 10; they correspond to picking one of the inner closed contours in figure 11 to bound the circulation in the middle layer. Such a configuration cannot persist since the upper layer flow exerts a stress around the available closed contours at the rim of the bowl and eventually accelerates a flow around them. This process deepens the bowl until all the closed contours have an inertial flow around them. The limiting situation, in which the bowl is as large as possible and abuts the northern boundary, corresponds to  $y_0 = 1$ . Although the above discussion has been couched in terms of the layer model, similar considerations must apply in a continuously stratified model; note how the bowl deepens and moves up against the northern boundary as  $y_0$  decreases to 1 in figure 13.

To summarize, the streamfunction is

$$\psi = \begin{cases} \frac{1}{2} (z + D)^2 (1 - y) & -D < z < 0 & (11.11a) \\ 0 & z < -D & (11.11b) \end{cases}$$

where

$$D = [6(1 - y)^{-1} (x - a) w_E(y)]^{1/3} \quad (11.12)$$

The surface  $z = -D(x, y)$  bounds the region containing the wind driven circulation from which the potential vorticity has been expelled. The region is deepest in the northwest corner of the basin and shoals as one

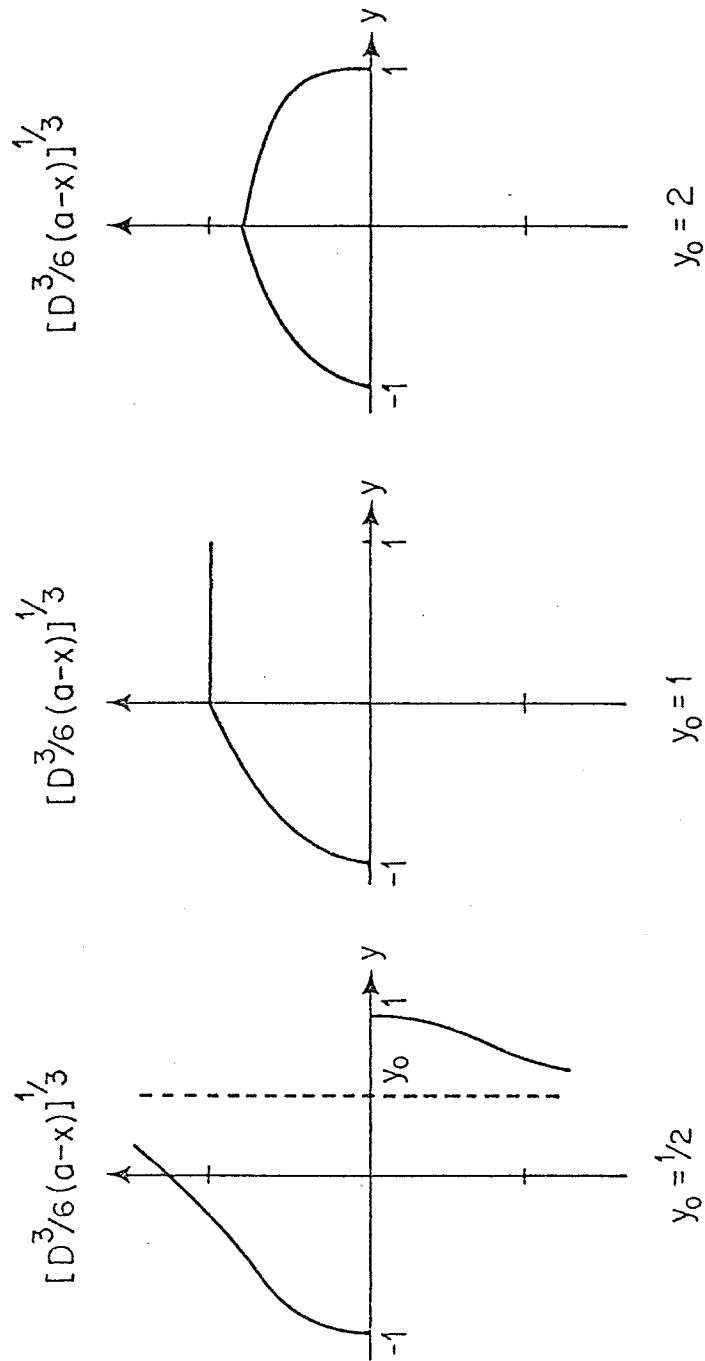


Figure 13. The shape of the bowl bounding the wind-driven circulation. This figure illustrates the consequences of varying the constant  $y_0$ . In the text it is argued that  $y_0 = 1$  is the preferred choice.

moves south and east, see figure 14. The streamlines corresponding to (11.10) are sketched in figure 15. This sequence clearly shows how the wind driven flow is compressed into the northwest corner of the basin as one moves downwards. This northwest shift of the gyre center is a well known feature of descriptive studies of the circulation, e.g. Worthington (1976) figures 24, 26, 29 and 41.

Some remarks on the relationship between the present theory and thermocline theories.

Before turning to the western boundary layer models which complete this chapter I shall digress and discuss the relationship of the present theory to thermohaline circulation theory, e.g., Needler (1967), Welander (1971) and for a recent review Veronis (1981).

The most important difference between the two theories has already been mentioned in section 1 viz. the present theory takes the basic stratification as given and calculates the wind-driven currents; thermohaline theory is more ambitious in that it attempts to calculate the density field and the wind-driven current simultaneously.

Because the present theory attempts to do less it is more successful at what it does do. For example the vertical length scale of the circulation is given by (1.13) and is not an adjustable parameter which can be picked to make the solution look like an observed circulation pattern. An example of this latter procedure is Welander's (1971) steady, ideal (i.e., nondiffusive) fluid thermocline model. In this development the existence of three conserved quantities  $q$ ,  $\rho$  and the Bernoulli

function  $B = p + \rho g z$  is exploited to obtain an elegant solution. In my opinion the most unsatisfactory aspect of the solution is the initial ad hoc specification:

$$q = a \rho + b B + c$$

where  $a$ ,  $b$  and  $c$  are arbitrary constants. The above specification leads to a tractable mathematical problem. The constants  $a$  and  $b$  are chosen to give the density field an inflection point at a desired depth and to adjust the thickness of the thermocline. I believe that the absence of such adjustable parameters is a desirable quality in a theoretical model.

It is clear, however, that the present model must be extended to include thermohaline effects; some of the deficiencies in the model can only be addressed by allowing the density surfaces to undergo large vertical excursions. For example, what of geostrophic contours which strike the vertical boundaries such as the base of the surface mixed layer? Presumably they are "blocked" yet it is likely they are qualitatively different from the coastally blocked contours which the present work has focused on. Is it possible to combine the wind-driven circulation model given here with a simple model of the abyssal circulation such as that of Stommel, Arons and Faller (1958) and Stommel and Arons (1960)?

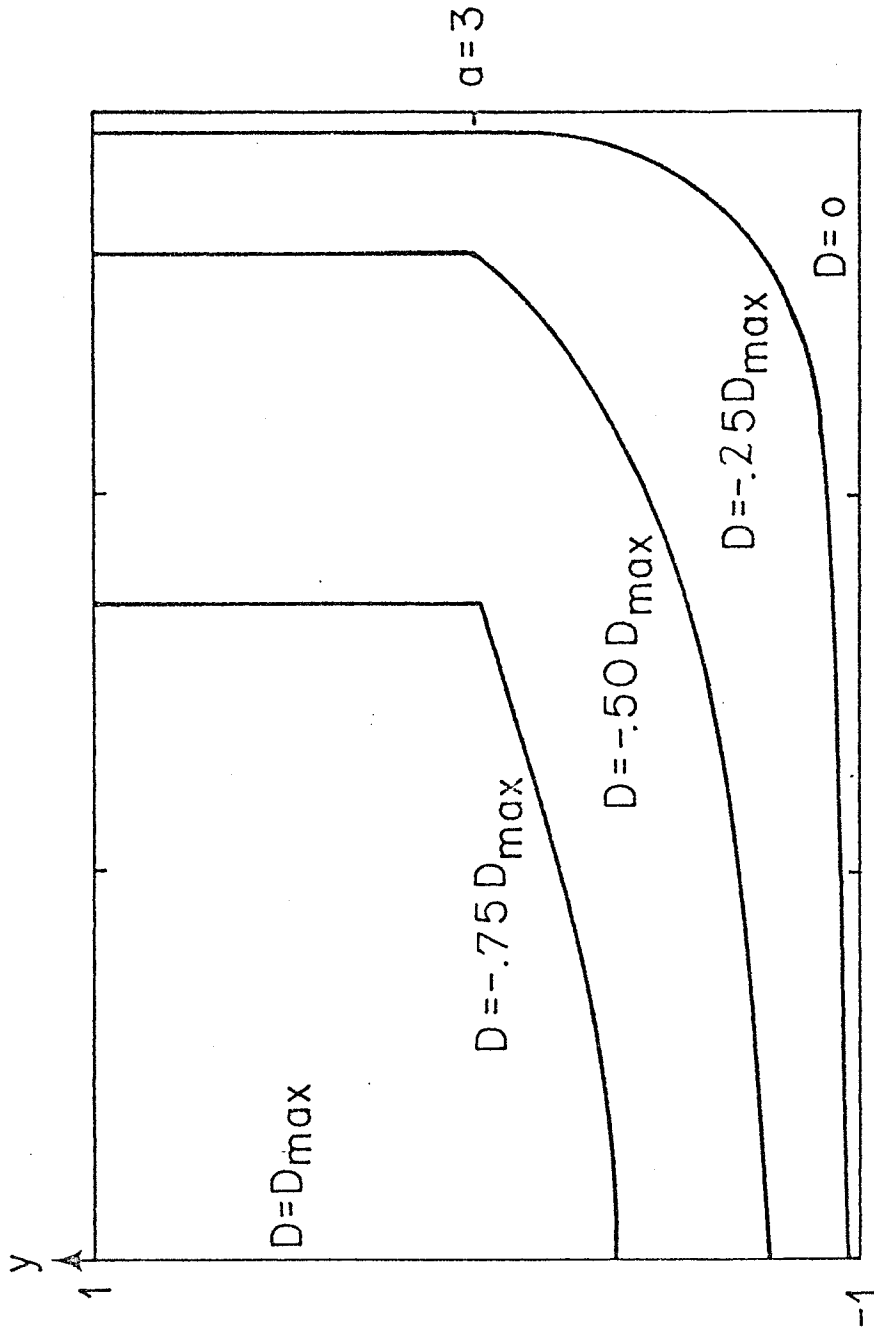


Figure 14. The depth of the wind driven circulation as a function of position from (11.12). The bowl is deepest at the line segment  $x = 0$ ,  $0 < y < 1$ . The circulation becomes shallower as one moves south and east.

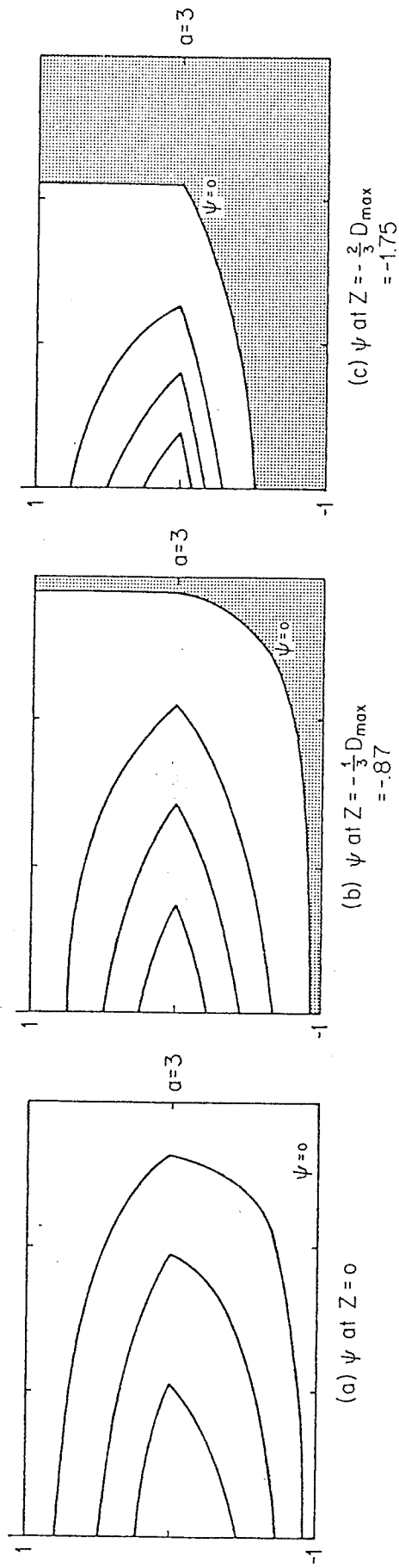


Figure 15. The streamlines from (11.11a) at various depths in the wind-driven gyre. There is no motion in the stippled regions outside the surface  $z + D = 0$ . The flow is confined to the region of uniform potential vorticity.

## 12. A Nondissipative Model of the Subsurface Western Boundary Layer.

### Some qualitative arguments concerning western boundary layer dynamics

The circulation patterns discussed in sections 10 and 11 and shown in figures 12 and 15 must be closed by appending western boundary layers. This is of course the same problem which arises in homogeneous circulation theory. In the baroclinic theory discussed here all the familiar difficulties of the homogeneous theory re-emerge, compounded by the addition of an extra spatial dimension.

One of the most vexing problems in the homogeneous circulation theory is the necessity of including some form of dissipation (i.e. an eddy viscosity) to remove the vorticity put into the fluid by the wind stress. Perhaps the most sophisticated example of this is Moore's (1963) damped stationary Rossby wave which is confined to the northwest corner of the basin and acts as a set of baffles to give the vorticity sufficient time to diffuse out of the basin (Pedlosky, 1979, section 5.10). Thus although this model, and the simpler ones due to Stommel (1948) and Munk (1950), are internally consistent, they are open to criticism because the structure of the western boundary layer depends strongly on how the smaller scale processes are parameterized. Fortunately the principal conclusion, viz. the boundary layer is on the west, requires only that the eddy viscosities be positive!

Now in the upper layer of a multilayer model the considerations in the previous paragraph are directly relevant. There is strong vorticity source of one sign,  $w_E$ , and so dissipation must be important on every streamline. Superficially at least it appears that the subsurface layers

may be simpler. Because there is no source in the potential vorticity equation there is no necessity for the dissipation to be strong. This suggests the interesting possibility that the subsurface western boundary layer dynamics are entirely inertial and their detailed structure is independent of how the dissipation is parameterized. Unfortunately, this is illusory, later in this section I shall present a model in which the frictional form of the upper layer boundary region "impresses" itself on the dynamics below.

The most direct way of seeing that the dissipation is important somewhere in the western boundary layer of a baroclinic model is to examine the density equation (1.6e), rather than the potential vorticity equation. As in section 2, if this equation is integrated over a closed streamline in a steady flow there results:

$$N^2 \iint_{\Psi} w \, dx \, dy = \iint (\text{dissipation}) \, dx \, dy \quad (12.1)$$

One cannot assume that the dissipation is negligible everywhere since a paradox results when the above equation is evaluated at  $z = 0$  where  $w$  is externally imposed and may have one sign.

This argument does not, however, exclude the possibility that the dissipation may all be vertically concentrated in the uppermost layer. Thus one can imagine a circulation in which all the dissipation is in the upper left hand corner of a zonal section, i.e. the western boundary layer region of the uppermost layer. In the layers below, the dissipation may be negligible everywhere in (12.1) so that if  $w < 0$  in the interior, e.g. (11.7), then  $w > 0$  in the western boundary layer. Note that the "upper left hand corner" dissipation has then performed the important task of

reversing the sign of  $w$  in the subsurface layers where, by hypothesis, the dissipation is negligible. The hypothesis can be tested with an eddy resolving general circulation model. If one integrates the time averaged density equation over a mean streamline a result similar to (12.1) is obtained in which  $w$  is the time averaged vertical velocity and the dissipation is the eddy heat flux. If one found that a significant amount of cancellation occurred in evaluating the integral on the left hand side the hypothesis of negligible subsurface dissipation would be confirmed.

This section is devoted to constructing an ad hoc model of the circulation described in the previous paragraph. This model is admittedly artificial; it must be kept in mind at all times that it has been specially contrived to illustrate a controversial hypothesis viz. that dissipation is negligible in subsurface western boundary layer regions.

The reason for examining the hypothesis described above is that unfortunately the homogenization arguments of chapter 2 appear to depend crucially on its validity. This is because (8.1) is ultimately substituted into line integrals which pass through western boundary layers; it is not obvious that the dissipative terms, neglected to obtain (8.1), are in fact small in these regions. Thus it is necessary to construct a western boundary layer, no matter how artificial, which shows it is possible to close the lower layer circulation of sections 10 and 11 nondissipatively.

The model - assume  $\psi_1$  is known

The equations used are the "equivalent two-layer" equations of section 10. The interior solutions found in that section will be denoted

by  $\sim$  in this section, thus:

$$\Psi_2 = \tilde{\Psi}_2(x,y) + \phi_2(x,y) \quad (12.2)$$

$$\{\text{total streamfunction}\} = \left\{ \begin{array}{l} \text{interior streamfunction} \\ \text{see (10.10) and (10.11)} \end{array} \right\} + \left\{ \begin{array}{l} \text{boundary layer} \\ \text{correction} \end{array} \right\}$$

The ad hoc, simplifying assumption I make is that  $\Psi_1$  is given by:

$$\Psi_1 = \{1 - e^{-\mu x}\} \tilde{\Psi}_1 \quad (12.3a)$$

$$\mu^{-1} \ll \text{east - west basin length scale} \quad (12.3b)$$

The form (12.3) is chosen because:

- (i) it satisfies the boundary conditions
- (ii) it reproduces the interior solution as  $\mu x \rightarrow \infty$
- (iii) it has a simple (perhaps the simplest) western boundary layer structure.

Other than the above there is no reason for choosing the particular form in (12.3a), the assumption is that all the unknown dissipative processes in the upper layer can be subsumed into the structure of the upper layer western boundary region in (12.3). Once  $\Psi_1$  is given, one can attempt to calculate  $\Psi_2$  in the western boundary layer using a completely dissipationless theory; one requires that

$$q_2 = \nabla^2 \Psi_2 + \beta y + F(\Psi_1 - 2\Psi_2) \quad (12.4a)$$

$$= \beta = \text{value of the potential vorticity} \quad (12.4b)$$

inside the closed  $q$ -contours, see  
(10.10) et seq.

at all points threaded by streamlines which pass through the region of homogenized  $q_2$  in the interior.

(12.4) is not as simple as it seems

It might appear that the solution of (12.4) is straightforward; one substitutes (12.2) and (12.3) into it and uses the interior result:

$$\beta = \beta y + F(\tilde{\psi}_1 - 2\tilde{\psi}_2) \quad (12.5)$$

to obtain a simple equation for  $\phi_2$ :

$$\phi_{2xx} - 2F\phi_2 = Fe^{-\mu x} \tilde{\psi}_1 \quad (12.6)$$

(it has been assumed that  $\phi_2$  varies rapidly only in the x-direction so that  $\phi_{2yy}$  is negligible). The solution of the above which satisfies the boundary condition:

$$\phi_2 = -\tilde{\psi}_2 \quad \text{at } x = 0 \quad (12.7)$$

is

$$\psi_2 = \tilde{\psi}_2 \left\{ 1 - e^{-\sqrt{2F} x} \right\} + \left( \frac{F}{\mu^2 - 2F} \right) \tilde{\psi}_1 \left\{ e^{-\mu x} - e^{-2F x} \right\} \quad (12.8)$$

I shall argue that (12.8) is not a physically satisfactory solution of the problem posed by (12.4). It has been derived so that its failings may be adequately discussed and used to motivate the more elaborate procedure ultimately used to solve (12.4).

The inadequacies of (12.8) become apparent when the streamlines are plotted. To do this I shall use a dimensional form of (11.10) as a model of the Ekman pumping:

$$w_E = -w_0 \left\{ 1 - |y| \right\} \quad (12.9)$$

Using the equivalent two layer model of section 10 it follows that

$$\tilde{\psi}_B = \left( \frac{H_1}{H} \right) \Psi (a - x)(1 - |y|) \quad (12.10a)$$

where:

$$\Psi = \frac{f_0 w_0}{\beta H_1} \quad (12.10b)$$

The advantage of (12.9) is that the  $\hat{q}_2$  and  $\Psi_2$  contours defined by (10.7) and (10.10) may be sketched without solving any transcendental equations.  $\hat{q}_2$  is given by (10.7):

$$q_2 = \beta y + F\Psi (a - x)(1 - |y|) \quad (12.11)$$

and is sketched in Figure 16. Note that the outermost closed  $\hat{q}_2$  contour is  $q_2 = \beta$ ; as explained in section 10,  $\tilde{\Psi}_2$  is nonzero only inside this contour where it is given by (10.10), explicitly:

$$\tilde{\Psi}_2 = \begin{cases} \frac{1}{3} (b_+ - x)(1 - y) & \text{if } y > 0 \\ \frac{1}{3} (b_- - x)(1 + y) - \frac{2\beta}{3F} & \text{if } y < 0 \end{cases} \quad (12.12a)$$

$$\quad (12.12b)$$

where:

$$b_+ = a - \frac{\beta}{F\Psi} \quad (12.13a)$$

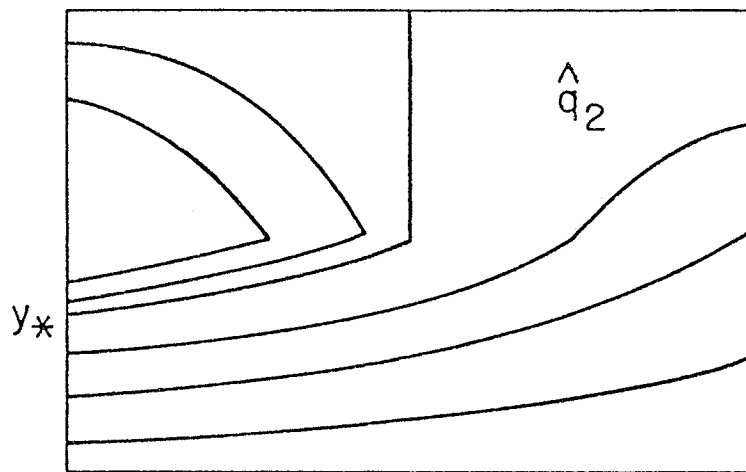
$$b_- = a + \frac{\beta}{F\Psi} \quad (12.13b)$$

Outside the contour  $q_2 = \beta$ ,  $\tilde{\Psi}_2 = 0$ .  $\tilde{\Psi}_2$  in (12.12) is sketched in figure 16. The boundary streamline,  $\tilde{\Psi}_2 = 0$ , cuts the western boundary at

$$y_* = \frac{2\beta}{F\Psi b_-} - 1 \quad (12.14a)$$

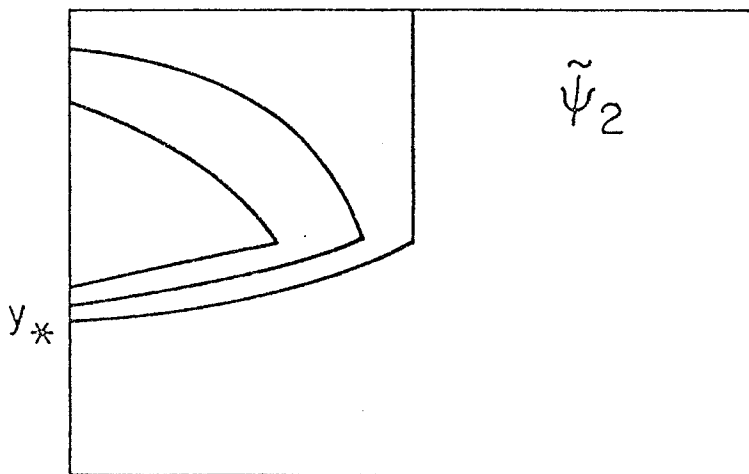
$$= \frac{\beta - aF\Psi}{\beta + aF\Psi} \quad (12.14b)$$

This expression shows neatly how the region of lower layer flow expands to fill the whole basin as the strength of the forcing increases:



(a)

$$\alpha F \psi / \beta = 2$$



(b)

Figure 16. The  $\hat{q}_2$  contours and lower streamfunction produced by (12.9).

$$\lim_{\Psi \rightarrow \infty} y_* = -1.$$

The western boundary layer streamlines calculated from (12.8), (12.10) and (12.12) are shown in figures 17 and 18. Figure 17 is a detailed sketch of the boundary layer; figure 18 has been included for clarity, it shows how the interior solution in figure 16 joins on to the boundary layer solution in figure 17. The most important point to note is the closed pocket of circulation in the southwest corner of the boundary layer. This circulation is confined to the boundary layer; because it is not connected to the interior region of homogeneous potential vorticity the condition after (12.4) is not satisfied. One could argue then that (12.8) applies only inside the streamline  $\Psi_2 = 0$  in figures 17 and 18 and that outside this region  $\Psi_2 = 0$ .

I believe this prescription is unsatisfactory since it makes the potential vorticity discontinuous on that part of the  $\Psi_2 = 0$  streamline which lies in the western boundary layer. One expects physically that arbitrarily small horizontal potential vorticity diffusion will ensure continuity of  $q$ .

Note that in the interior region, where the relative vorticity is negligible, the potential vorticity is continuous at  $\tilde{\Psi}_2 = 0$  since the interior streamfunctions are continuous there. In the western boundary layer, however, the relative vorticity contributes substantially to  $q$ . Consequently, continuity of potential vorticity at the bounding streamline in the western boundary layer is a stronger condition than in the interior. In the next subsection this condition will be used to construct what I hope is a more plausible boundary layer closure than (12.8).

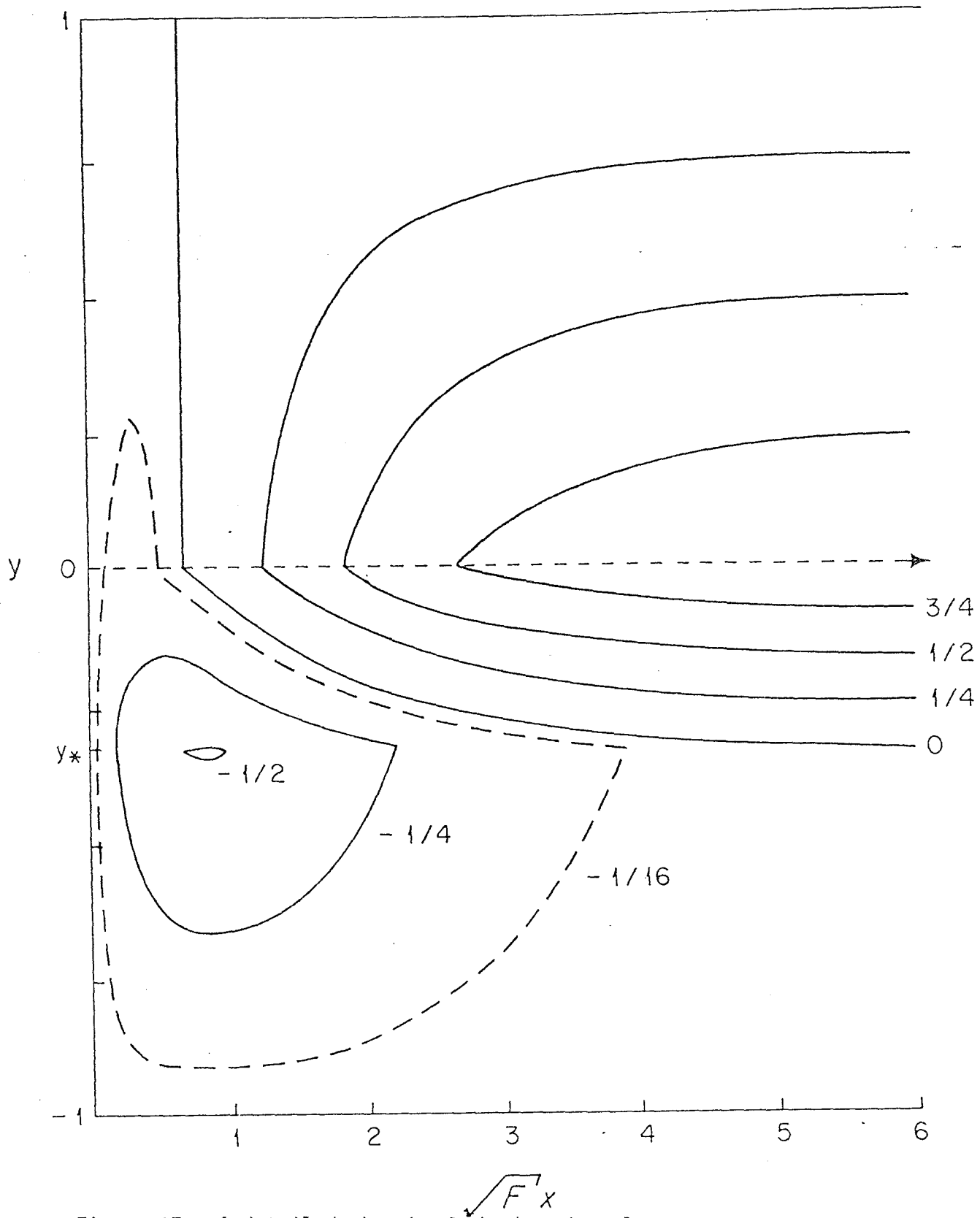


Figure 17. A detailed sketch of the boundary layer streamfunction calculated from (12.8) with  $\mu = \sqrt{F}$ . The extra dashed streamline is included to show the pocket of circulation in the southwest corner more clearly.

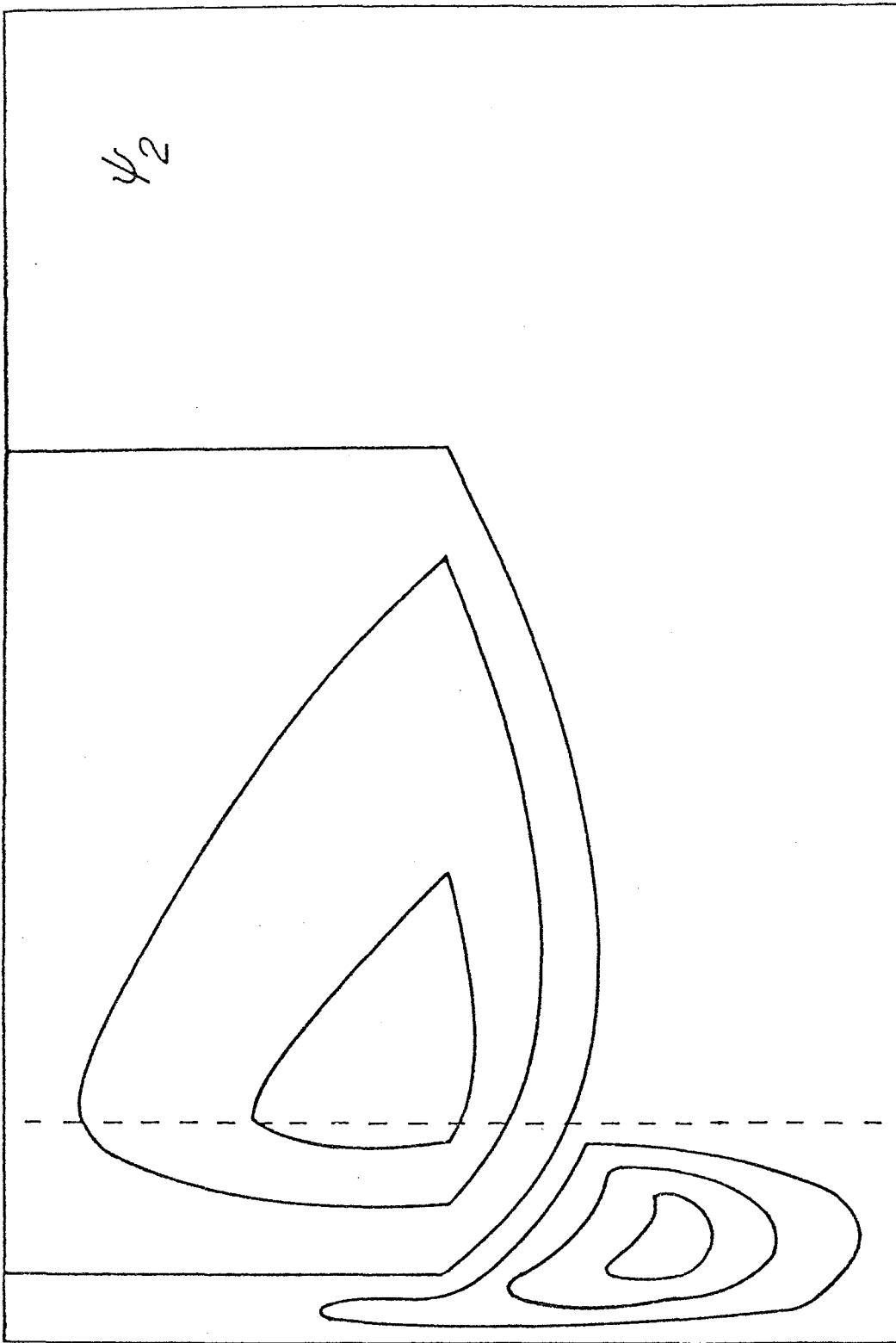


Figure 18. This figure shows schematically how the boundary layer circulation in figure 17 connects onto the interior circulation in figure 16.

It must be admitted, however, that requiring continuous potential vorticity is really a heuristic device which leads to a simple prediction of the location of the western edge of the region of homogeneous potential vorticity. Dr. W. Holland has recently run a three-layer, eddy resolving general circulation model (personal communication). The middle layer exhibits a large region of homogeneous potential vorticity which abuts the western boundary layer but not the coastal boundary. By contrast, the boundary condition (12.7) was used to obtain (12.8). These results suggest one should investigate the possibility that  $x = 0$  is not the western edge of the homogeneous  $q$  region. This means that only the right hand edge of the Gulf Stream will have uniform potential vorticity in the model developed below. Shielding the region of uniform potential vorticity from the coast is a region whose dynamics I shall not attempt to investigate.

A boundary layer with continuous potential vorticity -- formulation

The unusual structure of the boundary layers in figures 17 and 18 comes from requiring  $x = 0$  to be the western boundary of the region of homogeneous  $q$ . The structure of ensuing circulation suggests, however, that the western boundary of the homogeneous region is not the coast, but rather some initially unknown curve:

$$x = \xi(y).$$

$\xi(y)$  is the left hand portion of the streamline  $\psi_2 = 0$ , see figure 19. Matching requires that:

$$\lim_{y \rightarrow y_*} \xi(y) = \infty. \quad (12.15)$$

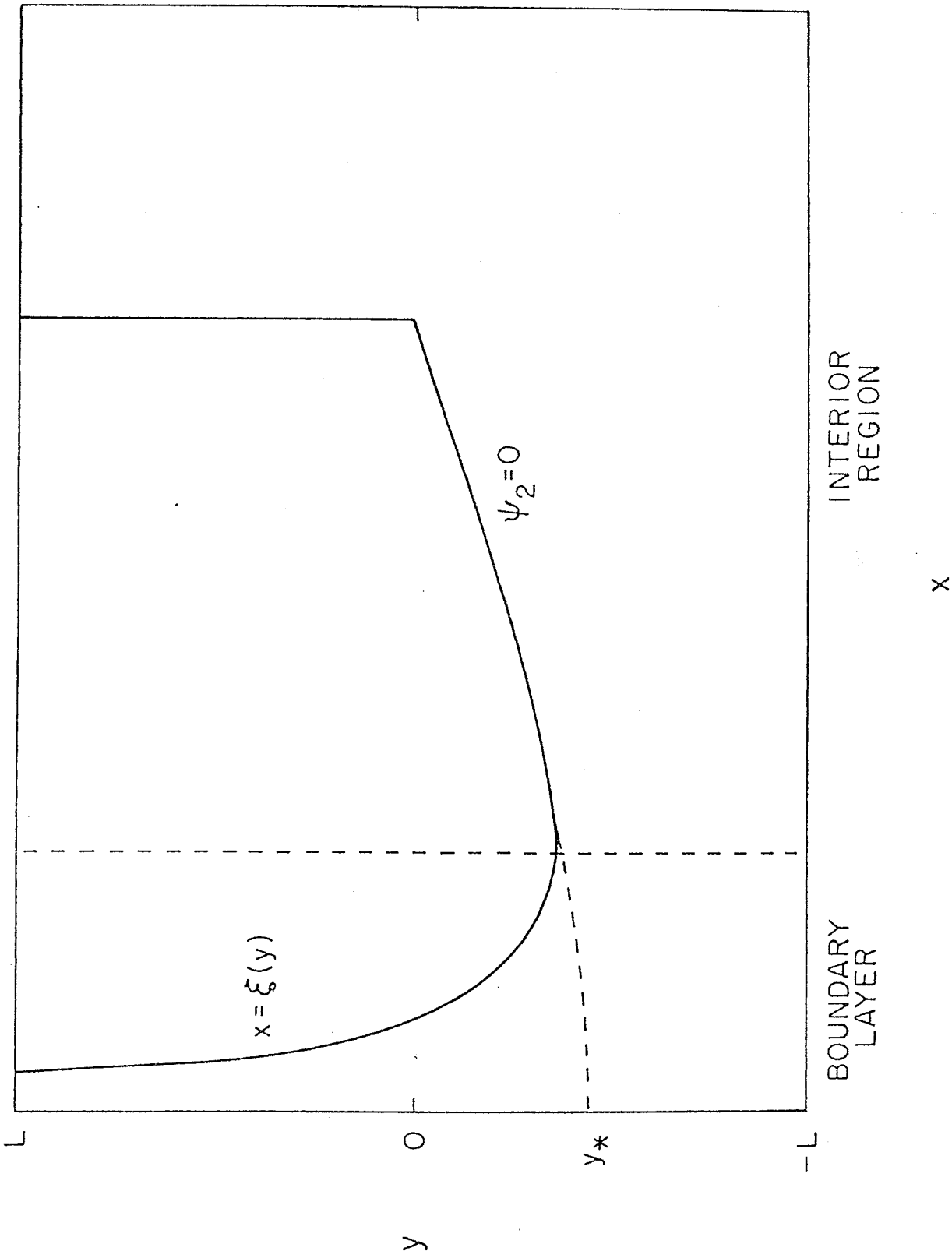
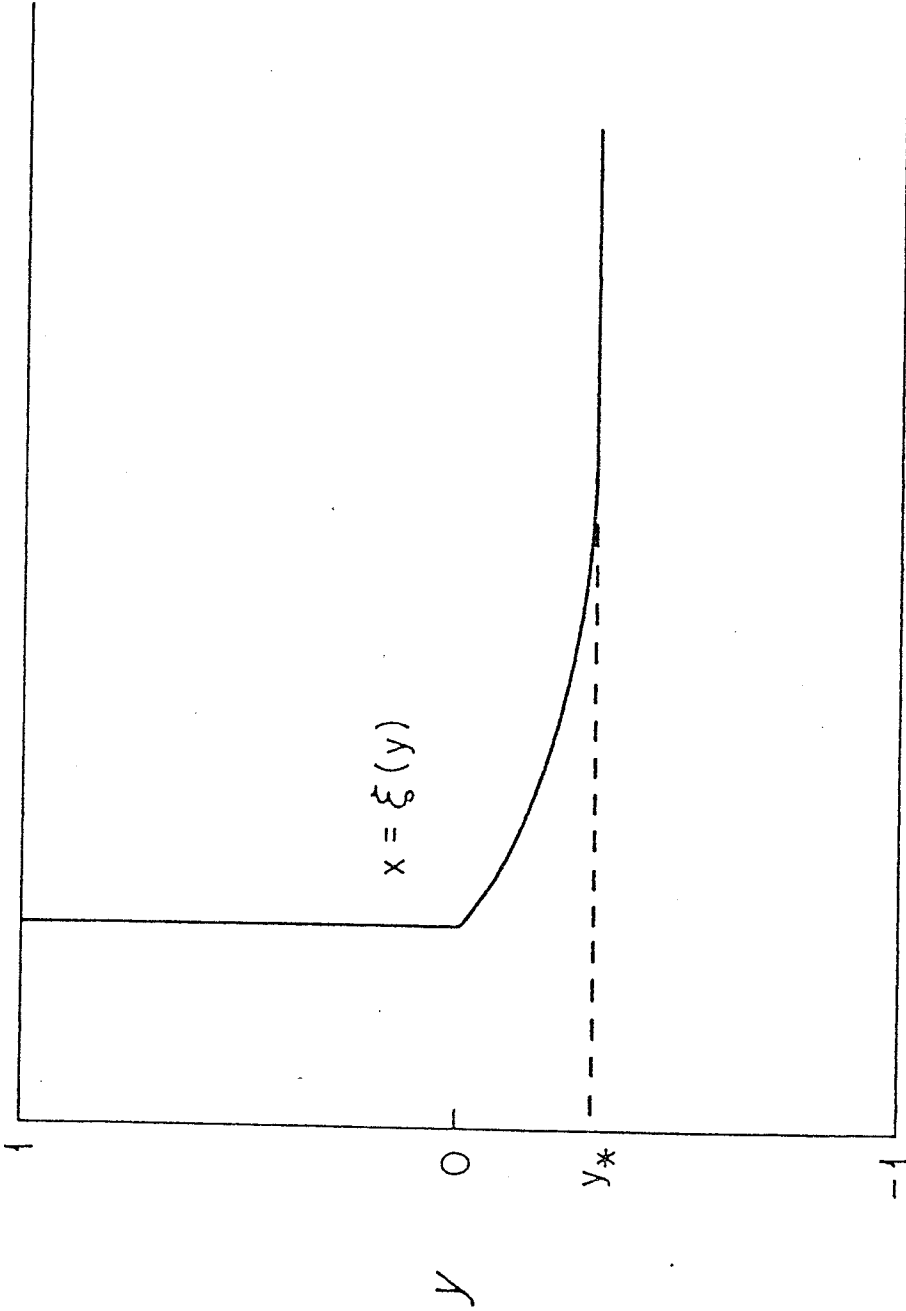


Figure 19. This figure illustrates the geometry discussed in the text. The curve  $x = \xi(y)$  is the left hand edge of the homogeneous potential vorticity region.



$\mu X$

Figure 20. The curve  $x = \xi(y)$  in the boundary layer calculated from (12.16). As  $y \rightarrow y^*$ ,  $\xi(y) \rightarrow \infty$ , as required by matching onto the interior.

Inside the streamline  $\psi_2 = 0$ , (12.4) applies. Outside,  $\psi_2 = 0$ .

This means that there is a narrow "sleeve":

$$0 < x < \xi(y)$$

in the western boundary layer. Inside the sleeve  $\psi_2 = 0$ . The sleeve contains the left hand edge of the Gulf Stream where the potential vorticity is nonuniform. The assertion that  $\psi_2 = 0$  in this region is obviously wrong. The impression one gets from examining Holland's numerical simulation is that fluid is entrained at  $y = y_*$  and swept northward along the sleeve. Thus, the sleeve is a conduit which deposits fluid with nonuniform potential vorticity at the northern boundary. Eddy mixing very rapidly destroys this potential vorticity signal so that the large region of homogeneous potential vorticity in the interior remains uniform. Prompted by human fatigability I shall not attempt to model this process.

The requirement that the potential vorticity be continuous enables one to calculate  $\xi(y)$  immediately. To the left of  $x = \xi(y)$  where  $\psi_2$  is zero and  $\psi_1$  is given by (12.3):

$$q_2 = \beta y + F \tilde{\psi}_1 (1 - e^{-\mu x})$$

while to the right of  $x = \xi(y)$

$$q_2 = \beta$$

so that continuity gives

$$\beta(1 - y) = F \tilde{\psi}_1(0, y) (1 - e^{-\mu \xi}) \quad (12.16)$$

Equation (12.16) is a transcendental equation which in principle can be solved for  $\xi(y)$ . This has been done in figure 20 for the particular forcing function (12.9).

There are several general properties of the solution of (12.16) which are worth noting. First, cast it in the form:

$$e^{-\mu \xi}(y) = 1 - \frac{\beta(1-y)}{F \tilde{\Psi}_1} \quad (12.17)$$

Now as  $y \rightarrow y_*$ ,  $\tilde{\Psi}_2 \rightarrow 0$  and  $\tilde{\Psi}_1 \rightarrow \left(\frac{H}{H_1}\right) \tilde{\Psi}_B$ . But from (10.7) and (10.10),

$\tilde{\Psi}_2 \rightarrow 0$  implies:

$$\beta y + F \left(\frac{H}{H_1}\right) \tilde{\Psi}_B \rightarrow \beta y + F \tilde{\Psi}_1 \rightarrow \beta$$

so that (12.17) implies:

$$e^{-\mu \xi} \rightarrow 0$$

which is the expected matching condition (12.15). The other interesting limit is  $y \rightarrow 1$ . To investigate this case it is convenient to use the particular solution (12.10) and (12.12). It is easy to see that these imply:

$$\tilde{\Psi}_1(0, y) = \left\{ \left(\frac{\beta}{3F}\right) + \frac{2}{3} a \Psi \right\} (1 - y)$$

so that (12.17) is:

$$e^{-\mu \xi}(1) = \frac{2aF\Psi - 2\beta}{2aF\Psi + \beta} \quad (12.18)$$

From (12.11), the condition for closed  $\hat{q}$  contours to exist is  $aF\Psi > \beta$ , so that  $\xi(1)$  in (12.18) exists; this means that the sleeve actually does extend all the way to the northern boundary, as in figure 19.

#### Solution of the boundary layer equations

In this subsection I present the solution of (12.4) subject to the boundary condition:

$$\psi_2 = 0 \quad \text{on } x = \xi(y).$$

The solution is found using the boundary layer decomposition in (12.2) and by assuming that the rapid boundary layer variation of  $\phi_2$  depends on the distance from the bounding streamline. To formalize this notion it is convenient to use

$$\rho = x - \xi(y)$$

(12.19a)

$$\eta = y$$

(12.19b)

as independent variables. Thus, the boundary layer correction is:

$$\phi_2 = \phi_2(\rho, \eta)$$

and since  $\rho$  measures distance from the bounding streamline:

$$\frac{\partial \phi_2}{\partial \rho} \gg \frac{\partial \phi_2}{\partial \eta}$$

It follows from (12.19) that

$$\nabla^2 \phi_2 = A(\eta) \frac{\partial^2 \phi_2}{\partial \rho^2} \quad (12.20a)$$

$$A(\eta) = 1 + \left(\frac{\partial \rho}{\partial y}\right)^2 \quad (12.20b)$$

$$= 1 + \left(\frac{\partial \xi}{\partial y}\right)^2 \quad (12.20c)$$

Substituting (12.2) into (12.4) and using (12.3) and (12.5) gives:

$$A(\eta) \phi_{2\rho\rho} - 2F\phi_2 = Fe^{-\mu(\rho + \xi(\eta))} \tilde{\Psi}_1(0, \eta) \quad (12.21)$$

Since the  $\eta$  dependence in (12.21) is parametric it is really no more complicated than (12.6). The solution which satisfies the boundary conditions:

$$\phi_2(0, \eta) = -\tilde{\Psi}_2(0, \eta)$$

$$\phi_2(\infty, \eta) = 0$$

is

$$\Psi_2 = \tilde{\Psi}_2 \left\{ 1 - e^{-\sqrt{2F/A} \rho} \right\} + \tilde{\Psi}_1 \left\{ \frac{Fe^{-\mu\xi}}{A\mu^2 - 2F} \right\} \left\{ e^{-\mu\rho} - e^{-\sqrt{2F/A} \rho} \right\} \quad (12.22)$$

where  $\xi$  is defined in (12.17),  $\rho$  in (12.19) and  $A$  in (12.20).

### Conclusion

The form of (12.22) shows that though dissipation is by construction negligible in the lower layer, the detailed form of the boundary layer depends strongly on the ad hoc frictional form of  $\Psi_1$  adopted in (12.3). The most important aspect of the solution is probably  $\xi(y)$ . Recall that this curve was calculated by requiring the potential vorticity to be continuous; it is clear from (12.17) that according to this principle  $\xi(y)$  depends strongly on the adjustable parameter  $\mu$ .

One might consider the possibility of determining  $\xi(y)$  using other criteria. For example, although  $q_2$  is continuous if  $\xi$  is given by (12.17),  $\frac{\partial \Psi_2}{\partial \rho}$  is not. As an alternative to (12.17) one could formulate the boundary value problem as in (12.19, 20 and 21) with  $\xi(y)$  as an initially unknown left hand boundary. In this way (12.22) is obtained.  $\xi(y)$  could now be calculated by requiring

$$\frac{\partial \Psi_2}{\partial \rho}(0, \eta) = 0 \quad (12.23)$$

i.e. continuity of  $\frac{\partial \Psi_2}{\partial \rho}$  rather than  $q_2$ . Equation (12.23) gives rise to a rather complicated differential equation for  $\xi$ . In view of the physical

inadequacies of the model this difficult mathematical problem does not deserve detailed attention. The point is, however, that apart from mathematical simplicity there is no compelling reason for believing that continuous potential vorticity is the correct condition to apply at  $x = \xi(y)$ . For this reason one may prefer to regard (12.22) as a lower layer boundary layer closure in which  $\xi(y)$  is an unknown curve which bounds the western edge of the homogeneous potential vorticity region.

Despite the inadequacies of (12.22) I believe that the principal objective of this section has been achieved. It has been shown how a specification of  $\psi_1$  enables one to construct a boundary layer closure for  $\psi_2$  in which dissipation is not directly important (i.e. the right hand side of (12.1) is small on every streamline passing through the boundary layer). As in homogeneous circulation models the theoretical lacunae, namely the arbitrary specification of  $\psi_1$  and  $\xi(y)$ , spring from an inadequate understanding of the role of dissipation in the western boundary.

### 13. A Frictional Model of the Western Boundary Layer

#### Introduction - a two layer model with interfacial friction.

To counterbalance the diagnostic approach of the previous section, in this section I shall attempt a more traditional, frictional western boundary layer closure. As in the simple, but self-consistent, models of Munk and Stommel, the relative vorticity is ignored, even in the boundary layer. The parameter range in which this neglect is rigorously justified is probably not oceanographically relevant. However, direct applicability to the oceans is not the primary purpose of models such as these, rather they focus our attention on specific processes by stripping away confusing detail. The model in the present section forces one to carefully consider the consequences strong vertical stress transmission in a western boundary layer. More specifically, in the circulation models of this section all the streamlines pass through frictionally dominated boundary layers in which (8.1) is invalid. The earlier arguments leading to potential vorticity homogenization do not apply and indeed the potential vorticity is not uniform inside the closed geostrophic contours of figure 11. Thus, this frictionally dominated model is informative because it forces one to confront a process which the machinations of section 12 deliberately side-stepped.

The formulation used in this section is the equivalent two layer model of sections 3 and 10:

$$J(\psi_1, q_1) = (f_{0W} w_E / H_1) + v \nabla^2 (\psi_2 - \psi_1) - \delta \nabla^2 \psi_1 \quad (13.1a)$$

$$J(\psi_2, q_2) = v \nabla^2 (\psi_1 - \psi_2) - \delta \nabla^2 \psi_2 \quad (13.1b)$$

$$q_1 = \beta y + F(\psi_2 - \psi_1) \quad (13.1c)$$

$$q_2 = \beta y + F(\psi_1 - 2\psi_2) \quad (13.1d)$$

In (13.1),  $v$  is an interfacial friction which transfers momentum vertically between the layers. In (13.1a),  $\delta$  is drag on the motionless deep, lowest layer. In (13.1a)  $\delta$  is an artificial "top-drag". The reason for including such a term is apparent when the barotropic mode equation is formed by adding (13.1a) and (13.1b):

$$\beta H \psi_{BX} = f_0 w_E - \delta H \nabla^2 \psi_B \quad (13.2a)$$

$$H \psi_B = H_1(\psi_1 + \psi_2) \quad (13.2b)$$

Equation (13.2a) is an equation for the barotropic mode alone and determines  $\psi_B$  everywhere, even in the western boundary layer. The problem with no "top-drag",  $\delta = 0$  in (13.1a), is more difficult analytically, but not really more informative physically.

In the following development the scaling  $v = O(\delta)$  will be assumed. There is no difficulty recovering  $v \gg \delta$  and  $v \ll \delta$  as special cases.

### Nondimensionalization

In section 12 the boundary layer analysis was done informally without nondimensionalizing the equations. The analysis in this section is more intricate and it is convenient to use nondimensional equations.

Temporarily denoting nondimensional quantities by  $*$ , the scalings are

$$(x, y) = L(x_*, y_*) \quad (13.3a)$$

$$\psi = UL\psi_* \quad (13.3b)$$

$$q = \beta Lq_* \quad (13.3c)$$

$$w_E = Ww_{E*} \quad (13.3d)$$

$$(v, \delta) = \beta L(v_*, \delta_*) \quad (13.3e)$$

where  $U$  is the typical horizontal velocity, given in terms of the external variables by

$$U = f_0 W / \beta H .$$

The nondimensional versions of (13.1) are then

$$J(\psi_{1*}, q_{1*}) = w_{E*} + v_* \nabla_*^2 (\psi_{2*} - \psi_{1*}) - \delta_* \nabla_*^2 \psi_{1*} \quad (13.4a)$$

$$J(\psi_{2*}, q_{2*}) = v_* \nabla_*^2 (\psi_{1*} - \psi_{2*}) - \delta_* \nabla_*^2 \psi_{2*} \quad (13.4b)$$

$$q_{1*} = y_* + F_* (\psi_{2*} - \psi_{1*}) \quad (13.4c)$$

$$q_{2*} = y_* + F_* (\psi_{1*} - 2\psi_{2*}) \quad (13.4d)$$

where

$$F_* = FU / \beta \quad (13.5)$$

The barotropic mode equation is

$$\psi_{B*} = w_{E*} - \delta_* \nabla_*^2 \psi_{B*} \quad (13.6)$$

where for convenience

$$\psi_{B*} = \psi_{1*} + \psi_{2*} \quad (13.7)$$

or equivalently

$$\psi_B = (H_1 / H) UL \psi_{B*}$$

The \*'s will now be dropped.

### Solution of the barotropic mode equation

The first order boundary layer solution of (13.6) when

$$\delta \ll 1$$

is well known:

$$\psi_B = (x - a)(1 - e^{-x/\delta}) w_E(y) \quad (13.8a)$$

$$= (1 - e^{-x/\delta}) \tilde{\psi}_B \quad (13.8b)$$

where  $\tilde{\psi}_B$  is the familiar Sverdrup solution.

An equation for  $\psi_2$  alone

Since  $\psi_B = \psi_1 + \psi_2$  is known, equation (13.4b) is:

$$J(\psi_2, \hat{q}) = \nu \nabla^2 \psi_B - (2\nu + \delta) \nabla^2 \psi_2 \quad (13.9a)$$

$$\hat{q} = y + F\psi_B \quad (13.9b)$$

The remainder of this section is devoted to the solution of (13.9a). The boundary condition is of course:

$$\psi_2 = 0$$

A preliminary simplification

It is easy to see that a particular solution of the inhomogeneous problem (13.9) (which does not, however, satisfy the boundary conditions) is  $(\frac{\nu}{2\nu + \delta}) \frac{\hat{q}}{F}$ . This observation suggests we represent  $\psi_2$  as:

$$\psi_2 = (\frac{\nu}{2\nu + \delta}) (q + \phi)/F \quad (13.10)$$

where  $\phi$  satisfies:

$$J(\phi, \hat{q}) = -\lambda \delta \nabla^2 \phi \quad (13.11a)$$

$$\lambda = 1 + 2(\nu/\delta) \quad (13.11b)$$

with boundary condition:

$$\phi = -y. \quad (13.11c)$$

Equation (13.11) is an advection-diffusion equation in which  $\phi$  is the "temperature" and  $\hat{q}$  the "streamfunction" producing the advection. The interior "streamlines" of this field have already been sketched for various values of  $F$  and  $w_E = -\cos(\frac{\pi}{2} y)$  in figure 11. In figure 21 I've shown the  $\hat{q}$  contours for  $F = 1$  in both the interior and the boundary layer with

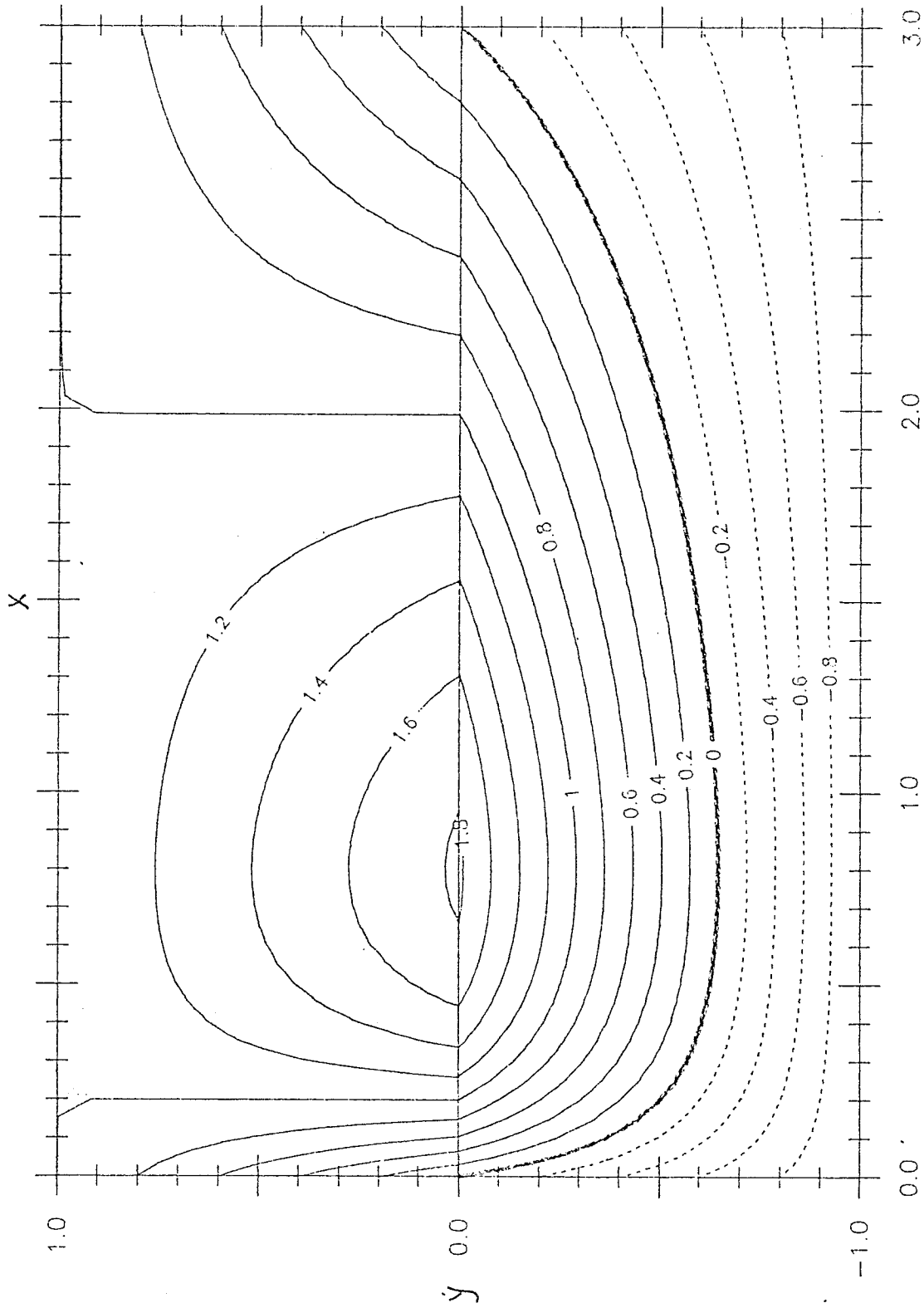


Figure 21. The function of  $\hat{q}$  defined by (13.9b). In the above sketch  $F = 1$ ,  $\delta = 0.45$ ,  $a = 3$  and  $w_E = -[1 - |y|]$ .

$w_E = -(1 - |y|)$ . Once again there is a region of closed  $q$  contours in the northwest corner of the basin.

After a discussion of the thermal analogy I shall begin the analysis of (13.11) by discussing two limiting cases:

$F = O(\delta)$  and  $F = O(\delta^{-1})$ . The interesting case  $F = O(1)$  is more complicated and is discussed last so that one may take advantage of the intuition generated by the limiting cases.

The thermal analogy and a general discussion of the role of the western boundary layer.

As mentioned previously, (13.11) is an advection-diffusion problem in which  $\hat{q}$  is a "streamfunction" and  $\phi$  the concentration of a passive scalar. Besides generating useful physical intuition, this analogy assures one that the problem is mathematically well-posed.

Physically, in the blocked regions, one can think of the "velocity-field",  $\hat{z} \times \nabla \hat{q}$ , as sweeping westward across the basin. Away from the diffusive western boundary layer the temperature  $\phi$  is constant on a streamline. In this way the eastern boundary condition is communicated to the blocked interior regions. In the closed regions the functional relation between  $\phi$  and  $q$  is unknown and since the Batchelor-Prandtl theorem is inapplicable, it can only be determined by an analysis of the diffusive western boundary layer.

The western boundary layer analysis of the model considered here is not a simple extension of the familiar techniques which are so efficacious in the Munk and Stommel models. From a mathematical point of view this is because  $\hat{q}$  varies on the boundary layer scale  $\delta^{-1}$ ; this means that both

terms in  $J(\phi, \hat{q})$  have equal magnitude and the boundary layer scaling produces partial rather than ordinary differential equations. This just reflects the way in which the  $q$  contours turn sharply north in the boundary layer, producing a narrow "pipe" in which both components of advection are as large as east-west diffusion.

The complications in the boundary layer analysis are not merely formal however. In the Munk and Stommel models the interior solution is known everywhere and the diffusive boundary layers are appended to satisfy the boundary conditions; if the frictional terms are identically zero the ensuing advection problem has no solutions which satisfy the boundary conditions. By contrast if the right hand side of (13.11a) were zero then

$$\phi = \begin{cases} -\hat{q} & \text{in the blocked regions} \\ \text{an arbitrary function of } q & \text{in closed regions} \end{cases}$$

is a solution which satisfies all the boundary conditions. The boundary layer analysis serves primarily to determine a unique functional relation between  $\phi$  and  $\hat{q}$  in the closed regions, i.e., unlike the more familiar problems, the boundary layer dynamics determines the interior solution in a substantial fraction of the basin.

Using the thermal analogy one can see intuitively how this happens. Consider a closed "streamline" in figure 21. In the interior diffusion is unimportant and "temperature" is constant on the "streamline". (Because the Batchelor-Prandtl theorem is inapplicable it may, however, vary from "streamline" to "streamline"!.) The "fluid" enters the boundary layer region in the south. The mathematical analysis of this southern entry

region will show that the boundary layer functions can satisfy two boundary values and so there is no trouble accomodating both (13.11c) and some arbitrary distribution of "entry temperature". The "fluid" then goes northward and because of diffusion its temperature changes in a way which reflects (13.11c) and the structure of  $\hat{q}$ . The "fluid" exits the boundary layer region, into the interior, in the north. The mathematical analysis of this northern exit region will show that the boundary layer functions can satisfy only one boundary value which must be (13.11c). The "temperature" at the exit region cannot be specified arbitrarily but is given by the limit of the boundary layer function as  $\xi = x/\delta \rightarrow \infty$ . This limit establishes the "temperature" distribution at the exit region and then the nondiffuse clockwise interior circulation of the closed  $\hat{q}$ -contours communicates this condition to the interior. Thus the northern "exit" section of the western boundary layer is acting rather like an eastern boundary in the classical theory, i.e., it provides a boundary condition for the interior circulation.

Limiting case 1:  $F = O(\delta)$

If:

$$F = \delta \hat{F}$$

$$\hat{F} = O(1)$$

then the  $\hat{q}$  contours are essentially lines of constant  $y$ . The solution of (13.11) has the form:

$$\phi = -y + \delta \phi(\xi, y) \quad (13.12a)$$

$$\xi = x/\delta \quad (13.12b)$$

The representation (13.12a) is slightly different from the more familiar boundary layer approximations used in geophysical fluid dynamics because the outer solution,  $\phi = -y$ , satisfies all the boundary conditions. The correction  $\hat{\phi}$  is necessary because:

$$\begin{aligned} J(-y, q) &= \hat{q}_x \\ &= -a\hat{F}e^{-x/\delta} w_E(y) + O(\delta) \end{aligned}$$

so that the outer solution alone produces an  $O(1)$  error in the boundary layer. From another perspective the contribution of  $\delta\hat{\phi}$  to  $\phi$  in (13.12a) is  $O(\delta)$  everywhere, but the contribution to  $\phi_x$  is  $O(1)$  in the boundary layer.

When (13.12a) is substituted into (13.11) and terms of  $O(\delta)$  are neglected there results:

$$\hat{\phi}_{\xi\xi} + \frac{1}{\lambda} \hat{\phi}_{\xi} = \left(\frac{a\hat{F}}{\lambda}\right) e^{-\xi} w_E(y), \quad (13.13)$$

the solution of which is:

$$\hat{\phi} = \left(\frac{a\hat{F}}{\lambda - 1}\right) [e^{-\xi} - e^{-\xi/\lambda}] w_E(y). \quad (13.14)$$

The final expression for  $\psi_2$  when (13.14) and (13.12a) are substituted into (13.10) is:

$$\psi_2 = \left(\frac{v}{2v + \delta}\right) \left[-1 + \left(\frac{\lambda}{\lambda - 1}\right) e^{-\xi} - \left(\frac{1}{\lambda - 1}\right) e^{-\xi/\lambda}\right] a w_E(y)$$

This expression for  $\psi_2$  should be contrasted with the calculation in section 3. As in that section  $\psi_2$  is  $O(1)$  in the boundary layer region; the  $O(\delta^{-1})$  abyssal currents provided the frictional stress to balance the wind stress.

#### Limiting case 2: $F = O(\delta^{-1})$

In this limit the simple Batchelor-Prandtl arguments of chapter 2

apply. Suppose:

$$F = \delta^{-1} \tilde{F}$$

$$\tilde{F} = O(1)$$

and that in the western boundary layer,  $x = O(\delta)$  and  $\frac{\partial}{\partial x} = O(\delta^{-1})$ . Then the Jacobian on the left hand side of (13.11a) is  $O(\delta^{-2})$  while the frictional term is only  $O(\delta^{-1})$  and one can conclude

$$\phi = F(\hat{q})$$

even in the frictional western boundary layer. The standard argument then shows that inside closed  $\hat{q}$  contours:

$$\phi = \text{constant.}$$

In fact since

$$\hat{q} = y + F\psi_B \approx \delta^{-1} \tilde{F}\psi_B$$

the closed  $\hat{q}$  contours occupy most of the basin.

#### The distinguished limit: $F = O(1)$

The analysis in this section depends heavily on taking the forcing to be

$$w_E = -[1 - |y|]. \quad (13.15)$$

In previous sections this particular form of the Ekman pumping was chosen for convenience; in this section, however, (13.15) is used because the boundary layer equations reduce to ordinary differential equations. Other forms of  $w_E$  lead to partial differential equations and I am unable to easily generalize the solution in this section.

With (13.15), the solution of (13.11) has the form:

$$\phi = A(\xi) - [1 + A(\xi)]y \quad \text{if } 0 < y < 1 \quad (13.16a)$$

$$\phi = B(\xi) + C(\xi)y \quad \text{if } y_* < y < 0 \quad (13.16b)$$

$$\phi = D(\xi) - [1 - D(\xi)]y \quad \text{if } -1 < y < y_* \quad (13.16c)$$

in the boundary layer,  $\xi = x/\delta = O(1)$ . In (13.16)  $y_*$  is the latitude at which the outermost closed  $\hat{q}$  contour cuts the western boundary, see figures 16, 22 and equation (12.14). In nondimensional variables:

$$y_* = \frac{1 - aF}{1 + aF} \quad (13.17)$$

Note how (13.16a,c) automatically satisfies the boundary conditions at

$|y| = 1$ . The boundary condition at  $\xi = 0$  requires

$$A(0) = B(0) = D(0) = 0 \quad (13.18a)$$

$$\text{and } C(0) = -1 \quad (13.18b)$$

When (13.16) is substituted into (13.11), ordinary second order differential equations for  $A$ ,  $B$ ,  $C$  and  $D$  are obtained. Continuity of the solution requires additional boundary "patches" of thickness  $\delta$  in the  $x$ -direction and thickness  $\delta^{1/2}$  in the  $y$ -direction. These patches are at  $y = 0$  and  $y_*$ ; their dynamics will be discussed later, for the moment accept (13.16) as the form of  $\phi$  over most of the western boundary layer.

Since the ordinary differential equations for  $A$ ,  $B$ ,  $C$  and  $D$  are second order, more boundary conditions than (13.18) are required to obtain a well posed problem. This leads us to consider the interior region,  $\xi = \infty$ .

#### Solution in the interior

In the interior the solution of (13.11a) is:

$$\phi = F(\hat{q}). \quad (13.19)$$

The function  $F(\hat{q})$  is determined by the boundary conditions. In the following discussion it will probably be helpful to refer to figure (16a) in which the "streamfunction"  $\hat{q}$  is sketched. In the closed region the

"flow" is clockwise while in the region of coastally blocked  $\hat{q}$  contours the flow is east to west. Thus in the blocked region  $\phi$  is determined by integrated westward along  $\hat{q}$  contours, using (13.11c) as an initial condition. In the region of closed  $q$  contours  $\phi$  is determined by integrating along  $q$  contours, starting at  $(x = 0, y > 0)$  and going

clockwise. The initial condition for this integration is obtained from the boundary layer analysis which provides the number  $A(\infty)$ . The integration finishes on the line segment  $(x = 0, y_* < y < 0)$  and provides an outer boundary condition for the boundary layer in this region. Thus the boundary layer in the region  $y > 0$  is qualitatively different from that in the region  $y < 0$ : when  $y > 0$  only one boundary condition  $A(0) = 0$ , is applied. This, together with the requirement that  $A(\infty)$  be bounded, determines  $A(\xi)$  uniquely. When  $y < 0$ , however, two boundary conditions, one at 0 and the other at  $\infty$ , are required to obtain a unique solution.

Consider first the region threaded by  $\hat{q}$  contours which strike the eastern boundary. In this region the function  $F$  which is compatible with (13.11c) is obviously:

$$\phi = -\hat{q} \quad (13.20)$$

The above result provides the  $\xi = \infty$  boundary condition for  $D$  in (13.16c); matching (13.20) and (13.16c) in the intermediate region  $(x \ll 1, \xi \gg 1)$  implies:

$$D(\infty) = -aF \quad (13.21)$$

Consider next the region inside the closed  $q$  contours with  $y > 0$ . Since the interior in this region is shielded from the condition (13.11c)

by the boundary layer (13.16a), we must consider the boundary layer dynamics to determine  $F$ . Later in this section I show that the equation for  $A$  has only one linearly independent solution which remains bounded as  $\xi \rightarrow \infty$ . Hence, the boundary layer equation for  $A$  must be solved using only one boundary condition, i.e. (13.18a). Thus the interior solution (13.19) must satisfy

$$\phi = A(\infty) - [1 + A(\infty)]y \quad (13.22)$$

at  $x = 0$ ; in (13.22)  $A(\infty)$  is a number which is known once the second order linear equation for  $A$  has been solved. Equation (13.22) determines  $F(\hat{q})$  by eliminating  $y$  between the expression for  $\hat{q}$  in the matching region ( $\xi \gg 1, x \ll 1$ ):

$$\hat{q} = y + aF(1 - y)$$

and (13.22) to obtain

$$\phi = \left( \frac{A(\infty) + aF}{1 - aF} \right) - \left( \frac{1 + A(\infty)}{1 - aF} \right) \hat{q}. \quad (13.23)$$

The important point to note about the above solution is that the western boundary layer has determined the interior solution (13.23) by setting the initial condition on the clockwise integration.

Finally consider the region of closed  $\hat{q}$  contours with  $y < 0$ . Apparently the solution (13.23) applies in this region as well. The boundary condition at  $\xi = \infty$  is determined by (13.23), which implies that in the matching region ( $\xi \gg 1, x \ll 1$ ):

$$B(\infty) + C(\infty)y = \left( \frac{A(\infty) + aF}{1 - aF} \right) - \left( \frac{1 + A(\infty)}{1 - aF} \right)(y + aF(1 + y))$$

or

$$B(\infty) = A(\infty) \quad (13.24a)$$

$$C(\infty) = \left( \frac{aF + 1}{aF - 1} \right) (1 + A(\infty)) \quad (13.24b)$$

$$= -\left(\frac{1}{y_*}\right) (1 + A(\infty)) \quad (13.24c)$$

Detailed solution in the boundary layer. Case 1:  $0 < y < 1$

Substituting (13.16a) into (13.11) with

$$\begin{aligned} \hat{q} &= y + F(a - x)(1 - e^{-\xi})(1 - y) \\ &\approx y + aF(1 - e^{-\xi})(1 - y) \end{aligned}$$

gives

$$\lambda A'' + [1 - aF(1 - e^{-\xi})] A' + aFe^{-\xi} A = -aFe^{-\xi} \quad (13.25)$$

The above equation can be transformed into Kummer's equation (Abramowitz and Stegun, 1968, pg. 504) by changing the independent variable to:

$$\zeta = -\left(\frac{aF}{\lambda}\right) e^{-\xi}$$

and defining:

$$A = -1 + \tilde{A}(\zeta) \quad (13.26)$$

The transformed equation is

$$\zeta \tilde{A}_{\zeta\zeta} + [b - \zeta] \tilde{A}_{\zeta} - \tilde{A} = 0 \quad (13.27a)$$

$$b = 1 - \lambda^{-1}[1 - aF] \quad (13.27b)$$

The above has two linearly independent solutions, the confluent hypergeometric functions  $M(1, b, \zeta)$  and  $U(1, b, \zeta)$ . The matching condition at  $\xi \rightarrow \infty$  corresponds to  $\zeta \rightarrow 0$  where:

$$\begin{aligned} M(1, b, \zeta) &\rightarrow 1 \\ U(1, b, \zeta) &\rightarrow \zeta^{1-b} \end{aligned}$$

If  $1-b$  is negative then  $U$  is not a physically acceptable solution.

However, since

$$1 - b = \lambda^{-1}[1 - aF],$$

and  $aF > 1$  is precisely the condition for the existence of closed  $\hat{q}$  contours, it follows that when the contours close only one boundary condition can be satisfied. Since  $A(\xi = 0) = 0$  corresponds to

$$\tilde{A} \cdot \left(-\frac{aF}{\lambda}\right) = 1$$

one has

$$\tilde{A} = M(1, b, \zeta) / M(1, b, -\frac{aF}{\lambda})$$

and from (13.26)

$$A = [-M(1, b, -\frac{aF}{\lambda}) + M(1, b, \zeta)] / M(1, b, -\frac{aF}{\lambda}) \quad (13.28)$$

Now that  $A$  is known, one can calculate  $A(\infty)$  and so through (13.23) determine  $\phi$  in the interior of the closed  $\hat{q}$  region. Since  $\xi \rightarrow \infty$  corresponds to  $\zeta \rightarrow 0$  and  $M(1, b, 0) = 1$ :

$$A(\infty) = -1 + [M(1, b, -\frac{aF}{\lambda})]^{-1}. \quad (13.29)$$

Detailed solution in the boundary layer. Case 2:  $y_* < y < 0$

---

Substituting (13.16b) into (13.11) gives

$$\lambda B'' + [1 + aF(1 - e^{-\xi})]B' - aFe^{-\xi}C = 0 \quad (13.30a)$$

$$\lambda C'' + [1 + aF(1 - e^{-\xi})]C' - aFe^{-\xi}C = 0 \quad (13.30b)$$

Subtracting (13.30b) from (13.30a) one finds that:

$$E = B - C$$

satisfies the simple equation:

$$\lambda E'' + [1 + aF(1 - e^{-\xi})]E' = 0.$$

The solution of the above which satisfies the boundary conditions (13.18) and (13.24) is

$$\frac{E(\xi)-1}{E(\infty)-1} = \frac{\int_0^{\infty} \exp[-\lambda^{-1} \{ (1+aF)\xi' + aFe^{-\xi'} \}] d\xi'}{\int_0^{\infty} \exp[-\lambda^{-1} \{ (1+aF)\xi' + aFe^{-\xi'} \}] d\xi'} \quad (13.31)$$

where from (13.24)

$$E(\infty) = A(\infty) - y_*^{-1}(1 + A(\infty))$$

and  $A(\infty)$  is given by (13.29).

Now that  $B - C$  is known, one can transform (13.30b) into Kummer's equation and again express  $C$  in terms of confluent hypergeometric functions. The previous change of independent variable turns (13.30b) into

$$\zeta C_{\zeta\zeta} + [b' - \zeta]C_{\zeta} + C = 0 \quad (13.32a)$$

$$b' = 1 - \lambda^{-1}(1 + aF) \quad (13.32b)$$

the solution of which is a linear combination of  $U(-1, b', \zeta)$  and  $M(-1, b', \zeta)$ . Unlike the solutions of (13.27a), both these solutions are well behaved at  $\zeta = 0$ , because  $1 - b' > 0$ . Thus both boundary conditions (13.18a) and (13.24b) can be satisfied.

Detailed solution in the boundary layer. Case 3:  $-1 < y < y_*$

Substituting (13.16c) into (13.11a) gives:

$$\lambda D'' + [1 + aF(1 - e^{-\xi})] D' - aFe^{-\xi} D = -aFe^{-\xi}.$$

As before this equation can be transformed into Kummer's equation. There are two well behaved solutions so that both (13.18a) and (13.21) can be satisfied.

Summary

The solution I've constructed is summarized in figure 22 and equations (13.10), (13.16), (13.23), (13.28) and (13.29).

Does the potential vorticity homogenize?

Suppose that  $\nu = \delta$  so that  $\lambda = 3$ . In this case the combination of interfacial and bottom drag on the lower layer is equivalent to horizontal diffusivity of potential vorticity. Previous arguments suggest that the potential vorticity should be uniform inside the closed  $q$  contours.

However, since

$$\begin{aligned} q_2 &= y + F(\psi_1 - 2\psi_2) \\ &= q - 3\psi_2 \\ &= -\phi \quad \text{(see (13.10))} \end{aligned}$$

this will not be the case unless:

$$\frac{1 + A(\infty)}{1 - aF} \ll 1 \quad (13.33)$$

so that  $\phi$  in (13.23) is uniform. The one case in which we can be certain that (13.33) applies is if  $F = O(\delta^{-1})$ , since this parameter condition allows the standard Batchelor-Prandtl proof to be applied. This is confirmed in Appendix A of this chapter where I show that

$$\begin{aligned} 1 + A(\infty) &= [M(1, b, -\frac{aF}{\lambda})]^{-1} \\ &\sim 2 + O((aF)^{-1}) \end{aligned}$$

as  $aF \gg \infty$ . This means that:

$$q_2 \sim 1 + \left(\frac{2}{aF}\right) (1 - \hat{q}) + O((aF)^{-2})$$

as expected.

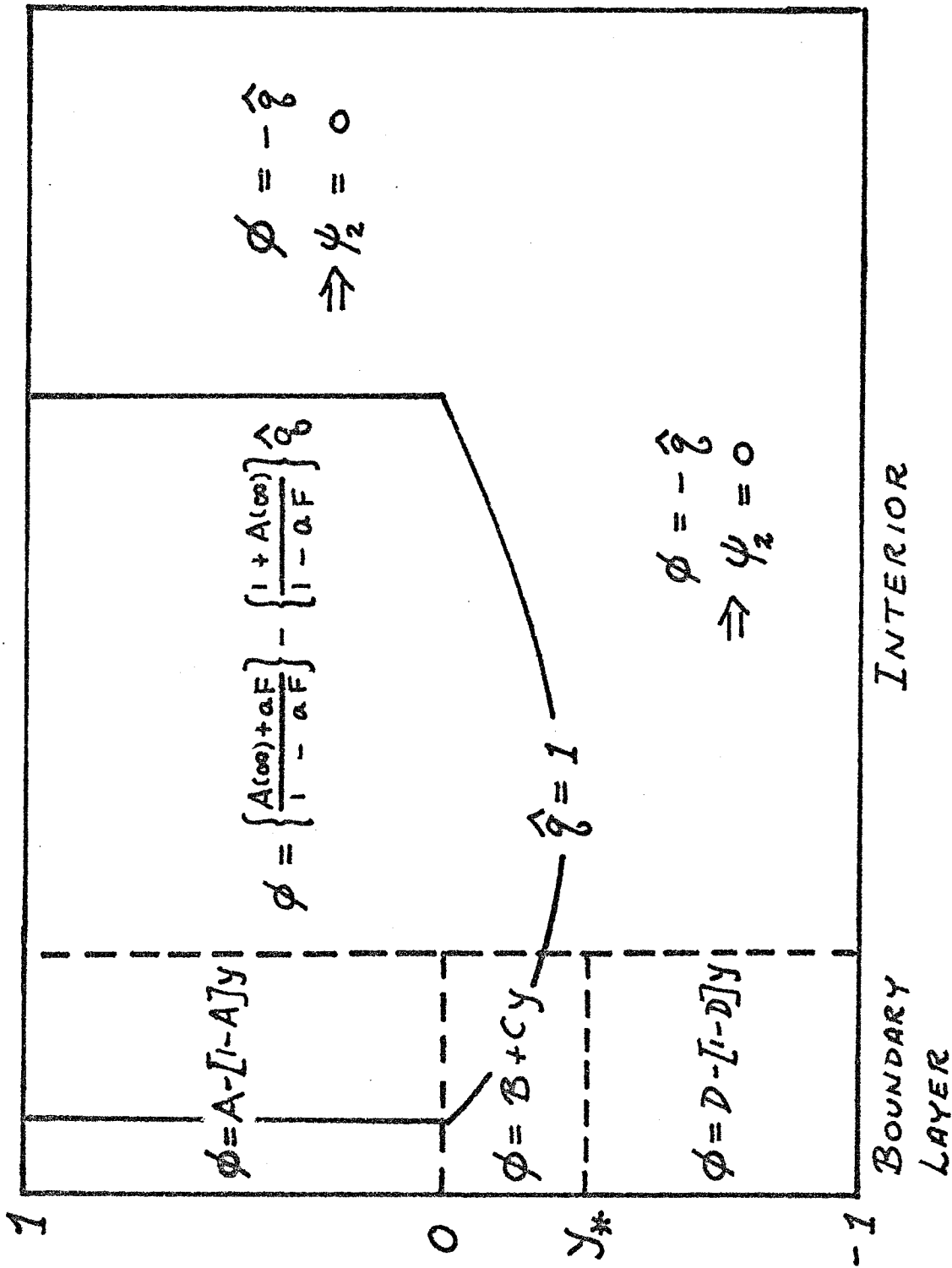


Figure 22. This figure summarizes the form of the solution in the various interior and boundary layer regions.

The boundary patches at  $y = 0$  and  $y_*$

The boundary patches are necessary to smooth the singularities in (13.16) at the points  $y = 0$  and  $y = y_*$ . At these points the representation (13.16) is discontinuous. It is plausible that this discontinuity can be removed by a diffusive boundary layer in which the heretofore neglected term  $\delta\phi_{yy}$  is order one. This suggests that the north-south scale of these patches is  $O(\delta^{1/2})$ .

I have not treated this problem completely; the preliminary analysis does not suggest any difficulty in principle, merely algebraic complexity. The possible extensions discussed in the next section are probably more deserving of attention.

Some extensions

The most unsatisfactory aspect of the model in this section is the top drag in (13.1a) which is introduced to obtain a simple equation for  $\psi_B$ . There are two alternative models which are less artificial physically, but more complex mathematically. In both these models, however, provided  $w_E$  is given by (13.15), an ansatz similar to (13.16) reduces the boundary layer dynamics to ordinary differential equations.

The two models are:

- (i) simply suppress the top drag in (13.1a). In this case the ordinary differential equations for the analogs of A, B, C and D are nonlinear.
- (ii) replace the top and bottom drag in (13.1a and b) by lateral friction,  $\nu \nabla^4 \psi_n$ . Once again the barotropic streamfunction can be calculated everywhere; this time it has a more complicated

Munk-type boundary layer structure.  $\Psi_1$  can then be eliminated from (13.1b) to obtain an equation for  $\Psi_2$  alone. In this case the analogs of A, B, C and D satisfy fourth order linear equations.

I am currently working on both of these models; my inchoate investigation suggests that the simpler model treated in this section displays what I consider to be the most interesting features of a frictionally dominated western boundary layer viz:

- (i) A range of latitudes, in this case  $0 < y < 1$ , in which only one imposed boundary condition can be satisfied by the boundary layer solution. Thus the boundary layer solution in this region imposes a boundary condition on the interior flow.
- (ii) A region of nonuniform potential vorticity in the interior which reflects the boundary condition imposed by the frictional layer.

Appendix A: Asymptotic expansion of  $M(1, b, -\frac{1}{3} aF)$  as  $aF \rightarrow \infty$  and

$$b = 1 - \frac{1}{3} (1 - aF)$$

In this appendix I shall calculate the asymptotic expansion of

$$M(1, \frac{2}{3} + k, -k)$$

as  $k \rightarrow \infty$ . This expansion is used at the end of section 13 to show that the potential vorticity becomes uniform as  $k = \frac{1}{3} aF$  becomes large.

Using the integral representation (Abramowitz and Stegun, 1968)

$$\frac{\Gamma(b-a)\Gamma(a)}{\Gamma(b)} M(a, b, z) = \int_0^1 e^{zt} t^{a-1} (1-t)^{b-a-1} dt$$

we have:

$$\begin{aligned} M(1, \frac{2}{3} + k, -k) &= (k - \frac{1}{3}) \int_0^1 e^{-kt} (1-t)^{k - \frac{4}{3}} dt \\ &= (1 - \frac{1}{3} k^{-1}) \int_0^k e^{-s} (1 - \frac{s}{k})^{k - \frac{4}{3}} ds \end{aligned}$$

or since

$$\lim_{k \rightarrow \infty} (1 - \frac{s}{k})^k = e^{-s}$$

one has, as  $k \rightarrow \infty$ ,

$$\begin{aligned} M(1, \frac{2}{3} + k, -k) &\sim \int_0^\infty e^{-2s} (1 - \frac{s}{k})^{\frac{4}{3}} ds \\ &\sim \frac{1}{2} + O(k^{-1}) \end{aligned}$$

CHAPTER 4  
Rossby Wave Action, Enstrophy and Energy  
in Forced Mean Flows

Abstract of Chapter 4

Assuming there is a separation in scale between the mean flow and fluctuations, the linearized potential vorticity equation is solved using the WKB method. Attention is focused on wave properties such as action and enstrophy which in some circumstances are conserved. In the most general case of Rossby waves supported by an arbitrary mean potential vorticity field,  $\bar{q} = f/h$ , and propagating through a forced mean flow neither action nor enstrophy is observed. It is shown that action is produced by the forcing which drives mean flow across  $q$  contours. while enstrophy is produced both by complicated  $q$  contours and by horizontal divergence of the mean flow.

#### 14. Introduction

This chapter has already been published, Young and Rhines (1980), in collaboration with my advisor. Dr. P. B. Rhines suggested the problem and provided physical insight in interpreting the conservation principles, especially as regards the integral balance results (15.10), etc. However, I undertook most of the writing and algebra and in the process discovered what is probably the most interesting result in this chapter viz. there are circumstances in which wave enstrophy is conserved when action is not. For these reasons I have decided to present the published paper, virtually unchanged, as a chapter of this thesis.

The interaction of Rossby waves with zonal mean flow has been extensively studied (see Dickinson, 1978, for a review). The energy density  $E$  of a Rossby wave train on a  $\beta$ -plane is not conserved as it propagates through a slowly varying mean flow. Instead, if the mean flow is zonal (i.e. unforced), the action density  $A = \omega^{-1}E$  defined by Bretherton and Garrett (1968) is conserved.

$$\partial A / \partial t + \nabla \cdot (\underline{C}A) = 0, \quad (14.1)$$

where  $\underline{C}$  is the group velocity and  $\hat{\omega}$  the intrinsic frequency.

If the mean flow is forced the problem is more complicated. Muller (1978) proved that  $A$  is not conserved by waves propagating through a slowly varying, forced mean flow on a homogeneous, constant depth,  $\beta$ -plane ocean. However, it is shown below that in this case the enstrophy density of the wave packet,

$$\begin{aligned} P &= (k^2 + l^2)E \\ &= -\beta kA, \end{aligned}$$

is conserved and that the analogous wave-potential enstrophy is conserved in a stratified, forced flow. When the mean flow is independent of  $x$ ,  $k$  (the  $x$ -wavenumber) is constant and  $P$  is proportional to  $A$ .

The purpose of this investigation is to derive the equations governing the change of quadratic wave properties such as  $E$ ,  $A$  and  $P$  in the general case of Rossby waves propagating through a forced mean flow in an ocean with slow depth variation. In particular our results are relevant in the gently forced interior of a homogeneous ocean where the Sverdrup balance for the mean flow  $(u,v)$  with depth  $h(x,y)$ ,

$$\bar{u} \bar{q}_x + \bar{v} \bar{q}_y = F, \quad (14.2)$$

$$\bar{q} = [f_0 + \beta y]/h(x,y).$$

obtains. As will be seen in Section 17 depth variations introduce several complications; in Section 15 we discuss the simpler problem of Rossby waves propagating vertically through a stratified incompressible fluid. In Section 16 a simple example illustrating the nonconservation of action in a forced mean flow is given.

### 15. Rossby Wave Trains in Three Dimensions

On a mid-latitude  $\beta$ -plane the linearized perturbation geostrophic potential vorticity equation in the Boussinesq approximation (see, e.g. Holton, 1975) is

$$q'_t - \bar{\psi}_y q'_{x'} + \bar{\psi}_x q'_{y'} - \psi'_{y'} \bar{q}'_x + \psi'_{x'} \bar{q}'_y = 0, \quad (15.1)$$

where

$$q' = \psi'_{xx} + \psi'_{yy} + (f_0^2 N^{-2} \psi'_z)_z,$$

$$\bar{q} = \bar{\psi}_{xx} + \bar{\psi}_{yy} + (f_0^2 N^{-2} \bar{\psi}_z)_z + \beta y.$$

Assume that there is a separation in scale between the mean flow and the perturbations and look for a solution of (15.1) using the WKB ansatz

$$\psi' = a(X, Y, Z, T) \exp \left\{ i\mu^{-1} \theta(X, Y, Z, T) \right\}. \quad (15.2)$$

where

$$(X, Y, Z, T) = \mu(x, y, z, t),$$

and

$$\mu = \frac{\text{Length (or time) scale of perturbations}}{\text{Length (or time) scale of waves}} \ll 1.$$

Equation (15.2) is substituted into (15.1) and equal powers of  $\mu$  collected to produce the hierarchy (dropping capitals)

$$\mu^0 : \hat{\omega}(k^2 + l^2 + f_0^2 N^{-2} m^2) + \beta k = 0, \quad (15.3)$$

$$\begin{aligned} \mu^1 : & \left( \frac{\partial}{\partial t} - \bar{\psi}_y \frac{\partial}{\partial x} + \bar{\psi}_x \frac{\partial}{\partial y} \right) [(k^2 + l^2 + f_0^2 N^{-2} m^2) a] \\ & - 2\hat{\omega} \underline{k} \cdot \nabla a - \hat{\omega} a \nabla \cdot \underline{k} - \beta a_x = 0, \end{aligned} \quad (15.4)$$

where

$$(k, l, m, \omega) = (\theta_x, \theta_y, \theta_z, -\theta_T),$$

and

$$\underline{k} = (k, l, f_0^2 N^{-2} m).$$

(It has been assumed that the Brunt-Väisälä frequency  $N$  varies on the same scale as the mean flow.) Eq. (15.3) is just the dispersion relation

$$\hat{\omega} = \omega + \bar{\psi}_y k - \bar{\psi}_x l = -\beta k / (k^2 + l^2 + f_0^2 N^{-2} m^2).$$

Eq. (15.4) describes the variation in amplitude of the wave packet, after a little algebra it can be put in the more intuitive form

$$\partial E / \partial t + \nabla \cdot (CE) = \frac{1}{2} a^2 K_i K_j \bar{v}_{i,j} + \frac{1}{2} a^2 K_3 K_i \partial \bar{v}_i / \partial z, \quad (15.5)$$

$$E = \frac{1}{4} (k^2 + l^2 + f_0^2 N^{-2} m^2) a^2,$$

$$(\bar{v}_1, \bar{v}_2) = (-\bar{\psi}_y, \bar{\psi}_x)$$

= the geostrophic part of  
the mean velocity field,

where  $i$  and  $j$  equal 1 and 2. The first term on the right-hand side of (15.5) is the conversion of mean kinetic energy to  $E$  by horizontal Reynolds stresses while the second term is the conversion due to vertical buoyancy flux. The derivation of (15.5) from the basic equations is given in Appendix A.

Surprisingly, the energy conversion terms on the right-hand side of (15.5) can be further simplified using the standard expressions for the rate of change of wavenumber along a packet trajectory (Lighthill, 1978)

$$\frac{dk}{dt} = -k \frac{\partial v_1}{\partial x} - l \frac{\partial v_2}{\partial x} - \frac{\partial \hat{\omega}}{\partial x}, \quad (15.6)$$

with analogous expressions for  $l$  and  $m$ . Since  $\hat{\omega}$  has no explicit  $x$  or  $y$  dependence it follows that

$$\frac{d}{dt} (K_i^2) = -2K_i K_j \bar{v}_{i,j}, \quad i, j = 1, 2,$$

$$\frac{d}{dt} (f_0^2 N^{-2} m^2) = -2K_3 K_i \left( \frac{\partial \bar{v}_i}{\partial z} \right),$$

and so (15.5) can be rewritten as

$$\begin{aligned} \partial P / \partial t + \nabla \cdot (\underline{CP}) &= 0, \\ P &= (k^2 + l^2 + f_0^2 N^{-2} m^2) E. \end{aligned} \quad (15.7)$$

Note that since

$$P = -\beta k A,$$

it follows that

$$\begin{aligned} \partial A / \partial t + \nabla \cdot (\underline{CA}) &= -A(d/dt)(\ln k) \\ &= k^{-1} A K_i \partial \bar{v}_i / \partial x, \quad i = 1, 2; \end{aligned}$$

A is conserved when the mean flow is unforced.

Integrating (15.7) over a volume which properly contains the wave train one finds

$$\frac{\partial}{\partial t} \iiint P dv = 0, \quad (15.8)$$

so that the total enstrophy is conserved. It is instructive to derive this result directly from (15.1). Multiply (15.1) by  $q'$  and average over a period to obtain

$$(\partial / \partial t) \left( \overline{\frac{1}{2} q'^2} \right) + \nabla \cdot \left( \bar{v} \overline{\frac{1}{2} q'^2} \right) + \overline{q' v'} \cdot \nabla \bar{q} = 0. \quad (15.9)$$

The crucial scale separation assumption implies

$$\nabla \bar{q} = \beta y + O(\mu^2).$$

so that (15.9) simplifies to

$$(\partial / \partial t) \left( \overline{\frac{1}{2} q'^2} \right) + \nabla \cdot \left( \bar{v} \overline{\frac{1}{2} q'^2} \right) + \beta \overline{q' v'} = 0. \quad (15.10)$$

Integrating (15.10) over a large volume containing the train reproduces (15.8). This derivation emphasises the importance of the scale separation assumption which ensures that  $\nabla \bar{q}$  is constant over the wave train. This restriction is also inherent in the WKB derivation, note how (15.3) and (15.4) are unchanged if  $\bar{q}$  is simply taken to be  $\rho y$ . This does not mean that the shear in the mean flow has been completely neglected; from (15.5) the WKB approximation accounts for the energy conversion associated with mean shear.

## 16. An Example of Nonconservation of Action

As a concrete example of nonconservation of wave action (but conservation of wave enstrophy) consider Rossby waves superimposed on a meridional flow in a homogeneous, constant depth ocean. Geisler and Dickinson (1975) analysed the critical level absorption of Rossby waves in such a flow. Because the fluid is homogeneous we can employ conservation of barotropic potential vorticity (see Appendix B) rather than the less exact conservation of geostrophic potential vorticity used in Section 15.

Since the mean flow is meridional the linearized potential vorticity equation is

$$\left[ \frac{\partial}{\partial t} + \bar{v}(\mu x) \frac{\partial}{\partial y} \right] \nabla^2 \psi' + \beta \psi'_x - \bar{v}_{xx} \psi'_y = 0. \quad (16.1)$$

The coefficients of (16.1) are independent of  $y$  and  $t$ , so a solution can be found in the form

$$\begin{aligned} \psi' &= \phi(X) \exp i(l y - \omega t), \\ X &= \mu x, \end{aligned} \quad (16.2)$$

where  $\omega$  and  $l$  are constants and  $\phi$  satisfies

$$\left\{ (\bar{v} - \frac{\omega}{l}) (\mu^2 \frac{d^2}{dX^2} - l^2) - \frac{i\beta}{l} \frac{d}{dX} - \mu^2 \frac{d^2 \bar{v}}{dX^2} \right\} \phi = 0. \quad (16.3)$$

The WKB solution of (16.3) is (see, e.g., Bender and Orszag, 1978)

$$\phi_{1,2} = [(\beta/2\omega)^2]^{-1/4} k_{1,2}^{-1/2} \exp[i\mu^{-1} \int^X k_{1,2} dX], \quad (16.4)$$

where  $k_1$  and  $k_2$  are the solutions of the quadratic equation

$$\hat{\omega} = \omega - l\bar{v}(X) = -\beta k(k^2 + l^2)^{-1}. \quad (16.5)$$

For a linear shear,  $\omega - l\bar{v} = \alpha X$ ,  $k_1$  and  $k_2$  are plotted in Figure 23.

From (16.3) and (16.4) it follows that

$$A(X) = \omega^{-1} E = -\frac{1}{4}(\beta k l)^{-1}(k^2 + l^2)^2, \quad (16.6)$$

so that

$$C_x A \text{ is proportional to } k^{-1}(X). \quad (16.7)$$

i.e. action is not conserved [cf. (14.1)] but

$$P = -\beta k A$$

is conserved. This can be deduced from the more general results of Section 15; simply suppress the term  $f_0^2 N^{-2} m^2$ .

It is interesting to solve the ray tracing problem for a wave packet in the linear shear  $\omega - l\bar{v} = \alpha X$ ; the ray equations are (Lighthill, 1978)

$$\frac{dk}{dt} = -\frac{\partial \omega}{\partial X},$$

so

$$k = k_0 - \alpha t,$$

and

$$\frac{dx}{dt} = \frac{\partial \omega}{\partial k},$$

so

$$\frac{1}{X} - \frac{1}{X_0} = \frac{\alpha^2}{\beta} t + \frac{\alpha l^2}{\beta} \left( \frac{1}{k} - \frac{1}{k_0} \right).$$

The  $x$  wavenumber decreases linearly with time. A wave packet which starts at A on Figure 23 moves East initially, is reflected at B, passes through the critical layer at C unscathed (Geisler and Dickinson, 1975), is reflected again at D and is finally absorbed at the critical layer near E. The WKB solution (16.4) is, of course, invalid at the turning points and the critical layer where (16.3) is singular.

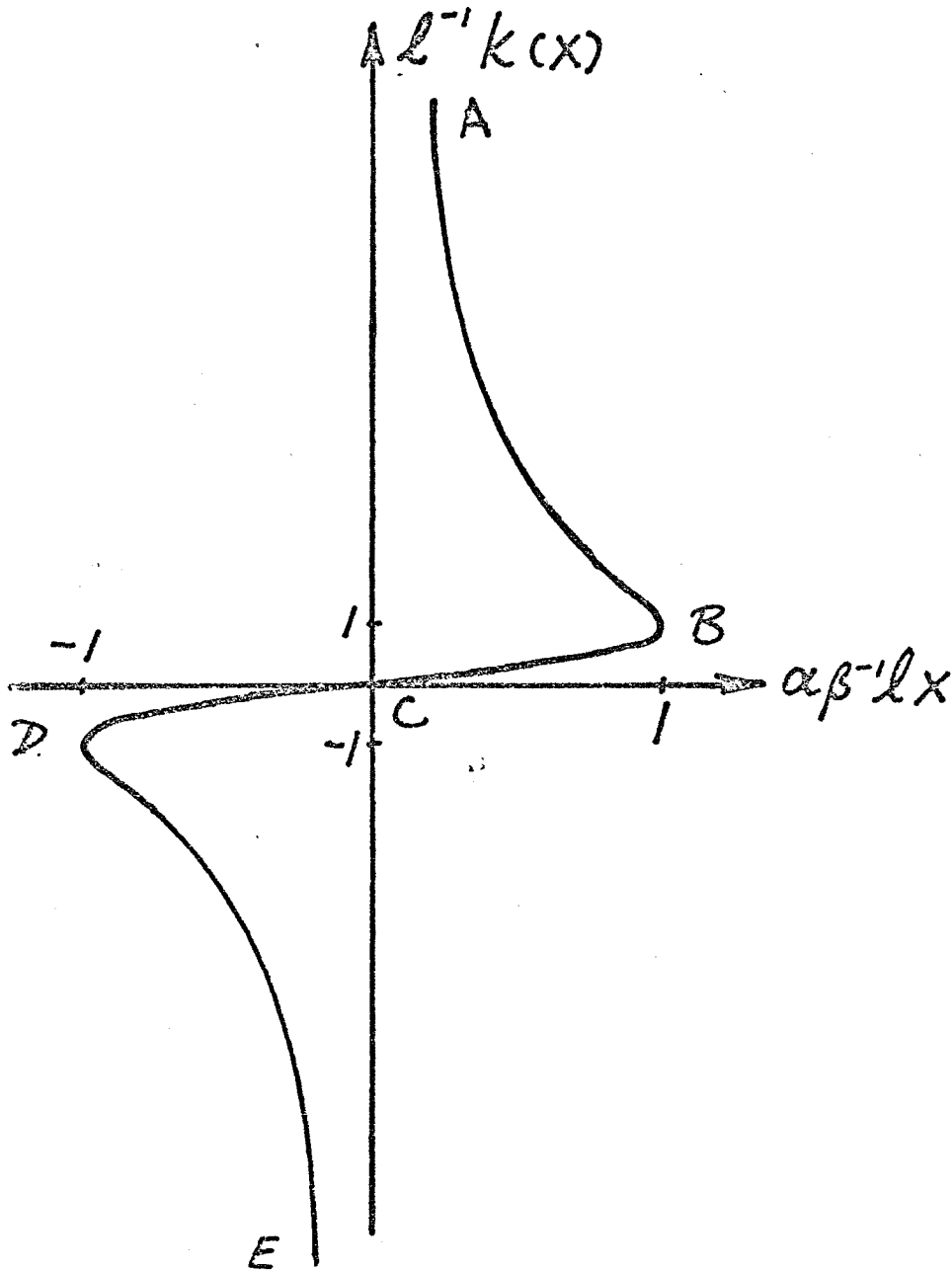


Figure 23. The solutions of (16.5) when  $\hat{\omega} = \alpha x$ . For each value of  $x$  there are two  $x$  wavenumbers; the waves on DCB have group velocities directed westward while those on AB and DE have eastward pointing group velocities. The critical layer is at  $x = 0$ ; as explained in Geisler and Dickinson (1975) only the short eastward travelling waves suffer critical layer absorption.

### 17. Rossby Wave Trains in an Ocean of Varying Depth

In section 15 we considered waves in a stratified fluid and used conservation of geostrophic potential vorticity. In this section we discuss waves in homogeneous fluid and use the more exact conservation of barotropic potential vorticity (see Appendix B),

$$\partial q' / \partial t + \bar{v} \cdot \nabla_2 q' + \underline{v}' \cdot \nabla_2 \bar{q} = -q' h^{-1} S, \quad (17.1)$$

where

$$q' = \zeta' / h, \quad \bar{q} = (f/h) + O(\mu^2), \quad (17.2)$$

$$\nabla_2 \cdot (h \underline{v}') = 0, \quad \nabla_2 \cdot (h \bar{v}) = S, \quad (17.3)$$

and

$$\nabla_2 = \frac{\partial}{\partial x} \hat{x} + \frac{\partial}{\partial y} \hat{y}.$$

The fluid source  $S$  in (17.3) is produced by the wind stress curl which pumps fluid out of the upper Ekman layer into the interior of the ocean. This is the forcing mechanism which gently drives mean flow across  $q$  contours according to the classical Sverdrup balance (see Appendix B)

$$\bar{v} \cdot \nabla_2 \bar{q} = h^{-1} \left\{ \nabla \times \underline{M} \cdot \hat{z} - \bar{q} S \right\}. \quad (17.4)$$

The mean forcing term  $S$  appears in the perturbation vorticity equation (17.1). This is in contradistinction to (15.1) where mean forcing, such as diabatic heating and mechanical stress  $M$ , appears only in the mean vorticity equation (14.2). Thus  $M$  and  $S$  are not equivalent,  $S$  can produce perturbation enstrophy (e.g. Appendix C) but  $M$  cannot.\*

---

\* Although, this distinction between  $M$  and  $S$  disappears at the level of quasi-geostrophic dynamics.

Because of (17.3), we can introduce a mass streamfunction

$$h\underline{v}' = \hat{\underline{z}} \times \nabla \psi', \quad (17.5)$$

and

$$q' = h^{-1} \zeta' = h^{-2} \left\{ \nabla^2 \psi' - \nabla_2 \ln h \cdot \nabla_2 \psi' \right\}. \quad (17.6)$$

The WKB ansatz

$$\text{leads to } \psi' = a(X, Y, T) \exp \left\{ i\mu^{-1} \theta(X, Y, T) \right\},$$

$$O(\mu^0): \hat{\omega} = h(\bar{q}_x l - \bar{q}_y k) / (k^2 + l^2), \quad (17.7)$$

$$O(\mu^1): (\partial/\partial t + \bar{\underline{v}} \cdot \nabla_2)(k^2 a) - \hat{\omega}(a \nabla_2 \cdot \underline{K} - a \underline{K} \cdot \nabla_2 \ln h + 2\underline{K} \cdot \nabla_2 a) \\ + (S/h - 2\bar{\underline{v}} \cdot \nabla_2 \ln h)(a k^2) + h \bar{q}_x a_y - h \bar{q}_y a_x = 0, \quad (17.8)$$

where it has been assumed that the depth  $h$  varies on the same scale as the mean flow and

$$\underline{K} = (k, l).$$

After considerable algebra (17.8) can be transformed into an energy equation (see Appendix A)

$$\partial E / \partial t + \nabla_2 \cdot (\underline{CE}) = 2EK^{-2} K_i K_j \left\{ \bar{v}_{i,j} - \frac{1}{2} \delta_{ij} \nabla_2 \cdot \bar{\underline{v}} \right\} + E \bar{\underline{v}} \cdot \nabla_2 \ln h, \quad (17.9)$$

where

$$E = \frac{1}{2} \overline{h \underline{v}'^2} = \frac{1}{4} h^{-1} a^2 K^2.$$

The right-hand side of (17.9) is the conversion of mean flow kinetic energy to wave energy by Reynolds stresses.

Eq. (17.9) can be rewritten using standard ray tracing results in two ways. Firstly using

$$dK_i / dt = -K_j \bar{v}_{j,i} - \hat{\omega}_{,i},$$

(see Lighthill, 1978) one obtains

$$\partial P / \partial t + \nabla_2 \cdot (\underline{C}P) = \frac{1}{2} h^{-1} a^2 \left\{ \underline{1} \underline{K} \cdot \nabla_2 (h \bar{q}_x) - \underline{k} \underline{K} \cdot \nabla_2 (h \bar{q}_y) \right\} - h \nabla_2 \cdot (h^{-1} \underline{v}) P, \quad (17.10)$$

where

$$P = (k^2 + l^2) E = \frac{1}{2} h \overline{\zeta'^2} = \frac{1}{2} h^3 \overline{q'^2}. \quad (17.11)$$

Secondly using

$$d\hat{\omega}/dt = - C_{ij} K_j \bar{v}_{i,j} + \bar{v} \hat{\omega}_{,i},$$

(Lighthill, 1978) one has

$$\partial A / \partial t + \nabla_2 \cdot (\underline{C}A) = - A (k F_y - l F_x) (k \bar{q}_y - l \bar{q}_x)^{-1}, \quad (17.12)$$

where

$$A = \hat{\omega}^{-1} E, \quad (17.13)$$

$$F = \overline{u q_x} + \overline{v q_y},$$

$P$  in (17.10) is the vertically integrated relative enstrophy in contrast to the integrated potential enstrophy appearing in (15.7). The right-hand side of (17.10) simplifies in two circumstances. If  $h$  is constant (17.10) becomes

$$\partial P / \partial t + \nabla_2 \cdot (\underline{C}P) = - \nabla_2 \cdot (\underline{v}) P, \quad (17.14)$$

while if  $\beta = 0$  and  $h = h_0 \exp(-\alpha x - \beta y)$  then

$$\partial P / \partial t + \nabla_2 \cdot (\underline{C}P) = - h \nabla_2 \cdot (h^{-1} \underline{v}) P. \quad (17.15)$$

In both cases the production of  $P$  is related to the horizontal divergence of the mean flow; simple scale analysis gives:

$$\text{fractional rate of change of } P \sim \nabla \cdot \underline{v} \sim |\underline{v}| \left\{ \text{Radius of the Earth} \right\}^{-1},$$

where it is assumed that the mean flow is in Sverdrup balance. In contrast:

$$\text{fractional rate of change of } E \sim |\underline{v}| L^{-1};$$

provided  $L$  is much less than the radius of the Earth  $P$  is more nearly conserved than  $E$ . The integral of (17.10) over a large region containing the disturbance is

$$\frac{\partial}{\partial t} \iint P dA + \iint h P \nabla_2 \cdot (h^{-1} \underline{v}) dA = 0. \quad (17.16)$$

This result is derived directly from (22) in Appendix C.

$A$  in (17.12) is the wave action;  $A$  is conserved provided  $F = 0$ , i.e. if the mean flow is unforced. The general source term in the Rossby wave action equation has not been given before and so the right-hand side of (17.12) is one of the principal results of this note.

## 18. Discussion

The wave quantities  $P$  and  $A$  have different and complementary governing equations [(compare (17.10) and (17.12)]. Roughly speaking, the source term in (17.10) is nonzero when the  $\bar{q}$  contours are complicated; in certain cases, such as a constant depth ocean, this source term vanishes and  $P$  is conserved. With extremely rough topography, not amenable to WKBJ analysis, topographic scattering produces wave enstrophy very efficiently. The production of  $A$  in (17.12) on the other hand is simply related to  $F = \bar{u}\bar{q}_x + \bar{v}\bar{q}_y$ .

The slow variation in amplitude of Rossby wave trains is determined at second order in the WKB expansion. At this level of approximation the  $\beta$ -effect is not equivalent to a sloping bottom and a mechanical stress  $M$  is not equivalent to Ekman divergence  $S$ . It is gratifying that  $A$  is conserved in this general case when the mean flow is unforced, this is further evidence for the faithfulness and consistency of the  $\beta$ -plane approximation.

Another major result of this chapter is embodied in (15.7); in vertically propagating Rossby waves the enstrophy is conserved even when the mean flow depends on  $x$ .

## Appendix A

Derivation of the energy equation

In this appendix (15.5) and (17.9) are derived; we prefer to obtain these energy equations from the equations of motion; they also follow from the WKB transport equations (15.4) and (17.8).

To get (15.5), start with the linearized, geostrophic Boussinesq equations of motion, retaining order Rossby number terms,

$$\bar{D}\underline{v}' + (\underline{v}' \cdot \nabla_2)\bar{\underline{v}} - \hat{z} \times f\underline{v}' + f_0 \nabla_2 \psi' = 0(\text{Rossby number})^2, \quad (\text{A1})$$

$$\bar{D}\partial\psi'/\partial z + (\underline{v}' \cdot \nabla_2)\partial\bar{\psi}/\partial z + w'N^2f_0^{-1} = 0(\text{Rossby number})^2, \quad (\text{A2})$$

$$\nabla_2 \cdot \underline{v}' + w'_z = 0(\text{Rossby number})^2, \quad (\text{A3})$$

where

$$\underline{v}' = (u', v'), \quad (\text{A4})$$

$$\bar{D} = \frac{\partial}{\partial t} + \bar{u} \frac{\partial}{\partial x} + \bar{v} \frac{\partial}{\partial y}. \quad (\text{A5})$$

Forming the combination of  $\overline{\underline{v}' \cdot (\text{A1})} + N^{-2} \overline{(\text{A3})\partial\psi'/\partial z}$  one has

$$\begin{aligned} & \bar{D} \left[ \frac{1}{2} \overline{\underline{v}' \cdot \underline{v}'} + \frac{1}{2} N^{-2} \overline{(\partial\psi'/\partial z)^2} \right] + \nabla \cdot \left\{ \overline{\psi' (\underline{v}' + w'\hat{z})} \right\} \\ & = - \overline{v'_i v'_j} \bar{v}_{i,j} + f_0 N^{-2} \overline{(\partial\psi'/\partial z) v'_i} (\partial\bar{\psi}/\partial z)_{,i}. \end{aligned} \quad (\text{A6})$$

Using the WKB ansatz (15.2) to evaluate the terms in (A6) to lowest nonzero order one recovers (15.5).

To get (17.9) start with the shallow water equations

$$\bar{D}\underline{v}' + (\underline{v}' \cdot \nabla_2)\bar{\underline{v}} - \hat{z} \times f\underline{v}' + f_0 \nabla p' = 0, \quad (\text{A7})$$

$$\nabla_2 \cdot (h\underline{v}') = 0. \quad (\text{A8})$$

Taking  $h\underline{v}'$ , (A7) one has

$$(\partial/\partial t)(\frac{1}{2}h\underline{v}' \cdot \underline{v}') + \nabla_2 \cdot (\frac{1}{2}h\underline{v}' \cdot \underline{v}' \underline{v} + f_0 h \underline{p}' \underline{v}') = -h \underline{v}'_i \underline{v}'_j \underline{v}'_{i,j} + S \frac{1}{2} \underline{v}' \cdot \underline{v}', \quad (A9)$$

where [see (17.3) and the subsequent discussion]

$$S = \nabla_2 \cdot (h\underline{v}). \quad (A10)$$

Using the WKB ansatz together with (A10) recovers (17.9) from (A9).

## Appendix B

### Derivation of the Barotropic potential vorticity equation

The shallow water equations in an ocean of varying depth  $h$  are

$$\underline{a}\underline{v}/\partial t + \hat{z} \times h\underline{q}\underline{v} = -\nabla B + \underline{M}, \quad (B1)$$

$$\nabla_2 \cdot h\underline{v} = S, \quad (B2)$$

where

$$B = \rho^{-1}p + \frac{1}{2} \underline{v} \cdot \underline{v},$$

$\underline{M}$  = mechanical stresses,

$S$  = mass source term,

$q = (\zeta + f)/h$  = barotropic potential vorticity

There are two forcing mechanisms,  $\underline{M}$  and  $S$ . The mass source  $S$  is a more realistic method of representing the divergent upper Ekman layer than the mechanical stress  $\underline{M}$ .

To obtain the barotropic potential vorticity equation take the curl of (B1) and use (B2) to get

$$\partial q/\partial t + \underline{v} \cdot \nabla_2 q = h^{-1} \{ \nabla \times \underline{M} \cdot \hat{z} - qS \}. \quad (B3)$$

The linearized fluctuation equation (17.1) follows from (B3). Note that if  $\underline{M}$  and  $S$  are mean forcing terms,  $S$  appears in the fluctuation equation but  $\underline{M}$  does not.

## Appendix C

Derivation of the integrated relative enstrophy equation (17.6)

Consider an ocean with  $\beta = 0$  and  $h = h_0 \exp(-\gamma y)$ , so the potential vorticity equation (17.1) can be put in the form

$$(\partial/\partial t + \bar{v} \cdot \nabla_2)(h^2 q') + (h^{-1} S - 2\bar{v} \cdot \nabla_2 \ln h)(h^2 q') + \gamma f_0 h v' = 0, \quad (C1)$$

$$h^2 q' = \nabla_2^2 \psi' + \gamma \psi'_y. \quad (C2)$$

If (C1) is multiplied by  $h q'$ , integrated over a large area and averaged (17.16) is recovered. In particular then the third term in (C1) vanishes completely since

$$\begin{aligned} \iint \exp(\gamma y) \psi'_x (\psi'_{xx} + \psi'_{yy} + \gamma \psi'_y) dx dy &= \iint \psi'_x \frac{\partial}{\partial y} (\exp(\gamma y) \psi'_y) dx dy \\ &= - \iint \exp(\gamma y) \{ \psi'_{xy} \psi'_y \} dx dy = 0 \end{aligned}$$

Note that if (C1) is multiplied by  $h^n q'$  the third term will vanish only when  $n = 1$ ; this suggests that out of the family of wave properties  $h^m q'^2$  the member  $m = 3$  will have the simplest conservation properties.

## CHAPTER 5

## Some Shear Dispersion Problems

## Abstract of Chapter 5

Two models of advection-diffusion in the oscillatory, sheared velocity field of an internal wave are discussed. My goal is to develop intuition about the role of such currents in ocean mixing through the mechanism of shear dispersion. The analysis suggests simple parameterizations of this process, equations (20.7) and (23.2a).

The solutions also incidentally illuminate a variety of other advection-diffusion problems, such as unsteady shear dispersion in a pipe and enhanced diffusion through wavenumber cascade induced by steady shearing and straining fields.

## 19. Introduction

I am in the process of preparing a paper for publication based on the content of this chapter in collaboration with Drs. P. B. Rhines and C. J. R. Garrett. Some of their ideas and insights have inevitably been included in the discussion given here; I have attempted to indicate explicitly the important sections which are not mine originally. The most important results in this chapter are embodied in (7), which I discovered independently of Dr. Garrett, and (35) which I discovered after Dr. Garrett persuaded me to look at shear dispersion in the velocity field (34).

The aim of this chapter is to examine some simple advection-diffusion models with the goal of developing intuition about the role of sheared oscillatory currents in mixing tracers in the ocean interior. The velocity fields considered are so simple that the advection-diffusion equation can often be solved exactly; I hope that my principal conclusions are robust enough to apply to the more complicated velocity fields associated with internal waves and inertial oscillations. In particular, it may be that the horizontal mixing of tracers by the combined action of vertical shear and vertical mixing is significant in both deep ocean and shelf regions and may provide an effective mechanism for horizontally dispersing tracer anomalies with vertical scales of order 100 m and horizontal scales of order 10 km. The solutions of the advection-diffusion models discussed here suggest simple parameterizations of this process.

Besides the real space phenomenon of shear dispersion our solutions also illustrate an important related process in Fourier space viz. the cascade to higher wavenumbers and the consequent enhanced dissipation produced by the shearing (and straining) of a large scale velocity field. This process is important even on basin scales; it is the mechanism by which peak concentrations are reduced. The ultimate problem is to predict the statistics of tracers in oceans with turbulence, waves and mean circulation all included. Besides the goal of understanding the interaction of turbulence and mean flow in shaping tracer distributions, one wants to know the sampling variability to be expected with turbulence of known intensity.

The theory of shear flow dispersion began with Taylor's (1953) realization that the sheared velocity profile in a pipe or channel would interact with cross-channel diffusion to produce an augmented along-channel dispersion. In this way a vertical sheet of dye is deformed by the shear and mixed vertically, producing a spreading plug of dye, almost uniformly distributed across the channel, which moves downstream at the cross channel averaged velocity. Since Taylor's work the subsequent developments have relied heavily on the simplifying approximations he introduced to obtain an analytic solution. These approximations amount to assuming that the tracer is almost uniformly distributed across the channel and so Taylor's theory applies only after the initial distribution of tracer has had sufficient time to spread across the channel.

The moment method of Aris (1956) and Saffman (1962) is not subject to the same limitations as Taylor's approximate theory and in principle it can provide precise information about the time evolution of certain integral moments (such as center of mass and moment of inertia) of tracer distributions. However in previous geophysical applications the limitations of Taylor's simpler theory have not been particularly restrictive because attention has been confined to shallow systems such as estuaries and streams [e.g., Fischer et al, (1980)]. An exception is Csanady's (1966) study of shear dispersion in an Ekman layer; because the region is semi-infinite, Taylor's theory does not apply and the moment method is used.

In this chapter I shall construct some exact solutions which illustrate the process of shear dispersion in an infinite region. These solutions may qualitatively describe processes in the ocean interior where the shearing (and straining) of internal waves and mesoscale currents can amplify smaller scale diffusive processes. Surprisingly, these exact solutions are in many ways mathematically simpler than both Taylor's approximate solution and those based on the moment method.

This analytic simplicity arises from two idealizations:

- (i) the region is infinite so it is not necessary to satisfy no flux boundary conditions;
- (ii) the horizontal velocity field is a linear function of the vertical coordinate.

In discussing horizontal shear dispersion by internal waves the second idealization is potentially misleading: it is observed that the

horizontal velocity fields of inertial oscillations have a jagged vertical structure with many sign reversals. Accordingly it is necessary to supplement the exact solutions with an approximate analysis of shear dispersion by a horizontal velocity field with an oscillatory vertical structure. It is found that the exact solution, based on the idealizations above, is misleading if the diffusivity is sufficiently large. However, "reasonable" estimates of the vertical diffusivity in the ocean suggest that shear dispersion by internal waves is closer to the small diffusivity limit where the idealized problem is directly relevant.

In section 20 we introduce the idealized model of advection-diffusion in an oscillatory shear flow. This problem is solved exactly using an advected coordinate system. The form of the solution motivates the introduction of an "effective horizontal diffusivity" which is equal to the actual horizontal diffusivity plus a term which arises from the interaction of the vertical shear and vertical diffusivity. In section 21 average properties of the model equation are discussed; by considering a time average over the period of the oscillatory shear flow the effective horizontal diffusivity, obtained formally in section 21, is heuristically derived. In section 22 the special case of a steady velocity field is discussed; this special case is qualitatively different from the oscillatory solutions in sections 20 and 21. In this section we also discuss the enhanced diffusion associated with a steady straining field. In section 23 we consider some oceanic applications of the results in sections 20 and 21; it is argued that an effective horizontal

diffusivity can be introduced for shear flows with more complicated spatial and temporal structure. Provided the diffusivity is sufficiently small this parameterization is similar to that obtained in sections 20 and 21. Attention is focused on inertial oscillations which might effectively disperse tracer anomalies with vertical scales of meters and horizontal scales of kilometers. In section 24 it is shown how the introduction of an advected coordinate can be used to simplify a very general class of advection-diffusion equations. This procedure might be useful if it was necessary to solve the shear dispersion problem for a particular velocity profile numerically. In most cases, however, the theory discussed in the earlier sections should provide an adequate qualitative description of the dispersion.

## 20. A Model Equation and its Solution

The model advection-diffusion equation we will solve is:

$$\theta_t + u \theta_x = \eta \theta_{xx} + K \theta_{zz} \quad (20.1)$$

$$\theta(x, z, 0) = \cos kx \cos mz \quad (20.2)$$

The velocity field is:

$$u = \alpha z \cos \omega t,$$

more general fields are considered in sections 23 and 24. In (20.1) and (20.2)  $x$  and  $z$  are horizontal and vertical coordinates,  $\eta$  and  $K$  are horizontal and vertical diffusivities and  $\theta$  is the tracer concentration. Previous work on this model equation in a bounded region using Taylor's method is summarized by Fischer (1976) and Fischer *et al.* (1980). Bowden (1965) first considered alternating currents like that in (20.1) in the context of tidal mixing in a shallow channel; time dependence of the shearing current is obviously a desirable feature in a model of shear dispersion by an internal wave. The steady limit,  $\omega \rightarrow 0$ , is an important special case and is qualitatively different from the unsteady case.

For simplicity we shall first solve (20.1) and (20.2) with  $m = 0$ , the case  $m \neq 0$  is more complicated algebraically and is treated in Appendix B. First note that the solution of (20.1) and (20.2) if  $\eta = K = 0$  is

$$\theta = \cos k\tilde{x} \quad (20.3)$$

where

$$\tilde{x} = x - (\alpha/\omega)z \sin \omega t. \quad (20.4)$$

The variable  $\tilde{x}$  is an advected coordinate. It is the initial position of the particle which is at  $x$  at time  $t$ . The solution (20.3) is simply a statement that when there is no diffusion each particle retains its initial value of  $\theta$ .

Now suppose  $\eta$  and  $\kappa$  are nonzero. The exact solution can be found by looking for a solution in the form

$$\theta = A(t) \cos k\tilde{x} \quad (20.5)$$

where  $A(0) = 1$ .

When (20.5) is substituted into (20.1) one finds:

$$\dot{A} = - \left\{ \eta k^2 + k^2 (\alpha/\omega)^2 \sin^2 \omega t \right\} A.$$

The solution of this simple differential equation gives:

$$\theta = \exp \left\{ -\eta k^2 t - \kappa k^2 \frac{1}{2} (\alpha/\omega)^2 \left[ t - \frac{\sin 2\omega t}{2\omega} \right] \right\} \cos k\tilde{x} \quad (20.6)$$

$A$  is plotted as a function of time in figure 24.

The solution (20.6) shows that the interaction between the shear flow with the vertical diffusion produces an "effective" horizontal diffusivity:

$$\eta_e = \eta + \frac{1}{2} (\alpha/\omega)^2 \kappa \quad (20.7)$$

(the limit  $\omega \rightarrow 0$  is singular and is discussed in the section 22). Equation (20.7) is one of the most important results in this chapter. It was derived independently by Dr. C. J. R. Garrett using a different method.

In order to illustrate the role of the effective horizontal diffusivity more clearly we use Fourier analysis to solve (20.1) with a more interesting initial condition:

$$\begin{aligned} \theta(x, z, 0) &= \frac{\sqrt{\pi}}{2a} \exp \left\{ -x^2/4a^2 \right\} \\ &= \int_0^\infty \exp \left\{ -a^2 k^2 \right\} \cos kx \, dk. \end{aligned} \quad (20.8)$$

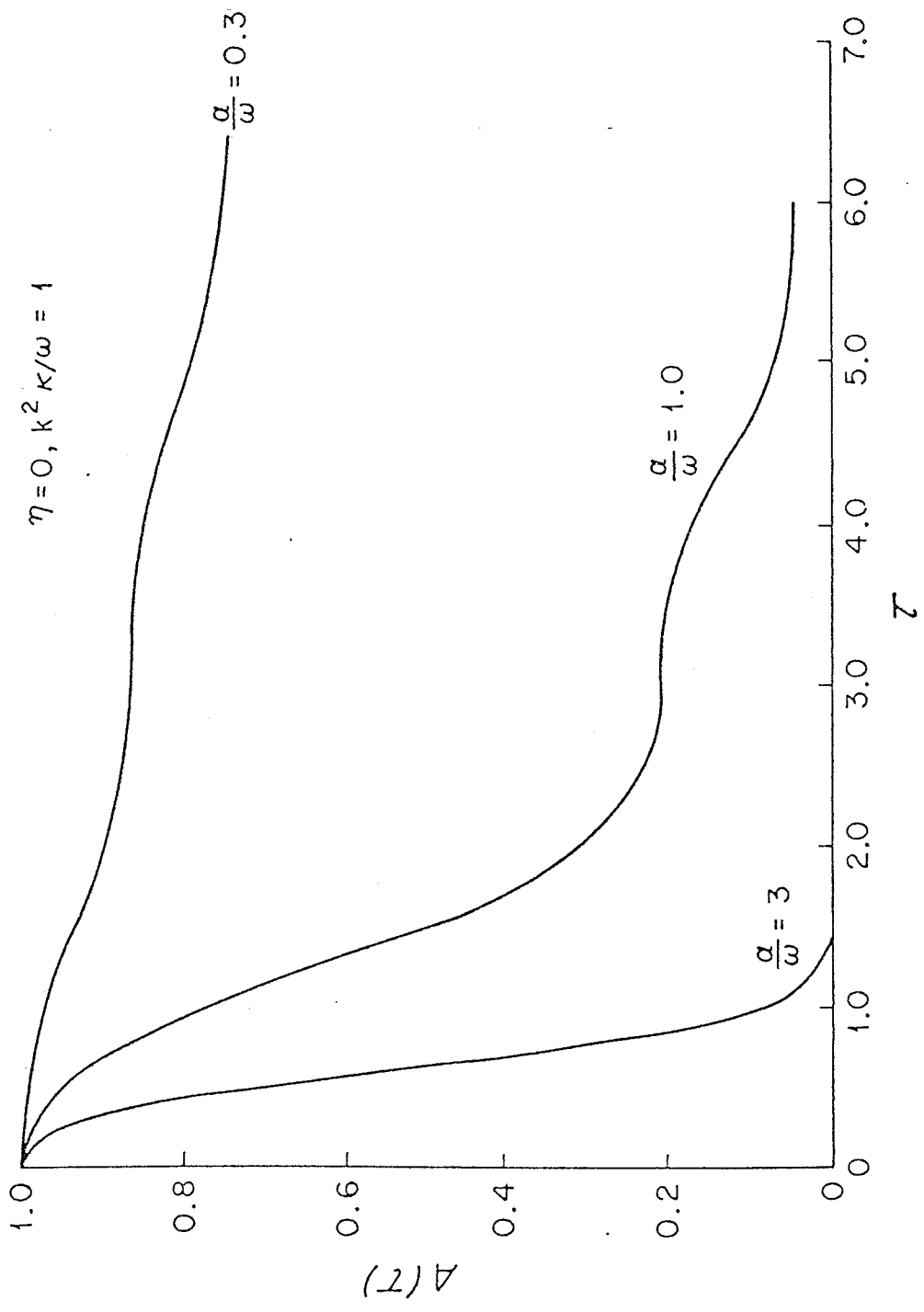


Figure 24. The amplitude  $A$  in (20.5) as a function of the nondimensional time  $\tau = \omega t$ . As  $\omega \rightarrow 0$  the decay is very rapid.

Since (20.6) is the solution of (20.1) with  $\cos kx$  as an initial condition, from (20.8) the solution with a Gaussian initial condition is:

$$\begin{aligned} \theta(x,z,t) &= \int_0^{\infty} \exp \left\{ -a^2 k^2 \right\} \exp \left\{ -\eta_e k^2 t + \frac{1}{2} (\alpha/\omega)^2 k^2 (\sin 2\omega t/2\omega) \right\} \cos k\tilde{x} \, dk \\ &= \frac{\pi}{2\tilde{a}} \exp \left\{ -\tilde{x}^2/4\tilde{a}^2 \right\} \end{aligned}$$

where  $\tilde{x}$  is defined in (20.4),  $\eta_e$  in (20.7) and

$$\tilde{a}^2 = a^2 + \eta_e t - \frac{1}{2} K(\alpha/\omega)^2 (\sin 2\omega t/2\omega) \quad (20.9)$$

Equation (20.9) shows clearly how the width of the Gaussian distribution of tracer increases linearly with time in a manner consistent with the interpretation  $\eta_e$  as an effective horizontal distribution. Note that even if the actual horizontal diffusivity  $\eta$  is identically zero the combination of a shear current and vertical diffusion produces horizontal spreading.

## 21. Average Properties of the Model Equation

In this section we consider time averaging (20.1) over a period; we will suppose that the diffusivities are small in the sense that:

$$\eta_{e^*} = \eta_e k^2 / \omega \ll 1. \quad (21.1)$$

The condition (21.1) ensures that the solution (20.6) is an oscillatory function of time modulated by a slow exponential decay; in fact:

$$\theta = e^{-\eta_{e^*}(\omega t)} \cos k\tilde{x} + O(\eta_{e^*}), \quad (21.2)$$

see the curve  $(\alpha/\omega) = .3$  in figure 24 which corresponds to  $\epsilon = .045$ .

Define a running time average by:

$$\bar{f}(t) = \frac{\omega}{2\pi} \int_{t - \frac{\pi}{\omega}}^{t + \frac{\pi}{\omega}} f(t') dt'.$$

In Appendix C it is shown that:

$$\bar{\theta} = e^{-\eta_{e^*}(\omega t)} \cos kx J_0(\alpha k z / \omega) + O(\epsilon) \quad (21.3)$$

where  $J_0$  is the Bessel function of zero order. This calculation is instructive because it illustrates some of the potential difficulties in interpreting time averaged Eulerian measurements. It is easy to see that the spatially averaged value of  $\theta$  is zero. Since the actual tracer pattern which is being swept around has equal amounts of positive and negative  $\theta$  this spatial average is less misleading than (21.3). The nonzero value of the time average can be understood intuitively by considering the record obtained by a fixed  $\theta$ -measuring instrument with a response time which is so

slow that it averages over many periods. The  $\theta$  pattern moves backwards and forwards and momentarily stops when its motion changes direction. Thus the time averaging Eulerian instrument is biased by the value of  $\theta$  which comes to rest at its position, and so spends the most time there.

$\bar{\theta}$  is a solution of the time average of (20.1):

$$\bar{\theta}_t + (\overline{u\theta})_x = \kappa \bar{\theta}_{zz} + \eta \bar{\theta}_{xx} \quad (21.4)$$

If the exact solution was unknown we would be unable to deduce (21.3) from (21.4) because of the flux term  $(u\theta)_x$ . There is however an instructive geometric argument, due to Dr. C. J. R. Garrett, which applies in the region:

$$\alpha k |z| / \omega \ll 1 \quad (21.5)$$

where  $u$  is small and this flux divergence negligible. This argument provides a simple explanation of why the effective horizontal diffusivity is given by (20.7). Of course (20.7) does not depend on (21.5) being satisfied; because of our inability to make a useful simplifying statement about  $(u\theta)_x$  we have been unable to produce a similar heuristic argument which explains (20.7) when  $\alpha k |z| / \omega > 1$ .

Begin by considering three  $\theta$ -contours which are initially parallel to each other and the  $z$ -axis and equally spaced at a distance  $\epsilon$ . At some later time the contours are tipped as in figure 25. Note that (21.1) ensures that each particle essentially keeps the same value of  $\theta$  over a period and so permits us to identify  $\theta$ -contours with material lines. Thus the vertical spacing of the  $\theta$ -contours has decreased from infinity to:

$$\delta = \epsilon / (\alpha / \omega) \sin \omega t \quad (21.6)$$

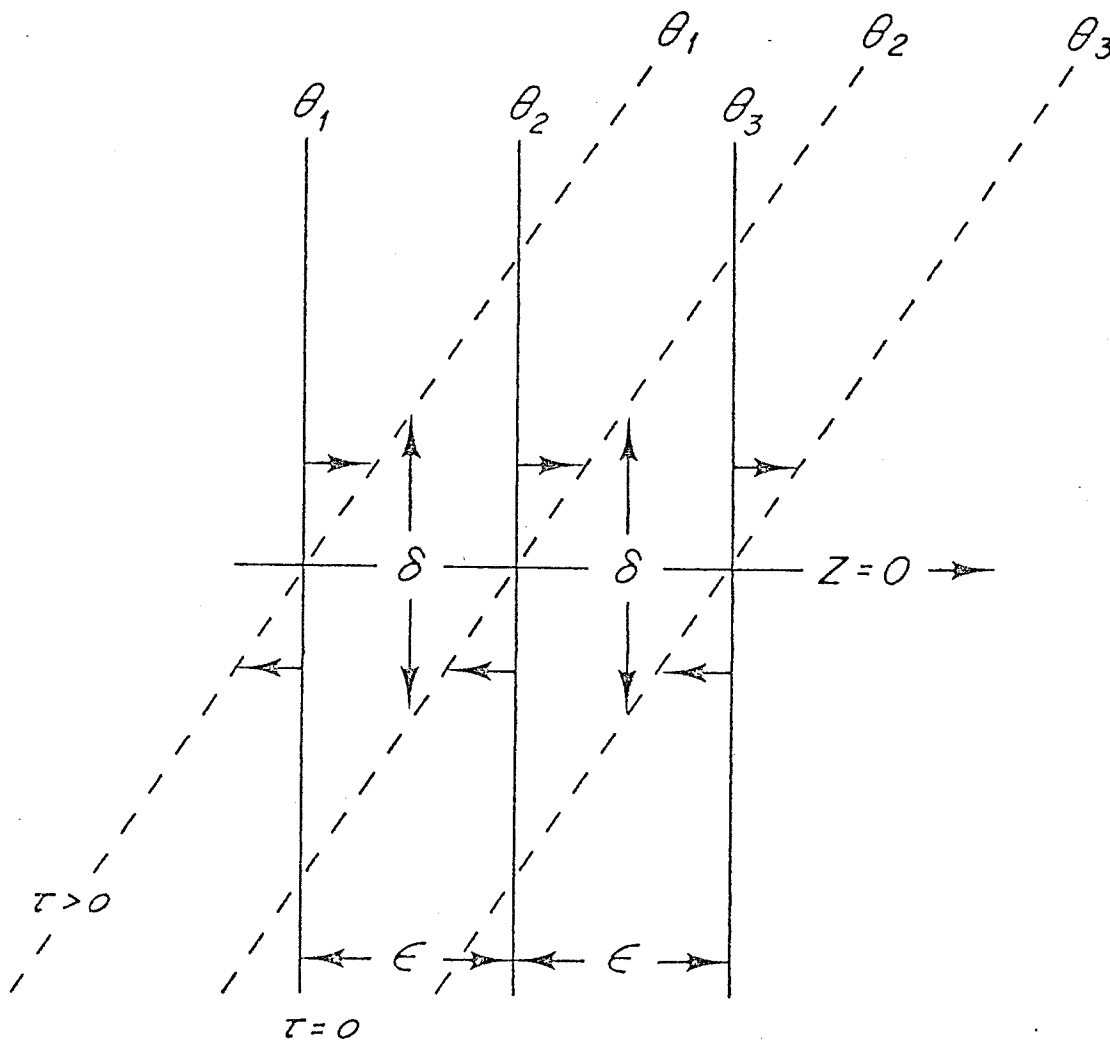


Figure 25. Illustration of the geometry referred to in the text to derive (21.8). Initially the three  $\theta$  contours are vertical and equally spaced by a distance  $\epsilon$ . The shear flows tips them as shown above.

Now if  $\epsilon$  is small (more precisely  $\epsilon \ll k^{-1}$ ) then

$$\begin{aligned} \kappa \theta_{zz} &\approx \kappa \left( \frac{\theta_1 - 2\theta_2 + \theta_3}{\delta^2} \right) \\ &= \kappa \left( \frac{\alpha}{\omega} \right)^2 \sin^2 \omega t \left( \frac{\theta_1 - 2\theta_2 + \theta_3}{\epsilon^2} \right) \\ &\approx \kappa \left( \frac{\alpha}{\omega} \right)^2 \sin^2 \omega t \theta_{xx} \end{aligned} \quad (21.7)$$

Time averaging (21.7) we see that

$$\kappa \bar{\theta}_{zz} = \kappa \frac{1}{2} \left( \frac{\alpha}{\omega} \right)^2 \bar{\theta}_{xx} \quad (21.8)$$

so that if  $(\overline{u\theta})_x$  is negligible in (21.4) then  $\eta_e$  is given by (20.7). Since:

$$J_0'' \approx -\frac{1}{2} J_0 \approx -\frac{1}{2}$$

when argument is small, (21.8) also follows from (21.3). This formal derivation shows how dependent the simple statement (21.8) is on the approximation (21.5).

From (21.3) we can also calculate the balance of terms in (21.4) when:

$$\alpha k |z| / \omega \gg 1.$$

In this case the argument of the Bessel function is large and consequently:

$$J_0'' \sim -J_0$$

so that

$$\kappa \bar{\theta}_{zz} \approx \left( \frac{\alpha}{\omega} \right)^2 \bar{\theta}_{xx}$$

$$\overline{u\theta}_x \approx \frac{1}{2} \kappa \left( \frac{\alpha}{\omega} \right)^2 \bar{\theta}_{xx}$$

Note how the flux divergence term has a counter-gradient sense.

## 22. Steady Velocity Fields: a Comparison of Shear with Strain

The solution of (20.1) when  $\omega=0$  can be found by simply taking the limit  $\omega \rightarrow 0$  in (20.6). This steady shear dispersion problem was originally considered by Dr. P. B. Rhines and served as my initial motivation for the class of problems discussed in this chapter. When  $\omega \rightarrow 0$  the first term in the Taylor series expansion of  $\sin 2\omega t$  cancels and we are left with;

$$\theta = \cos k\tilde{x} \exp \left\{ -nk^2t - \frac{1}{3} \alpha^2 k^2 t^3 \right\} \quad (22.1)$$

$$\tilde{x} = x - \alpha z t \quad (22.2)$$

As  $t \rightarrow \infty$  the above solution decays much more rapidly than (20.6). This is because the steady velocity field, unlike the oscillating field, persistently increases the  $\theta$ -gradients and enhances the diffusion. This point is illustrated more graphically when we consider the evolution of the "Gaussian patch" initial condition (20.8). The solution is

$$\theta(x,z,t) = \frac{\pi}{2\tilde{a}} \exp \left\{ -\tilde{x}^2/4\tilde{a}^2 \right\} \quad (22.3)$$

where  $\tilde{x}$  is given by (22.2) and:

$$\tilde{a}^2 = a^2 + \alpha z t + \frac{1}{3} \alpha^2 k^2 t^3 \quad (22.4)$$

It is impossible to define an effective horizontal diffusivity in this steady shear flow problem since it is clear from (22.4) that the patch expands much more rapidly than can be explained by an ordinary constant Fickian diffusivity. Saffman (1962) using the moment method found a similar  $t^{3/2}$  growth in the width of a cloud released at ground level into a semi-infinite atmosphere in which the velocity increases linearly with  $z$ .

Coincidentally the  $t^{3/2}$  expansion of the length scale in (22.4) is identical to that predicted by Richardson's "neighbour separation" theory of relative diffusion in a turbulent flow. In this problem the faster than  $t^{1/2}$  spreading occurs because a larger range of eddy sizes can act on the patch as its scale increases. This mechanism is very different from that in (22.4) where the  $t^{3/2}$  behaviour is produced by vertical diffusion from faster flowing regions into slowly flowing levels. The point is that one should not be too hasty in attributing  $t^{3/2}$  patch growth to relative diffusion, a steady shear flow is capable of producing the same behaviour.

There is a heuristic argument, similar to that in section 21, which explains the  $t^3$  term in (22.4) and provides some physical insight. Once again consider three  $\theta$ -contours, initially equally spaced by  $\epsilon$  and parallel to the  $z$ -axis as in figure 25. The contours are tipped by the shear flow so that their vertical spacing is

$$\delta = \epsilon/\alpha t$$

and consequently, as in section 21:

$$\kappa \theta_{zz} = \alpha^2 t^2 \kappa \theta_{xx} \quad (22.5)$$

Using (22.5) to replace  $\kappa \theta_{zz}$  in the steady version of (20.1) gives:

$$\theta_t + \alpha z \theta_x = (\eta + \alpha^2 t^2 \kappa) \theta_{xx} \quad (22.6)$$

Equation (22.6) means that the vertical shear is equivalent to a horizontal diffusivity which increases with time. It can easily be reduced to:

$$\theta_t = \theta_{xx}$$

by the change of variables

$$\tilde{t} = \eta t + \frac{1}{3} \kappa \alpha^2 t^3$$

$$\tilde{x} = x - \alpha z t.$$

This latter reduction is just another way of deriving the exact solution (22.1). The most important result is, however, (22.5) which relates the vertical and horizontal diffusion terms.

To quantify the notion that the shear flow amplifies the  $\theta$ -gradients until the enhanced diffusion rapidly destroys them it is helpful to compute the  $x$ -average average of  $\nabla \theta \cdot \nabla \theta$ :

$$\begin{aligned} \langle \nabla \theta \cdot \nabla \theta \rangle &= \lim_{L \rightarrow \infty} \frac{1}{2L} \int_{-L}^L \nabla \theta \cdot \nabla \theta \, dx \\ &= \frac{1}{2} k^2 (1 + (\alpha t)^2) \exp \left\{ -2\eta k^2 t - \frac{2}{3} \alpha^2 k^2 t^3 \right\} \end{aligned} \quad (22.7)$$

The right hand side of (22.7) is plotted as a function of the nondimensional time  $\tau = (\alpha t)$  in figure 26. The initial growth and eventual decay of the  $\theta$  gradients is as expected. What is not so obvious physically is what determines the time  $\tau_* = \alpha t_*$  at which the averaged squared gradient is a maximum. From (22.7) it easily follows that:

$$\tau_* - \left( \eta_* + \kappa_* \tau_*^2 \right) (1 + \tau_*^2) = 0 \quad (22.8)$$

where:

$$\eta_* = \eta k^2 / \alpha \quad \text{and} \quad \kappa_* = \kappa k^2 / \alpha$$

are nondimensional diffusivities. If  $\eta_* = 0$  ( $\kappa_*$ ) and  $\kappa_* \ll 1$  the relevant solution of the quartic is:

$$\tau_* = \kappa_*^{-1/3} - \frac{1}{3} \kappa_* \left( 1 + \frac{\eta_*}{\kappa_*} \right) + 0 \left( \frac{\eta_*}{\kappa_*} \right)$$

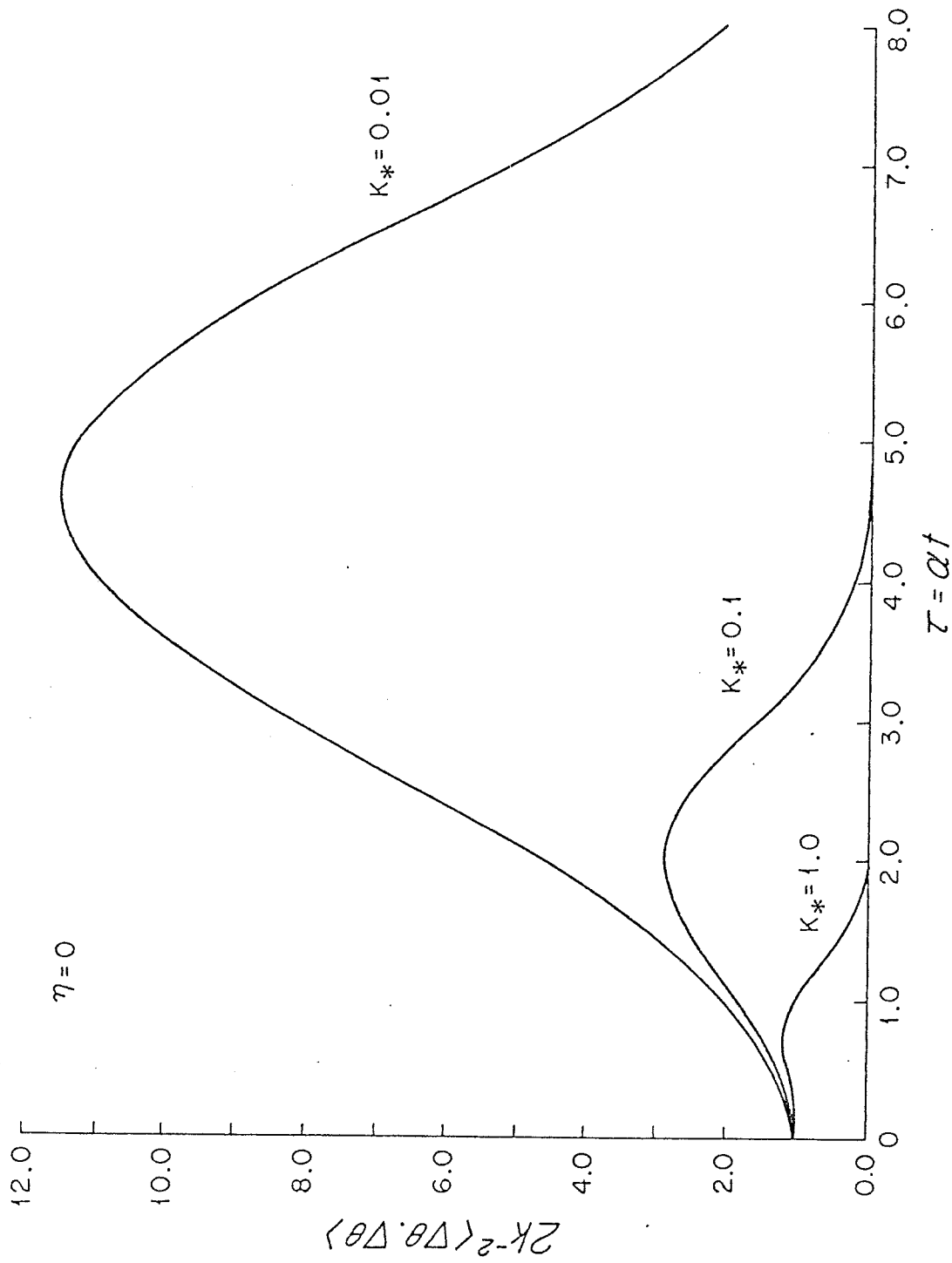


Figure 26. The growth and eventual decay of the average squared  $\theta$ -gradients in a steady shear flow for different values of the nondimensional diffusivity  $\kappa_* = k^2 \kappa / \alpha$ .

Reverting to dimensional units the above is:

$$\alpha t_* = \left( \frac{\alpha}{\kappa k^2} \right)^{1/3} + \text{smaller terms.} \quad (22.9)$$

The 1/3-power in (22.9) can be explained physically by forming the equation for the time rate of change of  $\langle \nabla \theta \cdot \nabla \theta \rangle$ . From (22.6) one has

$$\left\langle \frac{1}{2} \nabla \theta \cdot \nabla \theta \right\rangle_t + \alpha \langle \theta_x \theta_z \rangle = -(\eta + \alpha^2 t^2 \kappa) \langle \nabla \theta_x \cdot \nabla \theta_x \rangle \quad (22.10)$$

where the angular bracket denotes the x-average defined above (22.7). The first term in (22.10) increases initially because the shear creates some  $\theta_z$  and so the second term grows. Eventually however the third term dominates and the first term decreases. The maximum value of  $\langle \nabla \theta \cdot \nabla \theta \rangle$  is then achieved when the second and third terms have equal magnitudes. The time at which this occurs can be estimated using the following relations which apply as  $t \rightarrow \infty$ :

$$\frac{\partial}{\partial x} \sim k \quad \frac{\partial}{\partial z} \sim \nabla \sim \kappa \alpha t$$

It follows that:

$$\alpha \langle \theta_x \theta_z \rangle \sim \alpha k^2 (\alpha t)$$

$$(\eta + \alpha^2 t^2 \kappa) \langle \nabla \theta_x \cdot \nabla \theta_x \rangle \sim (\alpha t)^4 \kappa k^4 ;$$

when the right hand sides of the above are equated, (22.9) is recovered.

Note that if one naively estimated  $t_*$  as the time at which the shear time scale,  $\alpha^{-1}$ , equalled the diffusion time scale based on the decreasing length scale of the tracer distribution,  $[\kappa (k\alpha t)^2]^{-1}$ , the answer,  $\alpha t_* = (\alpha/\kappa k^2)^{1/2}$ , would be wrong; see (22.9).

This completes our discussion of diffusion in a steady shear. To conclude this section we will contrast this solution with one previously discussed by Batchelor (1959) and Phillips (1977) for diffusion in a steady strain. There are important qualitative differences between the two.

Consider the pure straining field:

$$(u,w) = (\beta x, -\beta z) \quad \text{and } \beta > 0, \quad (22.11)$$

the passive tracer  $\theta$  satisfies

$$\theta_t + \beta x \theta_x - \beta z \theta_z = \kappa \nabla^2 \theta \quad (22.12)$$

where for simplicity we've assumed that the horizontal and vertical diffusivities are identical. To solve (22.12) we begin by setting  $\kappa = 0$ . The solution of the resulting advection equation which satisfies the initial condition (20.2) is:

$$\theta(x,z,t) = \cos(ke^{-\beta t}x) \cos(me^{\beta t}z) \quad (22.13)$$

Note how the strain increases the vertical wavenumber exponentially with time, the shear only produced a growth linear in time.

To solve (22.12) with  $\kappa \neq 0$ , as in section 20, we look for a solution of the form:

$$\theta(x,z,t) = A(t) \cos(ke^{-\beta t}x) \cos(me^{\beta t}z) \quad (22.14)$$

When (22.14) is substituted into (22.12) and the resulting equation for  $A$  is solved there results:

$$\begin{aligned} \theta(x,z,t) &= \exp \left\{ \frac{\kappa}{2\beta} [k^2(e^{-2\beta t}-1) - m^2(e^{2\beta t}-1)] \right\} \cos(ke^{-\beta t}x) \cos(me^{\beta t}z) \\ &\rightarrow \exp \left\{ -\left(\frac{\kappa m^2}{2\beta}\right) e^{2\beta t} \right\} \cos(ke^{-\beta t}x) \cos(me^{\beta t}z) \quad \text{as } t \rightarrow \infty \end{aligned} \quad (22.15)$$

Comparing (22.15) with (22.1) it is clear that straining fields are much more effective than shearing fields at producing transfers to high wavenumbers and enhancing diffusion. One method of quantifying this is to calculate  $\langle \nabla \theta \cdot \nabla \theta \rangle$  from (22.15); for simplicity suppose  $m = k$  in which case

$$\langle \nabla \theta \cdot \nabla \theta \rangle = \frac{1}{2} k^2 \cosh(2\beta t) \exp\left[-\left(\frac{2\kappa k^2}{\beta}\right) \sinh 2\beta t\right]. \quad (22.16)$$

This exhibits the same qualitative behaviour as (22.7), an initial increase to a maximum followed by a rapid decrease to zero. The time at which the gradients are largest when  $\kappa k^2/\beta \ll 1$  is:

$$2\beta t_* = \ln[\beta/\kappa k^2] + (\text{smaller terms})$$

which should be compared to (22.9). If  $\alpha^{-1}$  and  $\beta^{-1}$  are comparable time scales we see that  $\langle \nabla \theta \cdot \nabla \theta \rangle$  peaks at a much smaller time in a straining field.

### 23. Oceanographic Applications: Shear Dispersion by Inertial Oscillations

The form of the effective diffusivity (20.7) suggests that the inertial oscillations will be the most important part of the internal wave band as far as shear dispersion is concerned. This is because they have the smallest frequencies combined with the largest vertical shears.

Before blithely inserting numerical estimates of  $\alpha$  and  $\omega$  for inertial oscillations into (20.7), it is advisable to consider possible complications associated with the structure of the velocity field of an inertial oscillation. Unlike the simple velocity field in section 20, the velocity field of an inertial oscillation is:

- (i) two dimensional, the horizontal velocity is circular polarized.
- (ii) rapidly oscillatory in the vertical, observations show there is significant vertical structure down to scales of 10 meters.

The first objection is easily disposed of; it is trivial to resolve equation (20.1) with a horizontal velocity:

$$(u,v) = (\alpha_1 z \cos \omega t, \alpha_2 z \sin \omega t) .$$

If  $|\alpha_1| = |\alpha_2|$  one finds an isotropic horizontal diffusivity given by (20.7).

To address the second objection, in Appendix D, we use the moment method to investigate (20.1) with:

$$u = u_0 \cos nz \cos \omega t \tag{23.1}$$

It is concluded that:

$$\eta_e = \eta + \frac{1}{4} \left( \frac{u_0}{\omega} \right)^2 \left( \frac{\delta}{1+\delta^2} \right) \tag{23.2a}$$

$$\delta = \kappa n^2 / \omega \quad (23.2b)$$

When  $\alpha \ll 1$ , (20.7) is recovered if we interpret  $\alpha^2$  as the mean square vertical shear,  $\frac{1}{2} n^2 u_0^2$ . If  $\delta \gg 1$  we find that  $n_e - n$  is inversely proportional to  $\kappa$ , a result strongly reminiscent of Taylor's (1953) steady pipe flow theory. This is not a coincidence, if  $\theta$  is initially independent of  $z$ , the velocity field (23.1) is such that  $\theta_z(x, z, t) = 0$  at  $z = 0$  and  $\pi/n$ . Thus the problem discussed in Appendix D can also be interpreted as shear dispersion in a pipe. The walls of the pipe are at  $z = 0$  and  $\pi/n$  where the velocity field (23.1) automatically ensures that the no flux boundary condition is satisfied.

This interpretation is additional motivation for considering shear dispersion in the velocity field (23.1). Previous studies of unsteady shear flows (Fischer et al., 1980) in pipes have used the velocity field of section 20. Since the no flux boundary conditions are not automatically satisfied the algebra is much more complicated and the final expression for  $n_e$  must be evaluated numerically. By contrast (23.1) is transparent and the limits  $\delta \rightarrow 0$  or  $\infty$  are easily extracted. This last point is important since there is some confusion in the literature about the limit  $\delta \rightarrow 0$ . Fischer et al. (1980) simply state that the dispersion coefficient is zero in this limit. The actual answer is given by (20.7) and explained physically in section 21. The physical argument assumes that as fluid particles are swept backwards and forwards, their  $\theta$  value is essentially unchanged over a period. This assumption becomes invalid when  $\delta \geq 0(1)$  and not surprisingly the effective diffusivity is no longer given by (20.7).

Order of magnitude estimates suggest that the limit  $\delta \ll 1$  is probably the most relevant for oceanic internal waves. Suppose we take as an upper bound for  $K$  the value suggested by Munk's (1966) model of the vertical advective - diffusive balance in the ocean interior. This is

$K = 1 \text{ cm}^2 \text{ s}^{-1}$ ; estimates based on the temperature microstructure using the method of Osborn and Cox (1972) give much lower values, typically  $K \sim 10^{-2} \text{ cm}^2 \text{ s}^{-1}$  e.g., Gregg et al (1973), Gregg (1977) and Gargett (1976). Thus for an inertial wave which has a vertical wavenumber of  $n \sim 5 \times 10^{-3} \text{ cm}^{-1}$  and a frequency  $\omega \sim f \sim 10^{-4} \text{ s}^{-1}$  one has  $\delta \sim \frac{1}{4}$ . Thus even with this extreme value of  $K$  the approximation:

$$\frac{\delta}{1 + \delta^2} \approx \delta$$

is good to within 10%. This estimate is rather sensitive to the value of  $n$ ; a careful calculation based on a shear spectrum is probably worthwhile.

Note, however, that even if we use  $n \sim 5 \times 10^{-2} \text{ cm}^{-1}$  and take

$K \sim 10^{-2} \text{ cm}^2 \text{ s}^{-1}$ , as suggested by finestructure measurements, the answer is unchanged.

Having established the  $\delta \ll 1$  is appropriate, one can use (20.7) to calculate  $\alpha_e$ . Assuming that the actual horizontal diffusivity  $n$  is negligible and that  $u_0 = 10 \text{ cm s}^{-1}$  it follows that

$$\begin{aligned} \alpha^2 &= \frac{1}{2} u_0^2 n^2 \\ &= \text{mean square vertical shear} \\ &= 10^{-3} \text{ s}^{-2} \end{aligned}$$

where  $n \sim 5 \times 10^{-3} \text{ cm}^{-1}$  was used. Hence

$$\eta_e = 5 \times 10^4 \kappa$$

since  $\omega \sim f \sim 10^{-4}$ . Thus shear dispersion in an oscillatory velocity field is capable of amplifying vertical diffusivities to produce much larger horizontal diffusivities.

The order of magnitude calculations in this section are rather rough; I believe, however, that the estimates for  $\eta_e$  which emerge from these calculations are interesting enough to justify a spectral calculation of  $\eta_e$  using an empirical shear spectrum.

24. Some Mathematical Extensions: Simplification of a General Class of Advection-Diffusion Problems

In this section we show that a rather general class of advection-diffusion problems can be simplified using advected coordinates. Specifically consider a passive tracer  $\theta$  which satisfies:

$$\theta_t + u(z,t) \theta_x + v(z,t) \theta_y = \eta(z) \nabla^2 \theta + [\kappa(z) \theta_z] z \quad (24.1)$$

$$\nabla^2 = \frac{\partial^2}{\partial x^2} + \frac{\partial^2}{\partial y^2}$$

$(u,v)$  = horizontal velocity

Note that the horizontal velocity fields do not depend on the horizontal coordinates and there is no vertical velocity. The shear field discussed in section 20 is an example of such a field. Less trivial examples are the velocity fields of an inertial oscillation and an Ekman layer. An example of a field which does not have this form is the strain field in section 22.

The advection-diffusion problem (24.1) is also the most general form which can be attacked using the moment method. In most cases (the problem in section 20 is an exception) this procedure is simpler than the method given here. For this reason the results in this section are not of primary importance. They are probably most useful in the rare cases when one wishes to determine the precise form of the evolving tracer distribution and so solves (24.1) numerically.

The solution of (24.1) if  $\eta = \kappa = 0$  is found by introducing advected coordinates:

$$\tilde{x} = x - \int_0^t u(z,t') dt'$$

$$\tilde{y} = y - \int_0^t v(z, t') dt'$$

If the initial condition is:

$$\theta(x, y, z, 0) = \theta_0(x, y, z)$$

then the solution is

$$\theta(x, y, z, t) = \theta_0(\tilde{x}, \tilde{y}, z)$$

A convenient class of initial conditions to consider is:

$$\begin{aligned} \theta_0 = & A_0(z) \cos kx \cos ly + B_0(z) \cos kx \sin ly \\ & + C_0(z) \sin kx \cos ly + D_0(z) \sin kx \sin ly, \end{aligned} \quad (24.2)$$

more general initial conditions can be constructed by Fourier analysis as in section 20.

When there is no diffusion the exact solution is obtained by replacing  $x$  and  $y$  in (24.3) by  $\tilde{x}$  and  $\tilde{y}$ . This motivates looking for a solution of the diffusive problem in the form

$$\begin{aligned} \theta = & A(z, t) \cos k\tilde{x} \cos l\tilde{y} + B(z, t) \cos k\tilde{x} \sin l\tilde{y} \\ & + C(z, t) \sin k\tilde{x} \cos l\tilde{y} + D(z, t) \sin k\tilde{x} \sin l\tilde{y} \end{aligned} \quad (24.3)$$

where  $A$ ,  $B$ ,  $C$  and  $D$  satisfy the initial conditions  $A(z, 0) = A_0(z)$ , etc. When (24.3) is substituted into (24.1) and the coefficients of like harmonics are equated one obtains four coupled linear evolution equations for  $A$ ,  $B$ ,  $C$  and  $D$ . The algebra is complicated and has been relegated to Appendix A. These equations are so complicated that it's not clear that the introduction of advected coordinates has actually been simplified (24.1). However, the dimensionality of the problem has been reduced from four to two and this might result in substantial savings if for some reason

it was necessary to solve (24.1) numerically. Moreover it's clear that (24.3) gives us some physical insight into how the structure of the tracer distribution changes as it is advected and diffused. As a special case suppose  $l = 0$  in (24.2), this ensures that the solution is independent of  $y$  at all times, even if  $v \neq 0$ . The four coupled equations in Appendix A reduce to

$$\dot{A} = - \left\{ \eta + \kappa \tilde{x}_z^2 \right\} k^2 A + (\kappa A_z)_z + k(\kappa \tilde{x}_z C)_z + k \kappa \tilde{x}_z C_z \quad (24.4a)$$

$$\dot{C} = - \left\{ \eta + \kappa \tilde{x}_z^2 \right\} k^2 C + (\kappa C_z)_z - k(\kappa \tilde{x}_z A)_z - k \kappa \tilde{x}_z A_z. \quad (24.4b)$$

Note how the solution in section 20 is recovered from the above; since

$\tilde{x}_{zz} = k_z = \eta_z = C_0 = A_{0z} = 0$  (24.2) reduces to

$$\begin{aligned} \dot{A} &= - \left\{ \eta + \kappa \tilde{x}_z^2 \right\} k^2 A \\ C &= 0 \end{aligned}$$

which immediately gives (20.6).

## Appendix A

### Algebraic details from section 24

Differentiating (24.3) with respect to  $z$  gives

$$\begin{aligned} e_z &= E(z,t) \cos k\tilde{x} \cos \tilde{l}\tilde{y} + F(z,t) \cos k\tilde{x} \sin \tilde{l}\tilde{y} \\ &+ G(z,t) \sin k\tilde{x} \cos \tilde{l}\tilde{y} + H(z,t) \sin k\tilde{x} \sin \tilde{l}\tilde{y} \end{aligned} \quad (A1)$$

where it is easily shown by direct calculation:

$$E = A_z + B\tilde{l}\tilde{y}_z + Ck\tilde{x}_z \quad (A2a)$$

$$F = -A\tilde{l}\tilde{y}_z + B_z + Dk\tilde{x}_z \quad (A2b)$$

$$G = -Ak\tilde{x}_z + C_z + D1\tilde{y}_z \quad (A2c)$$

$$H = -Bk\tilde{x}_z - C1\tilde{y}_z + D_z \quad (A2d)$$

(A1) and (A2) are important intermediate results if (24.1) is to be solved in a bounded geometry with no flux boundary conditions.

To obtain evolution equations the term  $(k\theta_z)_z$  must be evaluated from (A1). The resulting evolution equations are:

$$\dot{A} = -\eta(k^2 + 1^2)A + [\hat{E}_z + \hat{F}1\tilde{y}_z + \hat{G}k\tilde{x}_z]$$

$$\dot{B} = -\eta(k^2 + 1^2)B + [\hat{F}_z - \hat{E}1\tilde{y}_z + \hat{H}k\tilde{x}_z]$$

$$\dot{C} = -\eta(k^2 + 1^2)C + [\hat{G}_z - \hat{E}k\tilde{x}_z + \hat{H}1\tilde{y}_z]$$

$$\dot{D} = -\eta(k^2 + 1^2)D + [\hat{H}_z - \hat{F}k\tilde{x}_z - \hat{G}1\tilde{y}_z]$$

where

$$\hat{E} = \kappa E, \quad \hat{F} = \kappa F, \quad \hat{G} = \kappa G, \quad \hat{H} = \kappa H .$$

When the equations are independent of  $y$  the above simplify to (24.2).

## Appendix B

### Solution of (20.1) and (20.2) with $m \neq 0$

In this appendix I shall discuss the solution of (20.1) with the initial condition (20.2). It is easy to see that the solution has the form:

$$\theta = a(t) \cos k\tilde{x} \cos mz + b(t) \sin k\tilde{x} \sin mz \quad (B1)$$

$$a(0) = 1 \quad \text{and} \quad b(0) = 0 \quad (B2)$$

where  $\tilde{x}$  is defined in (20.4). Note that (B1) is a particular case of the general form discussed in section 24. When (B1) is substituted into

(20.1), the resulting evolution equations for a and b are:

$$\dot{a} = - \left\{ \kappa(m^2 + k^2 \tilde{x}_z^2) + \eta k^2 \right\} a + 2 \kappa m k \tilde{x}_z b \quad (B3)$$

$$\dot{b} = - \left\{ \kappa(m^2 + k^2 \tilde{x}_z^2) + \eta k^2 \right\} b + 2 \kappa m k \tilde{x}_z a \quad (B4)$$

The above are simplified to

$$\dot{\hat{a}} = 2 \kappa m k \tilde{x}_z b \quad (B5)$$

$$\dot{\hat{b}} = 2 \kappa m k \tilde{x}_z a \quad (B6)$$

by introducing:

$$\hat{a} = \exp \left[ \int_0^t \left\{ \kappa(m^2 + k^2 \tilde{x}_z^2) + \eta k^2 \right\} dt' \right] a \quad (B7)$$

$$\hat{b} = \exp \left[ \int_0^t \left\{ \kappa(m^2 + k^2 \tilde{x}_z^2) + \eta k^2 \right\} dt' \right] b \quad (B8)$$

Now observe that (B5) and (B6) have a first integral:

$$\begin{aligned} \hat{a}^2 - \hat{b}^2 &= \text{constant} \\ &= 1 \text{ from (B2), (B7) and (B8)} \end{aligned}$$

which can be used to put (B5) in the form:

$$\pm \frac{d\hat{a}}{\sqrt{\hat{a}^2 - 1}} = 2 \kappa m k \tilde{x}_z dt.$$

Integrating the above and using (B7) and (B8) we have finally

$$a = \exp[-(\eta_e k^2 t + \kappa m^2 t) + \frac{1}{4} \kappa k^2 (\alpha^2 / \omega^3) \sin 2\omega t] \cosh[2 \kappa m k (\alpha / \omega^2) (\cos \omega t - 1)] \quad (B9)$$

$$b = \exp[ \quad \quad \quad \text{As Above} \quad \quad \quad ] \sinh[ \quad \quad \quad \text{As Above} \quad \quad \quad ] \quad (B10)$$

where  $\eta_e$  is defined in (20.7). Note how (B9) and (B10) reduce to (20.6) when  $m = 0$ .

The evolution of the initial condition (20.2) can be described in terms of an effective horizontal diffusivity  $\eta_e$  and vertical diffusivity  $\kappa$

when:

$$\theta \approx \exp[-(\eta_e k^2 t + \kappa m^2 t)] \cos k\tilde{x} \cos mz$$

From (B9) and (B10) it follows that this simplification is valid when:

$$\eta_{e*} = \eta_e k^2 / \omega \ll 1$$

and  $2\kappa m k \alpha / \omega^2 \ll 1.$

The first condition is familiar from sections 20 and 21. When

$\eta_e = \frac{1}{2}(\alpha/\omega)^2 \kappa$ , the second reduces to

$$(m/k) \ll (\alpha/\omega) \eta_{e*}^{-1}$$

Since  $\eta_{e*} \ll 1$  and  $\omega/\alpha \ll 1$  are the most interesting cases, the above is not a very restrictive condition on the aspect ratio of the initial distribution.

## Appendix C

### Calculation of the time average in section 21

To emphasize that the  $J_0(\alpha k z / \omega)$  structure of  $\bar{\theta}$  in (21.3) is produced completely by the advection and is independent of the diffusivity we first calculate  $\bar{\theta}$  from the nondiffusive solution (20.3):

$$\theta = \cos k\tilde{x} \tag{C1}$$

$$= \cos kx \cos[(\alpha/\omega)z \sin \omega t] + \sin kx \sin[(\alpha/\omega)z \sin \omega t] \tag{C2}$$

The time average of (C2) is simple since:

$$\frac{\omega}{2\pi} \int_0^{2\pi/\omega} \cos[(\alpha/\omega)z \sin \omega t] dt = J_0[(\alpha/\omega)z \sin \omega t] \tag{C3}$$

$$\frac{\omega}{2\pi} \int_0^{2\pi/\omega} \sin[(\alpha/\omega)z \sin \omega t] dt = 0 ; \quad (C4)$$

(C3) is a well known integral representation of the Bessel function (Abramowitz and Segun, 1968) and (C4) follows from the antisymmetry of the integrand about the middle of the range.

When  $\epsilon$  defined in (21.1) is small the exponential multiplying  $\cos k\tilde{x}$  in (21.2) is virtually constant over a period and so when (21.2) is time averaged the exponential can be taken outside the integral with only  $O(\epsilon)$  errors.

#### Appendix D

##### An analysis of shear dispersion by (23.1) using the moment method

The problem investigated in this appendix is:

$$\theta_t + u\theta_x = \kappa\theta_{zz} + \eta\theta_{xx} \quad (D1a)$$

$$u = u_0 \cos nz \cos \omega t \quad (D1b)$$

$$\theta(x, z, 0) = \theta_0(x) \quad (D1c)$$

We will employ the moment method, the notation

$$\langle a \rangle = \int_{-\infty}^{\infty} a \, dx$$

is convenient. It follows from (D1) that

$$\langle \theta \rangle_t = \kappa \langle \theta \rangle_{zz} \quad (D2a)$$

$$\langle x\theta \rangle_t = \kappa \langle x\theta \rangle_{zz} + u \langle \theta \rangle \quad (D2b)$$

$$\langle x^2\theta \rangle_t = \kappa \langle x^2\theta \rangle_{zz} + 2u \langle x\theta \rangle + 2\eta \langle \theta \rangle \quad (D2c)$$

The solution of (D2a) is

$$\langle \theta \rangle = C_0 = \int_{-\infty}^{\infty} \theta_0(x) dx$$

and substituting this into (D2b) gives

$$\langle x\theta \rangle_t - \kappa \langle x\theta \rangle_{zz} = u_0 c_0 \cos nz \cos \omega t .$$

The solution of the above is:

$$\langle x\theta \rangle = (u_0 c_0 / \omega) (1 + \delta^2)^{-1} \cos nz \left\{ \delta \cos \omega t + \sin \omega t \right\} \quad (D3a)$$

+ (a decaying transient)

$$\delta = \kappa n^2 / \omega \quad (D3b)$$

Substituting (D3a) into (D2c) gives an equation for the second moment:

$$\langle x^2 \theta \rangle_t - \kappa \langle x^2 \theta \rangle_{zz} = 2(u_0^2 c_0 / \omega) (1 + \delta^2)^{-1} \cos^2 nz \cos \omega t \left\{ \delta \cos \omega t + \sin \omega t \right\} + 2\eta c_0 \quad (D4)$$

where we've neglected the transient in (D3a) by assuming  $\omega t \gg \delta^{-1}$ .

Equation (D4) can easily be solved exactly by decomposing the forcing term on the right hand side into its fundamental z and t Fourier components.

However, if one's sole interest is in how rapidly the dominant horizontal length scale of the distribution is expanding it suffices to consider the zero frequency components of the right hand side. Thus

$$\langle x^2 \theta \rangle = \left\{ \frac{1}{2} (u_0^2 c_0 / \omega) \delta (1 + \delta^2)^{-1} + 2\eta c_0 \right\} t + \left\{ \text{harmonic contributions} \right\} \quad (D5)$$

Equation (D5) shows the effective horizontal diffusivity is

$$\eta_e = \eta + \frac{1}{4} \left( \frac{u_0^2}{\omega} \right) \left( \frac{\delta}{1 + \delta^2} \right) \quad (D6)$$

For orientation it is instructive to consider (D6) in two limits:

$$\delta \ll 1 : \eta_e \approx \eta + (n u_0 / 2\omega)^2 \kappa \quad (D7a)$$

$$\delta \gg 1 : \eta_e \approx \eta + (u_0 / 2n)^2 \kappa^{-1} \quad (D7b)$$

(D7a) is the result obtained in sections 20 and 21 if  $\alpha^2$  is identified as the mean square shear,  $\frac{1}{2} n^2 u_0^2$ . In this limit the  $\theta$  value of a fluid particle is approximately constant over a period and the horizontal dispersion is due to the mechanism discussed physically in section 21. (D7b) is essentially Taylor's expression for the dispersion coefficient in a steady pipe flow, note  $n_e - n$  is inversely proportional to  $\kappa$ . The physical explanation of this surprising result is well known: in this limit the vertical diffusivity is so strong that a particle loses its initial value of  $\theta$  almost as soon as it is horizontally displaced. The enhanced horizontal dispersion is due, however, to the small excursion which is possible before  $\theta$  changes. The smaller the vertical diffusivity, the greater this excursion and the larger the horizontal dispersion. The pipe flow analogy is discussed further in section 23.

## References

- Abramowitz, M. and Stegun, I. A. (eds.), 1968. Handbook of Mathematical Functions. Dover, New York.
- Anderson, D.L.T., and A.E. Gill, 1975. Spin-up of a stratified ocean with applications to upwelling. Deep-Sea Research, 22, ~~709-732~~.
- Anderson, D.L.T., and P.D. Killworth, 1977. Spin-up of a stratified ocean, with topography. Deep-Sea Research, 24, 709-732.
- Andrews, D. G. and M. E. McIntyre, 1978. An exact theory of nonlinear waves on a Lagrangian-mean flow. Journal of Fluid Mechanics, 89, 609-646.
- Aris, R., 1956. On the dispersion of a solute in a fluid flowing through a tube. Proceedings of the Royal Society of London, A, 235, 67-77.
- Batchelor, G. K., 1956. On steady laminar flow with closed streamlines at large Reynolds number. Journal of Fluid Mechanics, 1, 177-190.
- Batchelor, G. K., 1959. Small scale variation of convected quantities like temperature in a turbulent fluid. Part I. General discussion and the case of small conductivity. Journal of Fluid Mechanics, 5, 113-133.
- Bender, C. M. and S. A. Orszag, 1978. Advanced Mathematical Methods for Scientists and Engineers, New York: McGraw-Hill.
- Bretherton, F. P. and C. J. R. Garrett, 1968. Wavetrains in inhomogeneous moving media. Proceedings of the Royal Society of London, A, 302, 529-544.
- Chandrasekhar, S., 1943. Stochastic problems in physics and astronomy. Reviews of Modern Physics, 15, 1-87.

- Charney, J.G., and G.R. Flierl, 1981. Oceanic Analogues of Large-scale Atmospheric Motions. In Evolution of Physical Oceanography: Scientific Surveys in Honor of Henry Stommel, B.A. Warren and C.I. Wunsch, eds., M.I.T. Press, Cambridge, Massachusetts and London, England.
- Csanady, G. T., 1966. Diffusion in an Ekman layer. Journal of the Atmospheric Sciences, 26, 414-426.
- Dickinson, R. E., 1978. Rossby waves -- long period oscillations of atmospheres and oceans. Annual Review of Fluid Mechanics, 10, 159-198.
- Fischer, H. B., and E. J. List, R. C. Y. Koh, J. Imberger and N. H. Brooks, 1979. Mixing in Inland and Coastal Waters. Academic Press.
- Flierl, G.R., 1978. Models of vertical structure and the calibration of two-layer models. Dynamics of Atmospheres and Oceans, 2, 341-381.
- Gargett, A. E., 1976. An investigation of the occurrence of oceanic turbulence with respect to fine structure. J. Phys. Oceanogr., 6, 139-156.
- Geisler, J. E. and R. E. Dickinson (1975). Critical level absorption of barotropic Rossby waves in a North-South flow. Journal of Geophysical Research, 80, 3805-3811.
- Gregg, M. C., and C. S. Cox and P. W. Hacker, 1973. Vertical microstructure measurements in the central north Pacific. J. Phys. Oceanogr., 3, 458-469.
- Gregg, M. C., 1977. Variations in the intensity of small scale mixing in the main thermocline. J. Phys. Oceanogr., 7, 436-454.
- Holton, J., 1975. The Dynamic Meteorology of the Stratosphere and Mesosphere, Meteorologic Monographs, 15, number 37, American Met. Soc.

- Leetma, A., P. Niiler, and H. Stommel, 1977. Does the Sverdrup relation account for the mid-Atlantic circulation? Journal of Marine Research, 35, 1-10.
- Lighthill, M.J., 1967. On waves generated in dispersive systems by travelling forcing effects, with applications to the dynamics of rotating fluids. Journal of Fluid Mechanics, 27, 725-752.
- Lighthill, J., 1978. Waves in Fluids, Cambridge: University Press.
- McEwan, A. D., R. O. R. Y. Thompson and R. A. Plumb, 1980. Mean flows driven by weak eddies in rotating systems. Journal of Fluid Mechanics, 99, 655-672.
- McWilliams, J. C., 1976. Large scale inhomogeneities and mesoscale ocean waves: a single stable wave field. Journal of Marine Research, 34, 423-456.
- Moffatt, H. K., 1978. Magnetic Field Generation in Electrically Conducting Fluids, Cambridge University Press.
- Moore, D.W., 1963. Rossby waves in ocean circulation. Deep-Sea Research, 10, 735-748.
- Muller, P., 1978. On the parameterization of eddy-mean flow interaction in the ocean. Dynamics of Atmospheres and Oceans, 2, 383-408.
- Munk, W.H., 1950. On the wind-driven ocean circulation. Journal of Meteorology, 7, 79-93.
- Munk, W. H., 1966. Abyssal recipes. Deep-Sea Res., 13, 707-730.
- Needler, G., 1967. A model for the thermohaline circulation in an ocean of finite depth. Journal of Marine Research, 25, 329-342.
- Osborn, T. R. and C. S. Cox, 1972. Oceanic finestructure. Geophys. Fluid Dyn., 3, 321-345.

- Pedlosky, J., 1979. Geophysical Fluid Dynamics. Springer Verlag.
- Phillips, O. M., 1977. The Dynamics of the Upper Ocean, 2nd ed., Cambridge University Press, London, 336 pp.
- Proctor, M. R. E., 1975. Non-linear mean field dynamo models and related topics. Ph.D. thesis, Cambridge University.
- Rhines, P., 1970. Edge-, bottom-, and Rossby waves in a rotating stratified fluid. Geophysical Fluid Dynamics, 1, 273-302.
- Rhines, P.B., 1977. The dynamics of unsteady currents. In The Sea: Ideas and Observations on Progress in the Study of the Seas, 6: Marine Modeling, E.D. Goldberg, I.N. McCave, J.J. O'Brien and J. H. Steele, eds., Wiley Interscience, New York.
- Rhines, P.B., and W.R. Holland, 1979. A theoretical discussion of eddy driven mean flows. Dynamics of Atmospheres and Oceans, 3, 289-325.
- Rhines, P. B., 1979. Geostrophic turbulence. Annual Reviews of Fluid Mechanics, 11, 401-441.
- Rooth, C., H. Stommel and G. Veronis, 1978. On motions in steady layered geostrophic models. Journal of the Oceanographical Society of Japan, 34, 265-267.
- Saffman, P. G., 1962. The effect of wind shear on horizontal spread from an instantaneous ground source. Quarterly Journal of the Royal Meteorological Society, 88, 382-393.
- Stommel, H., 1948. The westward intensification of wind-driven ocean currents. Transactions of the American Geophysical Union, 29, 202-206.
- Stommel, H. M., A. B. Arons, 1960. On the abyssal circulation of the world ocean -- I. Stationary planetary flow patterns on a sphere. Deep-Sea Research, 6, 140-154.

- Stommel, H. M., A. B. Arons, and A. J. Faller, 1958. Some examples of stationary planetary flow patterns in bounded basins. Tellus, 10, 179-187.
- Taylor, G. I., 1921. Diffusion by continuous movements. Proceedings of the London Mathematical Society, 20, 196-212.
- Taylor, G. I., 1953. Dispersion of soluble matter in solvent flowing slowly through a tube. Proceedings of the Royal Society of London, A, 219, 186-203.
- Van Kampen, N. G., 1976. Stochastic differential equations. Physics Reports (Section C of Physics Letters), 24, 171-228.
- de Verdiere, A. C., 1980. Quasigeostrophic turbulence in a rotating homogeneous fluid. Geophysical and Astrophysical Fluid Dynamics, 15, 213-251.
- Veronis, G., 1981. Dynamics of large-scale ocean circulation. In Evolution of Physical Oceanography: Scientific Surveys in Honor of Henry Stommel, B. A. Warren and C. I. Wunsch, eds., M.I.T. Press, Cambridge, Massachusetts and London, England.
- Weiss, N. O., 1966. The expulsion of magnetic flux by eddies. Proceedings of the Royal Society, Series A, 293, 310-328.
- Welander, P., 1960. A two-layer frictional model of wind-driven motion in a rectangular oceanic basin. Tellus, 18, 54-62.
- Welander, P., 1968. Wind-driven circulation in one- and two-layer oceans of variable depth. Tellus, 20, 1-15.
- Welander, P., 1971. Some exact solutions to the equations describing and ideal fluid thermocline. Journal of Marine Reserach, 29, 60-68.

Worthington, L. V., 1976. On the North Atlantic Circulation. The Johns Hopkins Oceanographic Series, 6, 110pp.

Young, W. R., and P. B. Rhines, 1980. Rossby wave action, enstrophy and energy in forced mean flows. Geophysical and Astrophysical Fluid Dynamics, 15, 39-52.